Superconductivity and Magnetism: Materials Properties and Developments

Andersen, Niels Hessel; Bay, Niels; Grivel, Jean-Claude; Hedegård, P.; McMorrow, D.; Mørup, S.; Kuhn, Luise Theil; Larsen, A.; La, B.

Published in:
Extended abstracts of the 24th Rsisø International Symposium on Materials Science

Publication date:
2003

Document Version
Publisher's PDF, also known as Version of record

RISØ

Superconductivity and Magnetism: Materials Properties and Developments

Editors

N. H. Andersen N. Bay J.-C. Grivel P. Hedegård D. McMorrow S. Mørup
L. T. Kuhn A. Larsen B. Lebech K. Lefmann P.-E. Lindelof S. Linderoth
N. F. Pedersen

24th Risø International Symposium
on Materials Science
2003

Superconductivity and Magnetism: Materials Properties and Developments

Risø National Laboratory
Roskilde, Denmark

ISBN 87-550-3244-3

ISSN 0907-0079

Superconductivity and Magnetism: Materials Properties and Developments

Extended abstracts of the 24th Risø International Symposium on Materials Science

10 – 13 September 2003

Editors

N.H. Andersen N. Bay J.-C. Grivel P. Hedegård D. McMorrow S. Mørup L. T. Kuhn A. Larsen B. Lebech K. Lefmann P.-E. Lindelof S. Linderoth N. F. Pedersen

RISØ NATIONAL LABORATORY
ROSKILDE, DENMARK

Risø International Symposium on

Superconductivity and Magnetism:
Material Properties and Developments

INTERNATIONAL ADVISORY COMMITTEE

LOCAL ORGANIZING COMMITTEE

Niels Hessel Andersen, Risø National Laboratory (Chairman)

Niels Bay, Technical University of Denmark

Jean-Claude Grivel, Risø National Laboratory
Per Hedegård, University of Copenhagen
Des McMorrow, Risø National Laboratory
Steen Mørup, Technical University of Denmark (Co-Chairman)
Luise Theil Kuhn, Risø National Laboratory
Ann Larsen, Risø National Laboratory (Secretary)
Bente Lebech, Risø National Laboratory
Kim Lefmann, Risø National Laboratory
Poul-Erik Lindelof, University of Copenhagen
Søren Linderoth, Risø National Laboratory

Preface

The discovery of new superconducting and magnetic materials with unexpected properties has revived a significant activity in the field ranging from basic science to developments for technological applications. Being considered as generally exclusive phases, superconductivity and magnetism may appear as separate topics, but they may co-exist and give rise to exotic phenomena.

The 24th Risø International Symposium on Materials Science:

SUPERCONDUCTIVITY AND MAGNETISM:
MATERIALS PROPERTIES AND DEVELOPMENTS

focuses on development of new materials, devices and applications, as well as experimental and theoretical studies of novel and unexplained phenomena in superconductivity and magnetism, *e.g.* within high-T_c superconductivity, magnetic superconductors, MgB_2, CMR materials, nanomagnetism and spin-tronics The aim is to stimulate exchange of ideas and establish new collaborations between leading Danish and international scientists. The topics are addressed by presentations from 24 invited speakers and by 41 contributed papers.

The Symposium is linked to two framework programmes granted by the Danish Technical Research Council to stimulate R&D within *"Nanomagnetism"* and *"New superconductors: mechanisms, processes and products".* Research groups at Risø National Laboratory, the Technical University of Denmark and the University of Copenhagen are working jointly to achieve the objectives. Neutron and synchrotron x-ray scattering are important techniques for the Danish research projects on magnetism and superconductivity. The Danish Natural Science Council via the Danish Neutron Scattering Centre, DANSCATT, and the synchrotron x-ray organisation DANSYNC have supplied support for these activities.

The symposium is organised jointly by the Materials Research Department at Risø National Laboratory, the Niels Bohr Institute for Astronomy, Physics and Geophysics at the University of Copenhagen, and the Department of Physics, the Department of Manufacturing Engineering and Management, and Ørsted•DTU at the Technical University of Denmark.

Financial support has been generously provided by Knud Højgaards Fond, Fabrikant Mads Clausens Fond, the Danish Technical Research Council, via the two framework programmes, the Danish Natural Science Council, via DANSYNC and DANSCATT, and Risø National Laboratory.

We thank all the people who have contributed to the programme and assisted in preparations for the Symposium.

Niels Hessel Andersen, Niels Bay, Jean-Claude Grivel, Per Hedegård,
Des McMorrow, Steen Mørup, Luise Theil Kuhn, Ann Larsen,
Bente Lebech, Kim Lefmann, Poul-Erik Lindelof, Søren Linderoth,
Niels Falsig Pedersen

CONTENTS

Invited Papers

Oral Contributed Papers

Posters Contributed Papers

Presentation of the ESS initiative in Lund

HISTORY OF MAGNETISM

J. M. D. Coey (Physics Department, Trinity College, Dublin 2, Ireland.)

The modern history of magnetism dates from the discovery of the electron, just over 100 years ago. Magnetism had been a problem since Ørsted demonstrated that a magnetic moment was equivalent to a current loop in 1821. The difficulty was to reconcile the magnetic moment of ferromagnetic iron for example with the corresponding huge surface current density of 1.76 MA/m. An explanation of the atomic and electronic nature of the perpetually-circulating currents required quantum mechanics and relativity in the guise of the Bohr theory of the atom and the Dirac theory of the electronic spin. Likewise the enormous molecular field postulated by Weiss to account for ferromagnetic order required the quantum mechanics of Pauli and Heisenberg for a fundamental, electrostatic explanation.

The generation from 1905 - 1930 was the Age of Understanding, but it was decades before much of practical value was to flow from it. A rather different approach, based on phenomenological theory and quantitative engagement with practical magnetic phenomena, typified by Neel, was successful in rationalizing the phenomenon of hysteresis and explaining the magnetism of magnetite and other oxides in terms of their crystal structure. Related studies of rock magnetism led to the establishment of the theory of global plate tectonics. Magnetism in the 1940s and 1950s had a focus on microwave and rf applications. In turn, nuclear and electronic magnetic resonance contributed powerful methods of investigating solids and liquids, and led to new forms of diagnostic imaging.

From 1960 onwards came an Age of Applications, when hard and soft magnetic materials, metals and insulators, proliferated in components for consumer goods, greatly expanding their traditional role in electrotechnology. Permanent magnets, which had overcome the 'shape barrier' with the development of hexagonal ferrites in the 1950s, came of age with the rare earth alloys Sm-Co and Nd-Fe-B, which enabled miniature electromagnetic drives - motors and actuators. Nevertheless, magnetism remained apart from electronics, the great mould-breaking technology of the age. Conventional electronics had ignored the spin on the electron, depending on charge currents alone. As lithography and thin film processes developed, along with electron microscopy and point probe techniques such as magnetic force microscopy, it became possible to realise and investigate magnetic thin-film structures and probe magnetic phenomena on mesoscopic length scales. Magnetic recording (a Danish invention) was the technology driver for 50 years, demanding and achieving exponential improvements in recording density and data rate.

Fert's discovery of giant magnetoresistance in an artificial magnetic multilayer in 1988 was a key step, which led quickly to the spin valve and the magnetic tunnel junction. Two-terminal spin electronics based on magnetoresistance is yields $6 \cdot 10^8$ devices/year and this may soon increase to 10^{16} with the commercialisation of MRAM. This is just the start: a whole new range of functionality awaits development as magnetism becomes ever more closely integrated with electronics in multi-terminal devices - the Age of Spin Electronics.

QUANTUM COHERENCE IN MAGNETS

Collin Broholm (Department of Physics and Astronomy, Johns Hopkins University, Baltimore, MD 21218, USA and NIST Center for Neutron Research, Gaithersburg, MD 20899, USA)

Magnetic materials are typically found in one of two qualitatively different states: Thermally disordered at high temperatures or spin ordered at low temperatures. In this talk I describe a third distinct state of an interacting spin system: quantum ordered magnetism.

I present neutron scattering data that provide evidence for quantum order in zero, one, two, and three-dimensional spin systems. $La_4Cu_3MoO_{12}$ contains spin-trimers that develop quantum order at low temperature where each trimer becomes a composite spin-1/2 degree of freedom.[1] Y_2BaNiO_5 is an antiferromagnetic spin-1 chain with an extensive one-dimensional Haldane ground state. I present scattering data that provide clear evidence for long-range coherence in the absence of conventional spin order.[2] $(C_4H_{12}N_2)Cu_2Cl_6$ (PHCC) is a frustrated bi-layer antiferromagnet with interactions that span a two-dimensional plane. I show that there are coherent triplet excitations and argue that competing interactions favour quantum order over spin order[3]. $Cu_2(C_5H_{12}N_2)_2Cl_4$ (CuHpCl) has a cooperative singlet ground state and was initially thought to be a spin ladder. However, neutron scattering data show that it is in fact a three-dimensional frustrated system with quantum order.[4]

Apart from describing and comparing the low temperature quantum ordered states in these pure systems, I shall also touch on the fascinating effects of impurities[5] and the field driven quantum phase transitions that can be accessed experimentally in several of these systems.[6]

REFERENCES

1. Y. Qiu, C. Broholm, S. Ishiwata, M. Azuma, M. Takano, R. Bewley, and W. J. L. Buyers, Cond-Mat/0205018
2. Guangyong Xu, J. F. DiTusa, T. Ito, H. Takagi, K. Oka, C. Broholm and G. Aeppli, Phys. Rev. B **54**, R6827 (1996)
3. M. B. Stone, I. A. Zaliznyak, Daniel H. Reich, and C. Broholm, Phys. Rev. B **64**, 144405 (2001).
4. M. B. Stone, J. Rittner, Y. Chen, H. Yardimci, D. H. Reich, C. Broholm, D. V. Ferraris, and T. Lectka, Phys. Rev. B **65**, 064423 (2002)
5. M. Kenzelmann, G. Xu, I. A. Zaliznyak, C. Broholm, J. F. DiTusa, G. Aeppli, T. Ito, K. Oka, and H. Takagi. Phys. Rev. Lett. **90**, 087202 (2003)
6. Y. Chen, Z. Honda, A. Zheludev, C. Broholm, K. Katsumata, and S. M. Shapiro Phys. Rev. Lett. **86**, 1618 (2001)

MORIN TRANSITION IN α-Fe_2O_3 NANO-PARTICLES INDUCED BY INTER-PARTICLE INTERACTIONS

C. Frandsen, S. Mørup (Department of Physics, Technical University of Denmark, Denmark), B. Lebech, K. Lefmann, S. N. Klausen, L. Theil Kuhn (Materials Research Department, Risø National Laboratory, Denmark), L. Keller (Laboratory for Neutron Scattering, ETH Zurich & Paul Scherrer Institute, CH-5232 Villigen, Switzerland)

In bulk α-Fe_2O_3 (hematite), the Morin transition takes place as a first order transition at $T_M \cong 263$ K. At T_M, the spin structure changes from being confined to lie in the rhombohedral (1 1 1) plane above T_M to lying along the [1 1 1] axis below T_M. With decreasing particle size, T_M decreases, and it has been reported that there is no Morin transition above 4 K in α-Fe_2O_3 particles smaller than ~ 20 nm in diameter. However, we have found that 9 nm α-Fe_2O_3 particles interacting with NiO nanoparticles show a gradual Morin transition at low temperatures.[1, 2] The Morin transition was neither observed in pure samples of the 9 nm α-Fe_2O_3 particles, nor when the α-Fe_2O_3 nanoparticles were exposed to Ni^{2+} or mixed with CoO particles.[2] Here, we present a combined Mössbauer and neutron diffraction study of α-Fe_2O_3 nanoparticles interacting with NiO nanoparticles. In Mössbauer spectra the Morin transition is clearly visible because the quadrupole shift, ε, changes from $\varepsilon = -0.1$ mms^{-1} above T_M to $\varepsilon = +0.2$ mms^{-1} below T_M. The spectrum of α-Fe_2O_3 nanoparticles mixed with NiO showed $\varepsilon \approx +0.2$ mms^{-1} at 20 K. With increasing temperature, up to ~ 160 K, there was a gradual change of the spectra, indicating a Morin transition. Over a range of temperatures ε was about 0 mms^{-1}, approaching -0.1 mms^{-1} around 160 K. The observations suggest that the sublattice magnetisation in a temperature range is neither fixed in the [1 1 1] direction nor in the (1 1 1) plane. At the highest temperatures, the analysis of the Mössbauer spectra is impeded by superparamagnetic relaxation. In neutron powder diffraction measurements, the data are not influenced by superparamagnetic relaxation and the gradual transitions can be followed by measuring the relative intensities and shapes of the magnetic [1 1 1] and [1 0 0] reflections.

REFERENCES

1. C.W. Ostenfeld and S. Mørup, Hyperfine Interact. C **5**, 83 (2002) 83
2. C. Frandsen and S. Mørup, J. Magn. Magn. Mater., in the press

TAILORING CMR MANGANITES

B. Raveau (Laboratoire CRISMAT, UMR 6508, 6 Boulevard du Maréchal Juin, 14050 CAEN Cedex 4 – France)

The discovery of colossal magnetoresistance in manganites has allowed new phenomena to be evidenced, which are most fascinating, such as charge orbital ordering and phase separation. The latter play an important role in the tailoring of these materials.

It has been shown very early that the average size of the A site cation and the size mismatch between different A-site cations are of capital importance for the optimisation of the Curie temperature of manganites. Nevertheless, to date, curiously, the utilisation of these compounds at room temperature under low magnetic fields remains a challenge. Based on the idea that the maximum intrinsic CMR at room temperature should appear for $T_c \sim T_{IM} \sim 300$ K, but should also require an optimum for double exchange, we demonstrate that intrinsic magnetoresistance can reach rather high values ranging from 14 % to 25 % at room temperature under 1.2 T, in different systems – $La_{1-x}Ag_xMnO_3$, $La_{2/3-x}Pr_xSr_{1/3}MnO_3$ and $La_{2/3}Sr_{1/3-x}Ca_xMnO_3$ – provided the Mn^{3+}/Mn^{4+} ratio is optimal for DE, i.e. close to 2.

Manganites involving small A-site cations such as $Ln_{1-x}Ca_xMnO_3$ series seemed at first sight useless for the CMR effect several years ago, since they were shown to be antiferromagnetic insulators. However, the existence of orbital-charge ordering in those oxides, in the form of stripes, in connection with the Jahn-Teller effect of manganese, and especially the metastability of the charge ordered state on the application of a magnetic field, make them also good candidates for the CMR. Based on the idea that charge-orbital ordering between manganese ions can be weakened and even destroyed by doping these materials with foreign cations at the Mn-sites, the CMR effect can be induced by Mn-site doping with magnetic cations (Cr^{3+}, Ru^{4+}/Ru^{5+}, Ni^{2+}, Co^{2+}, Rh^{3+}, Ir^{4+}), changing the magnetic phase diagram of these systems in a spectacular way. In fact, the appearance of CMR in these doped manganites is strongly connected to the existence of phase separation: small ferromagnetic regions are developed around the magnetic impurities, coexisting coherently with the antiferromagnetic insulating matrix. The latter regions are expanded as the doping element content increases, and as percolation is reached, an insulator metal transition is observed. In such phase-separated systems, the ferromagnetic metallic regions can extend on the application of a magnetic field, leading then to the CMR effect. The mechanism of the formation of such regions and of their extension is still an opened question. However, the studies of the field effect of those doped systems at low temperature (2 to 5 K) that are presently in progress, suggest strongly a martensic-like behaviour. One indeed observes that the magnetization, the resistivity and the specific heat of these oxides exhibit a step-like evolution versus the applied magnetic field, as a result of the opposition of the antiferromagnetic matrix to the development of the ferromagnetic regions.

Finally, the cationic ordering can also influence dramatically the magnetotransport properties of manganites. This is the case of the perovskite $LaBaMn_2O_6$. When prepared by direct synthesis at high temperature, this phase exhibits the classical cubic perovskite structure, and is ferromagnetic with a T_c of 270 K. When prepared by oxidation under an oxygen flow at rather low temperature (300°C) of the ordered oxygen deficient layered perovskite $LaBaMn_2O_5$, one obtains a stoichiometric tetragonal perovskite $LaBaMn_2O_6$, with a perfect ordering of the "La^{3+}" and "Ba^{2+}" layers alternately. The latter exhibits a much higher T_c ~ 335 K, showing the great effect of the geometry of Mn-O-Mn bonds upon the magnetotransport properties of manganites.

ENTANGLEMENT AND HOW TO MEASURE IT IN MAGNETS

G. Aeppli (University College London, UK and NEC Laboratories, USA), T. F. Rosenbaum (University of Chicago, USA), S. Ghosh (University of Chicago, USA), J. Brooke (NEC Laboratories and University of Chicago, USA), R. Parthasarathy (University of Chicago, USA) and S. N. Coppersmith (University of Wisconsin, USA)

We describe recent experiments, which probe a variety of quantum effects, most notably entanglement, in three-dimensional, insulating magnets. Of particular significance are the observation of tuneable quantum tunnelling of ferromagnetic domain walls[1], the discovery of hole burning and persistent oscillations in the bulk magnetization in frustrated magnets[2], and the puzzle of the smooth power law (in temperature) divergent susceptibility in the dilute dipolar coupled magnet.[3] The understanding of our data follows from consideration of the off-diagonal (in spin space) terms in the magnetic dipole interaction, which produce quantum mechanical mixing, or "entanglement", effects. Even though these terms are quite small, they dominate the low temperature physics and yield novel, yet easily measurable, quantum phenomena. We conclude with a discussion of implications for the problem of quantum computers.[4]

REFERENCES

1. J. Brooke, T. F. Rosenbaum and G. Aeppli, Nature **413**, 610 (2001)
2. S. Ghosh, R. Parthasarathy, T. F. Rosenbaum and G. Aeppli, Science **296**, 2195 (2002)
3. S. Ghosh, T. F. Rosenbaum, G. Aeppli and S. N. Coppersmith, preprint (2003)
4. J. Brooke, D. Bitko, T. F. Rosenbaum and G. Aeppli, Science **284**, 779 (1999)

MANIPULATING QUANTUM INFORMATION WITH SEMICONDUCTOR SPINTRONICS

David D. Awschalom (Department of Physics, University of California, Santa Barbara, California, 93106, USA)

Control over spins in the solid state forms the basis for nascent spintronics and quantum information technologies.[1] There is a growing interest in the use of electronic and nuclear spins in semiconductor nanostructures as a medium for the manipulation and storage of both classical and quantum information. Spin-based electronics offer remarkable opportunities for exploiting the robustness of quantum spin states by combining standard electronics with spin-dependent effects that arise from the interactions between electrons, nuclei, and magnetic fields. Here we provide an overview of recent developments in coherent electronic spin dynamics in semiconductors and quantum structures, including a discussion of temporally- and spatially-resolved magneto-optical measurements that reveal an interesting interplay between electronic and nuclear spins. In particular, we present electrical schemes for local spin manipulation based on g-tensor modulation resonance (g-TMR), functionally equivalent to electron spin resonance (ESR) but without the use of time-dependent magnetic fields.[2] The technique of g-TMR enables three-dimensional control of electron spins in nanometer-scale geometries using a single voltage signal. These optoelectronic results provide a compelling proof of concept that quantum spin information can be locally manipulated using high-speed electrical circuits.

Furthermore, recent dynamical measurements of hybrid ferromagnet/semiconductor heterostructures under optical illumination reveal that the nuclear spins become highly polarized at low temperatures.[3] We explore the potential for exploiting this behaviour to create complex nuclear domains and arrays in lithographically patterned structures. A time-resolved polarization microscope is used to directly image the nuclear landscape in hybrid nanostructures, and has led to the design of electrically controlled micron-scale nuclear polarization gates in semiconductors.[4]

These experiments investigate the electronic, photonic, and magnetic manipulation of electron and nuclear spins in semiconductor structures and focus on investigating the underlying physics for quantum information processing in the solid state.

REFERENCES

1.*Semiconductor Spintronics and Quantum Computation*, Series on Nanoscience and Technology (Ed. D. D. Awschalom, D. Loss, N. Samarth, Springer-Verlag, Berlin, 2002)
2. Y. Kato et al., Science **299***,* 1201 (2003)
3. R.J. Epstein et al., Phys. Rev. B **65**, 121202 (R) (2002)
4. J. Stephens et al., Phys. Rev. B **68**, 0413XX (R), (2003); R. J. Epstein et al., Phys. Rev. B **67**, 2413XX (R) (2003).

NEUTRON REFLECTIVITY STUDIES OF MAGNETIC MULTILAYERS

C. F. Majkrzak (National Institute of Standards and Technology, USA)

Historically, neutron elastic scattering studies have provided a wealth of important atomic scale information about the magnetic structures of condensed matter, a significant part of which could not have been obtained by any other means. In the beginning, magnetic neutron diffraction research was performed primarily on bulk crystals. In more recent years, advances in thin film deposition techniques have made it possible to synthesize a variety of new types of layered magnetic systems, with properties that can be tailored for studies of fundamental scientific interest as well as technological applications. Throughout this still ongoing development, neutron scattering techniques, especially polarized neutron reflectometry (PNR) and diffraction, have made and continue to make significant contributions to the understanding of the physical behavior of magnetic thin films and superlattices (see, for example, references.[1, 2]

Polarized neutron reflectometry can be divided into two broad categories, one of which corresponds to reflection measurements performed with the wavevector transfer Q normal to the film surface, commonly referred to as specular reflectometry, and the other to scattering done with some component of Q lying in the plane of the film. Analysis of the specular polarized neutron reflectivity, measured as a function of Q, yields the in-plane average of the vector magnetization depth profile along the surface normal, with a spatial resolution of less than a nanometer in certain cases. The nonspecular reflectivity, on the other hand, reveals in-plane magnetic structure, such as that associated with domains or artificially patterned surfaces. In this presentation, we will first briefly review what exactly makes PNR such an extraordinarily sensitive, and in some regards unique, probe of magnetic order in thin films and multilayers. We will also summarize the present state-of-the-art and new developments in experimental and theoretical PNR methods (see for example reference 3).

In the second part of the talk, we will discuss current relevant applications of PNR, including the study of giant magneto-resistance (GMR) film sandwiches and magnetic semiconductor films and superlattices[4], of particular interest to the relatively new field of ”spintronics”.

REFERENCES

1. C. F. Majkrzak, J. Kwo, M. Hong, Y. Yafet, D. Gibbs, C. L. Chien, and J. Bohr, Advances in Physics **40**, 99 (1991)
2. M. R. Fitzsimmons, S. D. Bader, J. A. Borchers, G. P. Felcher, J. K. Furdyna, A. Hoffmann, J. B. Kortright, I. K. Schuller, T. C. Schulthess, S. K. Sinha, M. F. Toney, D. Weller, and S. Wolf, Journal of Magnetism and Magnetic Materials, in the press
3. K.V.O'Donovan, J.A.Borchers, C.F.Majkrzak, O.Hellwig, and E.E.Fullerton, Physical Review Letters **88**, 672011(2002)
4. H. Kepa, G. Springholz, T. M. Giebultowicz, K. I. Goldman, C. F. Majkrzak, P. Kacman, J. Blinkowski, S. Holl, H. Krenn, and G. Bauer, Physical Review B, in the press

SPIN-BASED QUANTUM COMPUTING IN GaAs NANOSTRUCTURES

Daniel Loss (Department of Physics, University of Basel, Switzerland)

Spins of electrons offer the opportunity to store and manipulate phase coherence over length and time scales much larger than for charge, with promising applications in conventional and in quantum information processing [1,2].

The qubit is defined in terms of the spin of an electron [2], being localized in structures such as an atom, molecule, quantum dot etc. The desired manipulation of the spins (qubits), which includes single spin rotations, spin-spin interactions, and spin read-out, can be achieved by purely electric means in terms of gates which are externally controlled by voltage pulses (spin-charge-conversion).

I discuss schemes for using a single quantum dot as a spin filter and spin read-out device, and show how the spin decoherence time can be measured in a transport set-up. I address the issue of spin decoherence due to non-uniform hyperfine interactions with nuclei (being the dominant source of decoherence) and show that for electrons confined to dots the spin decay is non-exponential. If time permits I will also address the issue of entanglement in electron transport for quantum communication in nanostructures.

REFERENCES

1. "Semiconductor Spintronics and Quantum Computation", eds. D. Awschalom, D. Loss, N. Samarth, Springer, Berlin, 2002.
2. D. Loss, D.P. DiVincenzo, Phys. Rev. A 57 (1998) 120; cond-mat/9701055.

THEORY OF SPIN-TRANSPORT IN ONE-DIMENSIONAL QUANTUM-SPIN CHAINS:PROPOSAL FOR A NEW SPIN-BATTERY

Claudius Gros (University of the Saarland, Germany)

Transport of spin-degrees of freedom can be ballistic in low-dimensional quantum spin compounds even at finite temperatures, in contrast to the usual diffusive propagation in quasi-classical system. The ballistic transport of magnetic moments, which is due to additional conservation laws, leads to a non-decaying (in time) component of the magnetization current.

I present an overview of the theory[1, 2] of the unconventional transport of spin and energy in quantum-spin systems and discuss its applications to the quantum-spin compound Sr_2CuO_2 and the spin ladder system $Ca_9La_5Cu_{24}O_{41}$.

In the second part we discuss a novel magneto thermal effect recently proposed.[3] A temperature gradient applied to a quantum spin-chain in external magnetic field (see Fig.1) generates a net spin-current. The configuration thus acts as a spin-battery. We estimate the magnitude of the spin-current for a realistic experimental setup for the one-dimensional Heisenberg compound Sr_2CuO_2 and find a spin-current of 1.6×10^{15} magnetic moments per second for B = 10 T, ΔT = 10 K and a crystal with a cross-section of 1 mm^2. Note that an electric current of 1 A corresponds to 1.6×10^{19} electric charges per second.

REFERENCES

1. J.V. Alvarez and C. Gros, Phys. Rev. Lett. **89**, 156603 (2002)
2. J.V. Alvarez and C. Gros, Phys. Rev. Lett. 8**8**, 077203 (2002)
3. K. Louis and C. Gros, "Diverging magnetothermal response in the one-dimensional Heisenberg chain", Phys.Rev. B (in the press 2003)

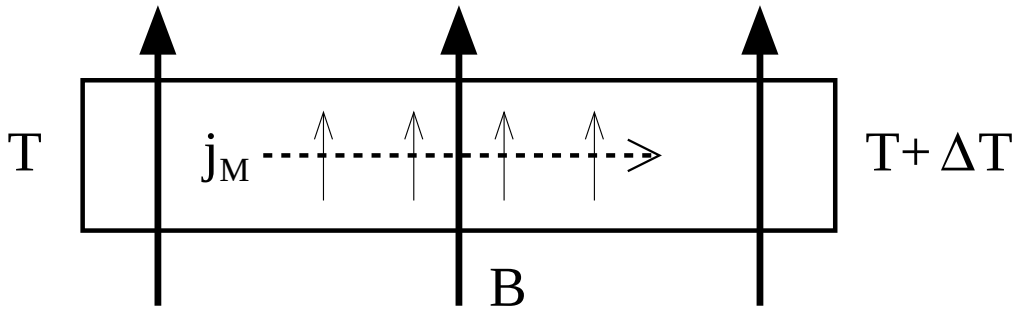

Fig. 1. Illustration of a quasi-one-dimensional magnetic insulator in the presence of an external magnetic field $\boldsymbol{B}$, and a longitudinal temperature differential ΔT. A magnetic current $\boldsymbol{j}_M$, with the moments aligned along $\boldsymbol{B}$ is induced.

SPIN-POLARIZED TUNNELING OF ELECTRONS FROM FERROMAGNETIC (Ga, Mn)As INTO GaAs

S. E. Andresen, B. S. Sørensen (Niels Bohr Institute fAPG, Ørsted Laboratory, University of Copenhagen, Denmark), J. A. C. Bland, C. M. Guertler (Cavendish Laboratory, University of Cambridge, United Kingdom), F. B. Rasmussen (Niels Bohr Institute fAPG, Ørsted Laboratory, University of Copenhagen, Denmark), J. Sadowski (Niels Bohr Institute fAPG, Ørsted Laboratory, University of Copenhagen, Denmark, MAX-lab, Lund University, Sweden, and Institute of Physics, Polish Academy of Sciences, Poland) and P. E. Lindelof (Niels Bohr Institute fAPG, Ørsted Laboratory, University of Copenhagen, Denmark)

For semiconductor spintronics, two of the prerequisites are efficient injection and efficient detection of spin-polarized carriers in a non-magnetic semiconductor. Both of these may be performed by electrical transport or by optical polarization.

We have studied electrical injection of spin-polarized electrons from (Ga, Mn)As in its ferromagnetic state into lightly doped n-type GaAs, similarly to the approach of Ohno *et al.*[1] and of Awschalom *et al.*[2] The injection occurs by tunneling from the valence band of (Ga, Mn)As to the conduction band of *n*-GaAs. Our aim is to study the influence of intense doping at the interface. Therefore, the tunneling barrier has been modified by the introduction of a Si delta-doped GaAs layer (doping level 10^{20} to 10^{21} cm^{-3}).

After tunneling, the injected electrons pass through 200 nm *n*-doped GaAs (also Si, 10^{16} cm^{-3}) and 40 nm of undoped GaAs before reaching a (Ga, In)As quantum well, where they recombine with holes coming from a region of *p*-GaAs (Be-doped, 10^{16} cm^{-3}) on the opposite side of the well. As a consequence of selection rules for the recombination in this case, the circular polarization of the emitted light equals the spin polarization of the electrons. In the *n*-GaAs the electron spin coherence length[3] is 0.1 mm, so practically no polarization is lost between interface and detector. The emitted light is observed from the sample edge in a direction parallel to the magnetic field, which is applied in the plane of the sample. The sample may be described as a light emitting diode (LED) with a magnetic film on the n-side. When bias on the whole structure corresponds to forward bias on the LED, negative carriers are injected from the magnetic layer.

The 240 nm layer of (Ga, Mn)As contained 4.2 % Mn. Magneto-optical Kerr measurements on the ferromagnetic layer revealed a Curie temperature of 68 K and a coercive field about 4 mT at 4.2 K. The hysteresis loop is approximately rectangular in shape; *i. e.* the magnetization is reversed in a rather narrow field interval.

At constant current through the structure, the circular polarization of light from the LED was measured as a function of magnetic field. The results show a hysteresis loop very similar to the Kerr measurements demonstrating that the injected carriers have a polarization that follows the (Ga,Mn)As magnetization. The maximum polarization (corresponding to saturated magnetization) was determined at three different currents and is shown in table 1. For comparison, Ohno *et al.*[1] reached 6.5 % and Awschalom *et al.*[2] obtained 0.82 %.

Current	*Polarization*	*Uncertainty*
4 mA	5.4%	0.3%
8 mA	5.6%	0.4%
12 mA	4.9%	0.1%

Table 1. Maximum circular polarization of light from the spin-LED, measured at various currents through the structure. Temperature was 4.2 K. The polarization seems to fall off at higher currents.

There are two features where our polarization curves differ from the Kerr results:

(a) At fields where the (Ga, Mn)As magnetization is saturated, there is still a weak, apparently linear field dependence of the polarization. This effect would correspond to a Zeemann splitting for a group of electrons with an effective *g*-value of −3.7.

(b) The center of the hysteresis loop is displaced to a position corresponding to about 15 % polarization at zero magnetic field. This offset is roughly independent of current. It is unclear at present whether the offset is due to an asymmetry of the quantum well or to some experimental artefact.

Further details of our work will be published elsewhere.[4]

REFERENCES

1. M. Kohda, Y. Ohno, K. Takamura, F. Matsukura and H. Ohno, Jpn J. Appl. Phys. **40**, L1274 (2001)
2. E. Johnston-Halperin, D. Lofgreen, R. K. Kawakami, D. K. Young, L. Coldren, A. C. Gossard and D. D. Awschalom, Phys. Rev B **65**, 041306 (2002)
3. J. M. Kikkawa and D. D. Awschalom, Nature **397**, 139 (1999)
4. S. E. Andresen, B.S. Sørensen, J.A.C. Bland, C. M. Guertler, F. B. Rasmussen, J. Sadowski, and P. E. Lindelof, J. Appl. Phys. (to appear Oct. 2003)

STRUCTURAL MODULATIONS IN $Sr_{14}Cu_{24}O_{41}$ AND THEIR RELATION TO CHARGE ORDERING

M. von Zimmermann (Hamburger Synchrotronstrahlungslabor at Deutsches Elektronen Synchrotron, Notkestr. 85, 22603 Hamburg, Germany), J. Geck, S. Kiele, R. Klingeler, and B. Büchner (II. Physikalisches Institut / Lehrstuhl A, RWTH Aachen, Huyskensweg, 52056 Aachen, Germany)

Spin chain and ladder materials are an exciting class of compounds since the basic structural unit is similar with high-T_c superconductors. While in the superconductors CuO_2 plaquettes form a 2-dimensional network, in ladders and chains materials they compose 1-dimensional arrays. $Sr_{14}Cu_{24}O_{41}$ is one such material that exhibits both chains and ladders in subsequent layers and it also shows superconductivity under pressure at a certain doping level. The average valence state of Cu in $Sr_{14}Cu_{24}O_{41}$ is 2.25 and the insulating ground state indicates that the holes are localized. Furthermore the existence of a spin gap in the chains has been explained by a lattice dimerization. We have investigated the structural properties of a single crystal of $Sr_{14}Cu_{24}O_{41}$ with high nergy (100 keV) x-ray diffraction, and find a strong incommensurate modulation of both chains and ladders, which persists up to high temperatures. This modulation is simply the result of the different c-axis lattice parameters of the chain and ladder structure, respectively. However, below 200 K the holes lock-in into the incommensurate modulation, as deduced from higher order superlattice reflections. Interestingly, at room temperature the chains form a 1-dimensional lattice, meaning that correlations between adjacent chains are almost absent. In contrast, at 10 K a 3-dimensional chain lattice is found. The temperature dependence of the chain lattice correlations indicates that thermal fluctuations give rise to the dimensional crossover.

THE MAGNETIC STATE OF $ErNi_2B_2C$ IN AN IN-PLANE FIELD

K. Nørgaard Toft, A. B. Abrahamsen, N. H. Andersen, D. F. McMorrow (Materials Research Department, Risø National Laboratory, Denmark), A. Jensen, J. Jensen, P. Hedegård (Niels Bohr Institute fAPG, Ørsted Laboratory, University of Copenhagen, Denmark), J. Klenke, K. Prokes, P. Smeibidl, S. Danilkin, V. Sikolenko (Hahn-Meitner-Institute, Germany), M. R. Eskildsen (Université de Genève, Switzerland) and P. C. Canfield (Ames Laboratories, USA)

We present a neutron-diffraction study of the magnetic structures of superconducting $ErNi_2B_2C$ in the presence of a magnetic field. At zero field, the magnetic structure is transversely polarized with $\boldsymbol{Q} = 0.55\boldsymbol{a}^*$ and the moments along the $\boldsymbol{b}$ direction. Transitions of $\boldsymbol{Q}$ between different commensurable values are observed when varying the field. The commensurable structures are analyzed in terms of a detailed mean-field model. Experimentally, the minority domain shows no hysteresis and stays stable up to a field close to the upper critical field of superconductivity, (H || [010]). Close to the upper critical field of superconductivity (H || [110]), we observe that $\boldsymbol{Q}$ rotates a small angle of about 0.5° away from the [100] direction.

In $ErNi_2B_2C$, the erbium ions are placed in a body-centered tetragonal lattice, with $a = b = 3.502$ Å^{-1} and $c = 10.558$ Å^{-1}. The Néel temperature is $T_N \approx 6$ K and the superconducting transition occurs at $T_c = 11$ K.[1] In this study, the magnetic structures of $ErNi_2B_2C$ are examined in general in the presence of a magnetic field, and specifically close to H_{c2}, in order to improve the understanding of the interdependence of superconductivity and magnetism.

A single crystal of approximate size $2\times3\times0.5$ mm^3 was prepared as described in Ref. 2. The neutron diffraction experiments were performed at BENSC using the E1 triple axes spectrometer and a 4 T horizontal cryomagnet for fields along [1 0 0] and [1 1 0]. The mean-field model includes crystal field parameters, RKKY-exchange, the classical dipole-dipole interaction, and a quadrupole coupling.[3] The crystal-field and quadrupole parameters have been established from neutron scattering and x-ray experiments. The exchange coupling has been derived from a fitting of the bulk magnetization[2,4] and neutron diffraction data[5].

At zero field, the magnetic domains with $\boldsymbol{Q} = \boldsymbol{Q}_A$ or $\boldsymbol{Q}_B$ are equally populated, but the application of the magnetic field along [010] suppresses the domain with the magnetic moments perpendicular to the magnetic field, i.e., the $\boldsymbol{Q}_B$ domain. The intensity of the minority domain is completely suppressed at 13 kOe, as shown in the lower left part of fig. 1. Surprisingly the minority domain shows no hysteresis. The minority domain was expected to be metastable in a field, and after being eliminated at some field, to be energetically unfavorable when decreasing the field. The critical field for the minority domain is close to the upper critical field of superconductivity, indicating that the existence of fluxlines might stabilise the minority domain. The ordering vector of the magnetic phase is $\boldsymbol{Q} = 11/20\boldsymbol{a}^*$ in zero field, and when applying a magnetic field $\boldsymbol{Q}$ increases in jumps to different commensurable structures. The period of the magnetic structure (for H || [010]) is presented in Fig. 1 and the dashed lines indicate the possible

commensurable values of $\boldsymbol{Q}$. For both field directions, the period changes as follows: $\boldsymbol{Q}$ = 0.55 to $\boldsymbol{Q}$ = 0.57 to $\boldsymbol{Q}$ = 0.58 or 0.59 and back to $\boldsymbol{Q}$ = 0.57. An overview of the states is presented in figure 2, where the black dots mark the measured data points. For both field directions two-phase regions exist in the transition from one structure to another, however due to different resolutions, this can be resolved only in the [110] case, indicated by striped areas. A peculiarity is a small, but clearly detectable rotation of the ordering vector, which occurs close to and above the superconducting critical field for H || [110]. This feature and the high field stability combined with a lack of hysteresis of the minority domain for H || [010], indicate possible connections to superconductivity, which cannot be confirmed in this study.

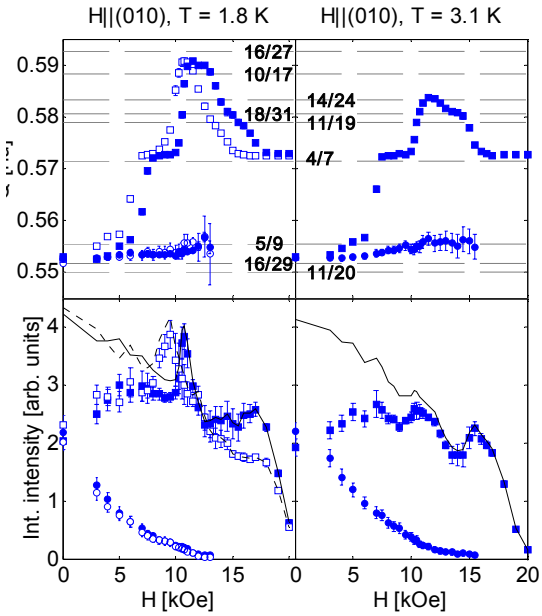

Fig. 1. Positions and integrated intensities of the majority domain measured at (200) – $\boldsymbol{Q}_A$ (squares) and of the minority domain (020) – $\boldsymbol{Q}_B$ (circles). The solid symbols represent the data obtained when increasing the field, and the open ones show the decreasing-field data. In the lower part of the figure, the sums of the magnetic intensities of the two domains are indicated by lines (solid: increasing field; dashed: decreasing field).

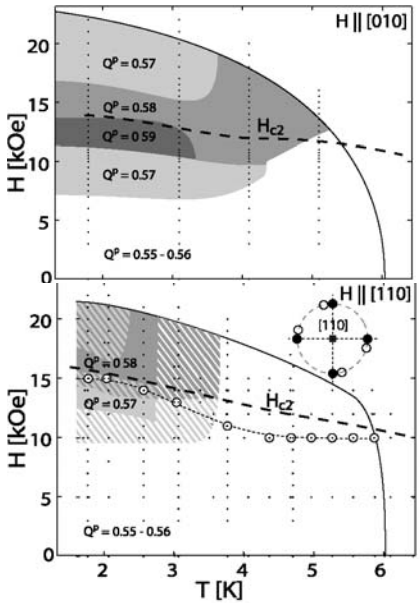

Fig. 2. Magnetic phase diagrams for fields applied along [010] and [110]. White and gray areas indicate single-phase regions, whereas striped areas represent two-phase regions. Bottom: A small orthogonal component $\delta\boldsymbol{Q} \approx -0.005\boldsymbol{b}^*$ appears above the dashed line with open circles. The insert shows the rotation of the magnetic reflections.

The Danish Technical research Council via the Framework Program on Superconductivity and the Danish Natural Science Research Program via DANSCATT support this work. The EU Commision under contract HPRI-CT-2001-00138 supports the neutron diffraction experiments at BENSC. P.C.C acknowledges support from the U.S.D.O.E., W-7405-Eng.-82.

REFERENCES

1. J. W. Lynn *et al.* Phys. Rev. B **55**, 6584 (1997)
2. B. K. Cho *et al.*, Phys. Rev. B **52**, 3684 (1995)
3. J. Jensen, Phys. Rev. B **65**, 140514 (2002)
4. P. C. Canfield *et al.*, Physica C **262B**, 249 (1996)
5. S.-M. Choi *et al.*, Phys. Rev. Lett. **87**, 107001 (2001)

SUPERCONDUCTIVITY, STATUS AND PERSPECTIVES

H. R. Ott (Laboratorium für Festkörperphysik, ETH Zürich, Switzerland)

The research area of superconductivity was, for many years, dominated by the phenomenon of high-T_c superconductivity. The discovery of Bednorz and Müller in 1986 inspired a wide range of activities, including materials science, experiments probing the physical properties of the relevant materials, the copper oxides, in their normal and superconducting state, and a wealth of different theoretical approaches, aiming at explaining this electronic instability at unprecedented high temperatures. Indirectly, it also lead to a lot of work in magnetism and it revived the interest in oxide materials in general. Additional impact was felt in research on low dimensional systems and the general problem of describing the ground state of metals.

Somewhat less prominent but, nevertheless, of equal scientific interest were the developments concerning the occurrence of superconductivity in heavy electron metals and in organic conductors. In metals with heavy mass electrons, the main difficulties are posed by dominating many body effects in the electronic subsystem in the normal state and unconventional characteristics of the superconducting phase. In this context, the appearance of quantum critical points was and is discussed in great detail. The organic conductors exhibit clear features of low dimensionality and also here, the description of the electronic subsystem is highly non trivial.

Quite recently it was shown that also rather simple metallic compounds exhibit superconductivity at, conventionally viewed, anomalously high temperatures. The example is the binary compound MgB_2 and it may well be that it represents a case where lucky coincidences lead to a critical temperature of the order of 40 K.

In view of this wide range of different kinds of aspects that may be considered, it is clear that only a selection of topics can be handled reasonably in a limited amount of time. Hence the main emphasis will be addressed to aspects of unconventional phenomena in both the normal and the superconducting state of these different materials, mainly in cuprates and heavy-electron metals. It will be shown, in what respects these materials are different from common metals and why, most likely, new concepts in the description of their ground states need to be considered. Although quite different in many aspects, these materials also share some similarities in their features and therefore, comparisons will be made where appropriate.

Since many details of these unconventional superconductors are not yet understood in detail, it is clear what kind of tasks lay ahead in future research on superconductivity. Although it is usually an unexpected discovery of a new superconductor that captures the interest of researchers but naturally cannot be predicted, it is clear that still a lot of difficult problems, which are related to, the known superconductors, have not yet been solved.

CHEMICAL AND STRUCTURAL CHARACTERIZATION OF THE COBALT OXYHYDRATE SUPERCONDUCTOR $Na_{0.3}CoO_2 \cdot 1.3H_2O$

R. J. Cava (Department of Chemistry and Princeton Materials Institute, Princeton University, Princeton, New Jersey, USA)

Since the discovery of superconductivity in layered copper oxides in 1986[1], solid state chemists have been searching for other families of superconductors that might help shed light on the superconducting mechanism of the cuprates. Structurally layered oxide superconductors such as Sr_2RuO_4[2] have been reported in the interim, but they are clearly fundamentally different from the cuprates both chemically and physically. The recent discovery of superconductivity near 4 K in a layered sodium cobalt oxyhydrate, $Na_{0.35}CoO_2 \cdot 1.3H_2O$, is a hopeful sign that superconductors related to the cuprates may be found.[3] The crystal structure of the superconducting phase is hexagonal, based on close packed layers of edge-sharing CoO_2 octahedra perpendicular to the *c* axis, separated by intercalant layers consisting of Na and H_2O. The layered, triangular lattice of Co ions is of particular interest to theorists due to the geometrical magnetic frustration displayed by triangular systems and the importance of the triangular lattice to the original exposition of the RVB theory.[4] Unexpected spin-charge dynamics, seen in the unusually high Seebeck coefficient and transport properties of a related compound, $Na_{0.7}CoO_2$[5, 6], suggest that interactions between magnetism and charge transport are indeed important in this chemical system.

In this talk, I will describe our work in this system. We have found, for example, that the oxyhydrate superconductor is one of a series of hydrated phases of $Na_{0.3}CoO_2$. Furthermore, through careful analysis of thermogravimetric data we have shown that the superconducting phase is chemically unstable at body temperature, implying that it cannot be touched during handling without subsequent treatment[7]. It also changes its water content in response to changes in humidity at ambient temperature, implying that it must be handled only under special humidifying conditions. This degree of chemical instability is unprecedented for superconductors, indicating that if high quality physical property measurements are to be performed on this important superconductor, extreme attention to ambient conditions will be required.

By varying the amount of Na in the superconducting phase through variation in the method of deintercalation of sodium from the non-superconducting end-member $Na_{0.7}CoO_2$, we have been able to investigate the change of superconducting temperature with electronic band filling. The results of this study will be described. We have found that both the superconducting transition temperature and the DC magnetization in the superconducting state vary strongly with Na content, and indicate that the optimal superconducting composition is $Na_{0.3}CoO_2 \cdot 1.3H_2O$. In spite of the ambient temperature synthesis employed, which might be expected to give rise to inhomognetities in composition, the optimal superconducting region is very narrow in electron count.

I will also describe our neutron-diffraction studies of the crystal structures of both superconducting and non-superconducting phases in this system.

Several factors are critical for understanding the superconductivity of $Na_xCoO_2 \cdot 1.3H_2O$. Observations that the lower hydrates with closer CoO_2-CoO_2 interplanar distances are not superconducting above 2 K indicate that the two dimensional character of the structure is important. The maximum in T_c as a function of the Na content establishes the optimal chemical doping level for superconductivity. An analogy between the layered copper oxide and layered cobalt oxide superconductors is seen in the decreased T_c for both underdoped and overdoped materials. The optimal doping level for superconductivity is clearly higher with respect to the Mott-Hubbard-like half filled two-electron band in $Na_xCoO_2 \cdot 1.3H_2O$ (+0.3 electrons) than in the copper oxides (+0.15 electrons or holes). This fact appears to be disturbing to some theorists. It may be indicative of a fundamental difference between the two types of superconductors. On the other hand it may reflect the influence of as yet unknown structure – electronic state correlations in the cobalt oxides.

This work was done through extensive collaborations with M. L. Foo, R. E. Schaak, T. Klimczuk, H. W. Zandbergen, Yayu Wang and N. P. Ong at Princeton University, Q. Huang and J. W. Lynn at The Center for Neutron Research, NIST, Gaithersburg MD, USA, and B. G. Ueland and P. Schiffer, Department of Physics, Pennsylvania State University, State College, Pennsylvania, USA. It was supported by the US National Science Foundation and the Department of Energy, Basic Energy Sciences.

REFERENCES

1. J. G. Bednorz, and K. A. Müller, Z. Phys. B **64**, 189-193 (1986)
2. Y. Maeno, H. Hashimoto, K. Yoshida, S. Nishizaki, T. Fujita, J. G. Bednorz, and F. Lichtenberg, Nature **372** 532-534 (1994)
3. K. Takada, H. Sakurai, H. Takayama-Muromachi, F. Izumi, R. A. Dilanian, and T. Sasaki, Nature **422**, 53 – 55 (2003)
4. P. W. Anderson, Mat. Res. Bull. **8** 153-160 (1973)
5. I. Terasaki, Y. Sasago, and K. Uchinokura, Phys. Rev. B **56**, R12685 (1997).
6. Yayu Wang, N. S. Rogado, R. J. Cava, and N. P. Ong, Nature **423** 425 (2003)
7. M. L. Foo, R.E. Schaak, V. L. Miller, T. Klimczuk, N. S. Rogado, Yayu Wang, G. C. Lau, C. Craley, H. W. Zandbergen, N. P. Ong, and R. J. Cava, Sol. St. Comm., in the press.

BORIDE SUPERCONDUCTORS: FROM $LuNi_2B_2C$ TO MgB_2

Paul C. Canfield (*Iowa State University, USA*)

In this presentation I will review some of the features that make $LuNi_2B_2C$ (as well as other members of the RNi_2B_2C series) and MgB_2 specifically clear examples of how differently superconductivity can manifest itself in intermetallic systems. Results of thermodynamic and transport measurements on pure and doped versions of these compounds will be presented and discussed. Broadly speaking $LuNi_2B_2C$ presents an example of how many experimentalists tended to think about the search for higher T_c values in intermetallics compounds. MgB_2 on the other hand, with a T_c value of nearly 40 K, presents an extreme example of intermetallic superconductivity: two gap superconductivity coming from two distinct bands with very different electron phonon coupling.

INFLUENCE OF MAGNETISM ON FLUX LINE LATTICE IN $TmNi_2B_2C$ SUPERCONDUCTOR

A. B. Abrahamsen (Materials Research Deparment, Risø National Laboratory, Denmark), M. R. Eskildsen (University of Notre Dame, USA), N. H. Andersen (Risø National Laboratory, Denmark), P. C. Canfield (Ames Laboratory, USA)

We have examined the phase boundary of the square flux line lattice in $TmNi_2B_2C$ using small angle neutron scattering and the transition into a rhombic lattice for $H > 2$ kOe is found to scale with the upper critical field $H_{c2}(T)$ of the superconductor. The influence of the magnetic Tm-ions on the flux line lattice symmetry in the paramagnetic state seems only indirect through the shape of the upper critical field.

A co-existence of superconductivity and magnetic ordering of the rare earth moment in the form of a spin-density wave (SDW) is observed in the borocarbide series RNi_2B_2C, when the rare earth is R = Tm, Er, Ho or Dy. The presence of the rare earth moments polarises the conduction electrons, which mediates the indirect RKKY interaction between different moments. However, the superconducting state is also formed by the conduction electrons and a strong interplay between magnetism and superconductivity is seen. In the case of R = Tm a quite complicated phase-diagram of the flux line lattice symmetries is found when the applied field is oriented along the c-axis of the tetragonal crystalline unit cell[1], as shown on Fig 1. The critical temperature is T_c = 11 K and the maximum upper critical field H_{c2} = 10 kOe is found at T = 5 K. At lower temperatures H_{C2} shows a minimum as the magnetic ordering of the q_{mI} and q_{mII} SDW is setting in at T_N = 1.5 K. In the paramagnetic phase $T_N < T < T_c$ a smooth transition from a rhombic to a square flux line lattice is seen as the applied field in increased from the lower critical field H_{c1}. This transition is driven by non-local electrodynamics, which favours a four-fold symmetric current and field pattern, depending on the underlying Fermi surface symmetry, when the field profile of the flux lines is highly overlapping[2]. Insert D and A illustrates the change from an almost hexagonal to a square flux line lattice, which is common for even the non-magnetic borocarbides R = Y and Lu.[3] A transition back into a rhombic symmetry is observed as the applied field is increased towards the upper critical field H_{c2}. Small angle neutron scattering (SANS) has been used to measure the azimuthal width of the diffraction spots from the square flux line lattice. The transition field H_{c2} between the A and B phase was determined as the field, where the width increased above the resolution of the SANS camera and insert B shows two rhombic lattices clearly resolved.

It has been argued that the square flux line lattice would not exist close to H_{c2}, because the separation between the flux lines is larger for the rhombic than the square lattice, whereby the loss of condensation energy is smaller when the superconducting order parameter is suppressed in between the flux lines as the vortex cores start to overlap.[3] Thus the AB phase transition is expected to coincide with the crossover from intermediate to high flux line density, which is often defined by the field where the

flux line separation a is a factor $C_{IH} \approx 4$ larger than the superconducting coherence length ξ.[4] Flux quantization for the square flux line lattice gives a relation between magnetic flux density B and the separation between the flux lines

$$\Phi_0 = B\,a^2$$

The coherence length ξ is connected to the upper critical field B_{C2} by inserting $a = \sqrt{2\pi}\xi$, whereby it is seen that the AB phase transition scales with the upper critical field by

$$\frac{B_{AB}}{B_{C2}} = \frac{2\pi}{C_{IH}^2}$$

From the AB phase boundary of figure 1 one gets an estimate of C_{IH} = 3.96-3.45, which is in qualitative agreement with the definition of the crossover from intermediate to high flux line density.

It is suggested that the square flux line lattice exist between a lower phase boundary (AD) determined by non-local electrodynamics and an upper boundary (AB), where the vortex cores start to overlap. Thus the influence of the magnetic Tm-ions on the flux line lattice symmetry seems only to be indirect through the shape of the upper critical field $H_{c2}(T)$ curve in the paramagnetic phase.

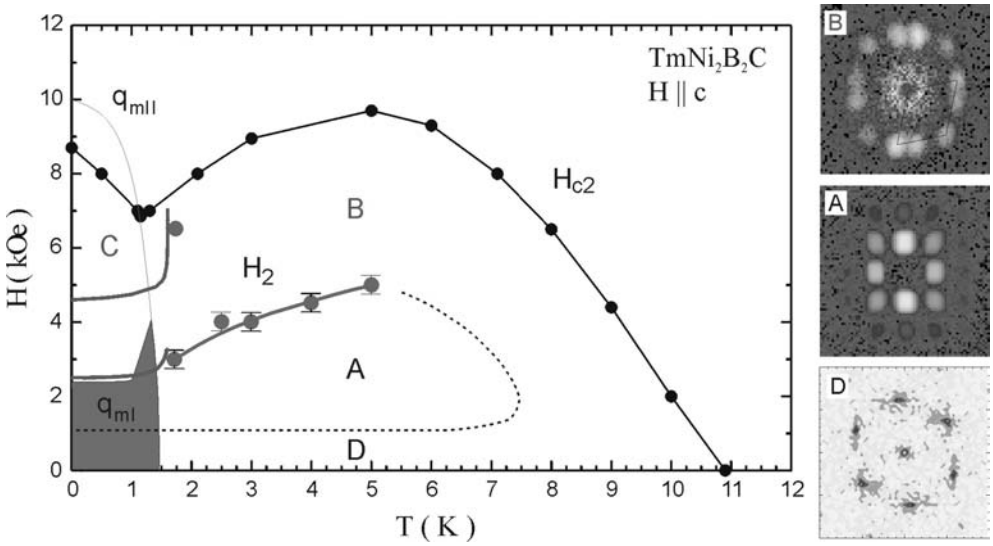

Fig. 1. Phase diagram of $TmNi_2B_2C$ showing square (A) and different rhombic flux line lattices (B, C, D). It is suggested that the AB phase boundary has a positive slope, because it scales with the upper critical field H_{c2}. Insert D: Magnetic decoration showing rhombic lattice at H = 20 Oe and T = 4.2 K, A: Square lattice at H = 2.0 kOe and T = 2.3 K, B: Rhombic lattice at H = 6.5 kOe and T = 1.7 K.

REFERENCES

1. M.R. Eskildsen *et.al.*, NATURE **393**, 242 (1998)
2. V.G. Kogan *et.al*, Phys. Rev. B. **55**, R8693 (1997)
3. M.R Eskildsen *et.al*, Phys. Rev. Lett. **86**, 5148 (2001)
4. E.H. Brandt, Rep. Prog. Phys. **58**, 1465(1995)

A NOVEL SUPERCONDUCTING STATE IN THE SUPERCONDUCTING FERROMAGNETIC RUTHENO-CUPRATES

C. W. Chu (Department of Physics and Texas Center for superconductivity, University of Houston, Houston, Texas, Lawrence Berkeley Laboratory, Berkeley, CA, and Hong Kong University of Science and Technology, Hong Kong), Y. Y. Xue, A. Baikalov, J. Cmaidalka, and R. L. Meng, (Department of Physics and Texas Center for superconductivity, University of Houston, Houston, Texas)

One salient feature of a superconductor is the expulsion of magnetic flux below its transition temperature T_c. A Type II superconductor will be in the Meissner state (MS) with an equilibrium diamagnetic moment $Ms = -H/4\pi$ when H is smaller than its lower critical field (H_{c1}). A distinct $dMs/dH > 0$, on the other hand, is expected either under higher H or in the spontaneous vortex state (SVS), which is predicated when superconductivity and ferromagnetism coexist. Here we report the observation of a novel superconducting state in the polycrystalline superconducting ferromagnetic rutheno-cuprates below T_c, where:

(1) The spontaneous vortices occur;

(2) dMs/dH is negative and H-independent up to an apparent H_{c1}, a reminiscence of the MS;

(3) This H_{c1} does not depend on temperature but varies with the particle size of the single-grain powders.

These are in strong contrast to what is typically expected of either MS or SVS. We attribute these to the combination of the anisotropic superconductivity, the fine granularity of the compounds and the unusually long penetration depth, which makes the polycrystalline rutheno-cuprates a naturally occurred mesoscopic superconducting system.

FOURIER TRANSFORM SCANNING TUNNELLING SPECTROSCOPY (FT-STS): A NEW PERSPECTIVE ON THE ELECTRONIC STRUCTURE OF CUPRATES

J.C. Séamus Davis (Department of Physics, LASSP, Cornell University, Ithaca, NY 14850, USA), K. McElroy (Department of Physics, LASSP, Cornell University, Ithaca, NY 14850, USA and Department of Physics, University of California, Berkeley, CA 94720, USA), J.E. Hoffman, D.-H. Lee (Department of Physics, University of California, Berkeley, CA 94720, USA), H. Eisaki (AIST, 1-1-1 Central 2, Umezono, Tsukuba, Ibaraki, 305-8568 Japan) and S. Uchida (Department of Physics, University of Tokyo, Yayoi, 2-11-16 Bunkyoku, Tokyo 113-8656, Japan)

Angle-resolved photoemission (ARPES) studies have been remarkably successful in mapping the momentum-space characteristics of the electronic excited states in the high-T_c superconducting cuprates. However, since high-T_c superconductivity develops from atomically localized electrons and exhibits nanoscale disorder, a pure momentum-space description of electronic structure may not be sufficient. Instead, simultaneous information on electronic structure in both the real-space and momentum-space may be required. I will describe atomic-resolution scanning tunneling spectroscopy studies which achieve these apparently contradictory aims.

We apply the Fourier transform scanning tunnelling spectroscopy (FT-STS) technique. The tip-sample differential tunnelling conductance ($g=dI/dV$) is spatially mapped at each bias voltage V. The result, $g(\vec{r},\omega)$, is proportional to $LDOS(\vec{r},\omega)$, the local density of states at location $\vec{r}$ and energy $\omega = eV$. The $\vec{q}$-vectors of any spatial modulations in $g(\vec{r},\omega)$ are then determined from the locations of peaks in $g(\vec{q},\omega)$, the Fourier transform magnitude of $g(\vec{r},\omega)$.

Using these FT-STS techniques, we have begun to explore the relationship between the real-space and momentum-space characteristics of the electronic structure in the cuprate $Bi_2Sr_2CaCu_2O_{8+\delta}$ (Bi-2212). Weak incommensurate LDOS-modulations which disperse with energy are ubiquitous in this system. A typical series of $g(\vec{q},\omega)$ measured on an optimally doped Bi-2212 sample at 4.2K is shown in Fig. 1.

It has been proposed that these LDOS-modulation patterns are produced by scattering-induced quasiparticle interference[1] and that their evolution with energy is due to the momentum-space electronic structure of the system. And, indeed, analysis of our data within the context of such models yields the Fermi surface and the d-wave superconducting energy gap $|\Delta(\vec{k})|$ in reasonable agreement with ARPES[2]. Our earlier observation of intense spatial variations in the superconducting electronic structure at the nanoscale[3] was viewed in the context of granular superconductivity. However, by applying FT-STS, we can now better understand these observations as a very unusual type of electronic disorder located in a specific part of momentum space near k=(π,0). Finally, FT-STS studies of local electronic states at individual impurity atoms[4] are also beginning to reveal new insights.

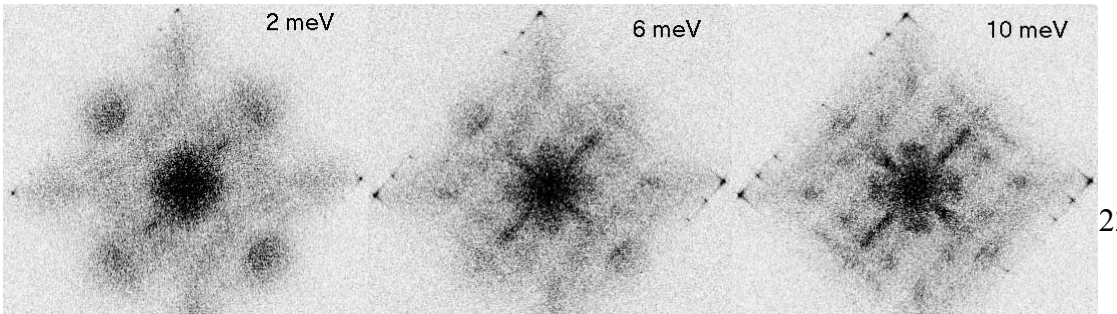

Fig. 1: These $g(\vec{q},\omega)$ are the Fourier transforms of *LDOS* images taken at 4.2K in the same 65nm square FOV at six different energies. Within the reciprocal unit cell, one can identify up to 16 different wavevectors as the dark spots in any given $g(\vec{q},\omega)$ image. It is obvious that these spots move to different locations with changing energy.

[1] Byers J. M., Flatté M. E., Scalapino D. J., *Phys. Rev. Lett.* 71, 3363 (1993); Wang Q. and Lee D.-H., PHYS REV B 67 020511 2003; Zhang D. & Ting C.S., cond-mat/0209318; T. Pereg-Barnea, M. Franz, cond-mat/0306712; L. Capriotti, D.J. Scalapino, R.D. Sedgewick, cond-mat/0302563.

[2] Hoffman *et al*, *Science 297* 1148 (2002); McElroy *et al*, *Nature* 422 592 (2003).

[3] ***Pan* et al, Nature 413 *282 (2001); Lang* et al Nature 415*, 412 (2002).***

[4] Hudson *et al, Science 285*, 88 (1999); Pan *et al*, *Nature 403*, 746 (2000); Hudson *et al Nature 411* 920 (2001).

DIRECT OBSERVATIONS OF TRIANGULAR TO SQUARE FLUX LATTICE TRANSITIONS IN HIGH T_c SUPERCONDUCTORS AND THEIR RELATIONSHIP TO *d*-WAVE EFFECTS

E. M. Forgan, S. P. Brown, D. Charalambous, E. C. Jones (School of Physics and Astronomy, University of Birmingham, Birmingham B15 2TT, UK), A. Erb (Walther Meissner Institut, D-85748 Garching, Germany) and J. Kohlbrecher (SINQ, Paul Scherrer Institut, CH-5232 Villigen, Switzerland)

We have used the technique of small-angle neutron scattering to observe magnetic flux lines in a low twin-density $YBa_2Cu_3O_7$ single crystal up to high fields, as a function of temperature and field direction. We find that with the field perpendicular to the CuO_2 planes, the flux lattice structure at low temperatures changes smoothly from a distorted triangular co-ordination to nearly perfectly square as the magnetic induction approaches 10 T. The orientation of the square flux lattice and the variation of the transition with temperature is as expected from recent *d*-wave theories.[1] However, the orientation is 45° from that recently observed[2] in $La_{1.83}Sr_{0.17}CuO_{4+\delta}$.

REFERENCES

1. J. Shiraishi el al., Phys. Rev. B **59**, 4497 (1999)
2. R. Gilardi et al., Phys. Rev. Lett. **88**, 217003 (2002)

VORTEX MATTER IN NANOSTRUCTURED SUPERCONDUCTORS

Victor V. Moshchalkov (Laboratory for Solid State Physics and Magnetism, K. U. Leuven, Celestijnenlaan 200 D, B-3001 Leuven, Belgium)*

Flux confinement phenomena have been studied in individual superconducting nanoplaquettes, their clusters and huge arrays (films with nano-engineered periodic pinning arrays (PPA)). In individual nano-plaquettes of the different form (loops, discs, triangles and squares) the superconducting critical temperature Tc(H) was measured resistively and also calculated from the linearized Ginzburg-Landau equations. Novel symmetry consistent vortex patterns have been identified for triangles and squares. To keep the imposed symmetry, vortex-antivortex pairs can be spontaneously formed, for example, in an equilateral triangle with two flux quanta applied, antivortex is formed in the centre and the three vortices sit in the three corners, thus complying with the symmetry (see also Nature **408**, 833 (2000); PRL **86**, 1323 (2001)). Stability of the vortex-antivortex molecules in type-I equilateral mesoscopic triangles has been demonstrated (PRL **90**, 147003 (2003). In films with the PPA (lattices of antidots or magnetic dots) pronounced peaks at integer and rational fields have been revealed in dc- and ac-magnetisation and transport measurements. The peaks are attributed to certain stable vortex configurations. These configurations can be directly visualised by using different vortex imaging techniques: magnetic decoration, Lorentz and scanning Hall probe microscopy (PRL **90**, 237001 (2003)). The combination of the local probe techniques with the bulk probes has made it possible to identify correctly all relevant vortex patterns (multi quanta and composite vortex lattices, interpenetrating sublattices of strongly and weakly pinned vortices, etc) responsible for the strong enhancement of the critical current. In Pb films with a periodic array of magnetic dots with perpendicular magnetic anisotropy *field-induced superconductivity* has been observed. This effect can be seen in any superconducting film combined with a nano-engineered dipole field compensator (PRL **90,** 197006 (2003)).

This work was supported by the Belgian IUAP, the Flemish GOA and FWO Programmes and the ESF “VORTEX” Programme.

* In collaboration with: G. Teniers, M. Lange, M. Morelle, S. Raedts, D. Golubovic, J. Bekaert, A. Silhanek, W. Pogosov, M. Van Bael, B. Y. Zhu, L. F. Chibotaru, A. Ceulemans, S. Bending.

INTERPLAY BETWEEN VORTEX AND Cu-SPIN DYNAMICS IN LSCO

Joël Mesot (Laboratory for Neutron Scattering, Paul Scherrer Institute and ETHZ, 5232 Villigen, Switzerland)

As illustrated by their complex phase diagrams, the transition metal oxides possess remarkable electronic properties. It is not rare to observe a metal-insulator phase transition accompanied by orbital, magnetic and/or charge instabilities. In order to better identify the relevant interactions controlling their macroscopic properties, it is crucial to obtain precise energy- and momentum-resolved information about the fundamental excitations in these materials. Neutron scattering and photoemission spectroscopy provide powerful and complementary tools to investigate the subtle interplay that may exist between the spin and electronic degrees of freedom in the transition metal oxides.

The following neutron results obtained on the high-temperature superconductor $La_{2-x}Sr_xCuO_{4+\delta}$ (LSCO) as a function of doping, temperature and magnetic field will be presented:

Vortex lattice

Using small angles neutron scattering we have succeeded, for the first time, to measure a well-ordered vortex lattice structure at all doping regimes of LSCO. While in the underdoped regime, a hexagonal lattice could be observed only at very low fields, in the optimally to overdoped regime a field-induced transition from hexagonal to square coordination (see Fig. 1) occurs at around 0.4 T.[1] A similar phase transition has been recently observed in optimally doped YBCO[2] but at much higher fields (≈ 9 Tesla) and with an orientation of the square lattice rotated by 45° when compared to the LSCO case. In order to explain the observed vortex structures, possible scenarios[3] that include the anisotropies of the electronic and superconducting gap structures will be discussed.

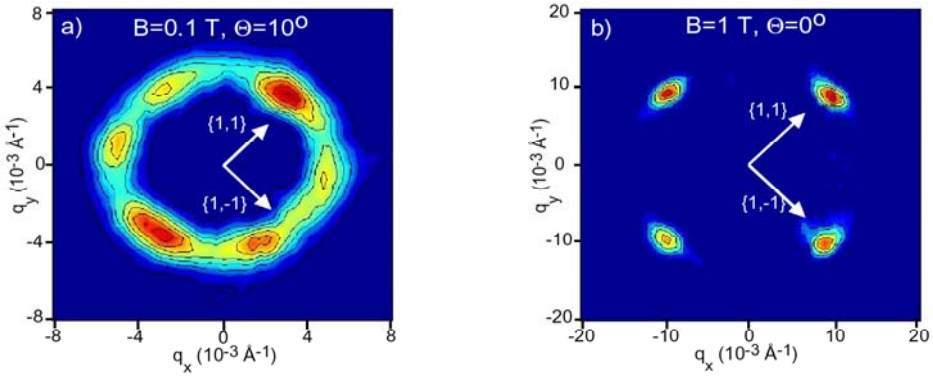

Fig. 1. Small angle neutron scattering patterns taken on LSCO (x = 0.17) at B = 0.1 T (left) and 1 T (right), T = 1.5 K.

Cu-spin dynamics in the Abrikosov state

Our inelastic neutron scattering studies of the spin dynamics in the mixed phase of LSCO show that, in the slightly overdoped phase, the application of a magnetic field of 5 T ($\approx$ 1/10 H_{c2}) induces a spectral weight redistribution centred at the spin gap energy.[4] This result obtained in the Abrikosov state, together with those reported by Lake *et al*. in the underdoped[5] and optimally[6] doped regimes, possibly reveal the existence of an additional doping-dependent energy scale.

Moreover, in the slightly overdoped regime of LSCO, we do observe that the opening of the spin gap seems to track the irreversibility/melting line, rather than T_c, thus underlining an unusual interplay between the vortex- and spin- dynamics in LSCO.[4] The suppression of the spin gap in the vortex fluid phase can be understood qualitatively by considering the dynamical nature of the vortices.[6] This interpretation is supported by earlier measurements of the Hall conductivity, which suggest that an additional degree of freedom (e.g. Cu-spin) couples to the vortices above the melting line.[7]

REFERENCES

1. R. Gilardi *et al.*, Phys. Rev. Lett. **88**, 217003 (2002)
2. T. Forgan *et al.*, to be published.
3. N. Nakai *et al.*, Phys. Rev. Lett. **89**, 237004 (2002)
4. R. Gilardi *et al.*, submitted
5. B. Lake *et al.*, Nature **415**, 299 (2002)
6. B. Lake *et al.*, Science **291**, 1759 (2001)
7. G. D'Anna *et al.*, Phys. Rev. Lett. **81**, 2530 (1998)

NEW ROOM TEMPERATURE FULLERENE BASED ORGANIC FERROMAGNETS

K.V. Rao (Department of Materials Science-Tmfy-MSE, Royal Institute of Technology, SE-10044 Stockholm, Sweden)*

We report the discovery of ferromagnetism with a Curie temperature well above room temperature, in a non-metallic compound consisting of C_{60} and the paramagnetic organic molecules 2,2 diphenyl 1-picryl hydrazyl (DPPH) as well as 2,2,6,6 tetramethyl-4 oxy-piperidinooxy (TMOP). Samples containing approximately 90 weight percent of the magnetic phase, determined by superconducting quantum interference device (SQUID) magnetometry measurements, have been obtained by mixing nominal 1:1 molar ratios of C_{60} and DPPH (or TMOP) dissolved in benzene at ambient conditions. The absence of magnetic metallic elements down to the parts per billion range is shown by inductively coupled plasma mass spectrometry (ICP-MS). Synchrotron x-ray diffraction measurements on agglomerated particles attracted to a magnet at room temperature, showed no evidence of crystallinity. Ferromagnetic resonance (FMR) and SQUID magnetometry results show clear indications of soft ferromagnetism extending to much above room temperature in both the above materials. The temperature dependence of the saturation magnetization of the ferromagnetic phase follows the expected $T^{3/2}$ law for low-lying spin wave excitations. The obtained values for the spin wave stiffness constant are found to be close to what is usually observed in amorphous materials, which is one order of magnitude larger than is known for crystalline ferromagnets.

Similar results are also obtained when pristine C-60 is exposed to ultra-violet light for extended time. The ability to obtain photolysed C-60 based room temperature ferromagnets opens a new approach to fullerene electronics. A simple mechanism in terms of local spins arising from the local C-O bonds appears to stabilize the long-range ferromagnetic order in these novel non-metallic materials.

The ability to produce patterned ferromagnetic films of C-60 based ferromagnets on various substrates using ink-jet technology will also be presented.

(*) with Lioubov Belova, Wolfgang Voit, Frank J. Owens (*Army Armament Research, Development, and Engineering Centre, Picatinny, NJ*) and Zafar Iqbal (*Dept. of chemistry and chemical Engineering, NJTI, NJ, USA)*

FERROMAGNETIC III-V SEMICONDUCTOR MATERIALS AND DEVICES

Hideo Ohno (Laboratory for Electronic Intelligent Systems, Research Institute of Electrical Communication, Tohoku University, 2-1-1 Katahira, Aoba-ku, Sendai 980-8577, Japan)

Ferromagnetism in transition metal doped III-V compounds has its origin in hole mediated magnetic interaction and offers integration of ferromagnetism with existing nonmagnetic III-V heterostructures.[1] These structures allow us to explore a new dimension of spintronic devices. A mean-field theory based on exchange between carrier spin and Mn spin, indicates that the properties of ferromagnetism in magnetic III-V's depend critically on the hole concentration. By the use of insulating-gate field-effect transistor structure to modulate carrier concentration, isothermal reversible electrical switching of the ferromagnetic phase transition has been realized. This can be used to electrically assist magnetization reversal, a fundamental process for recording bits in magnetic materials. Furthermore, ferromagnetic/nonmagnetic semiconductor multilayers has been shown to exhibit tunnel magnetoresistance as well as interlayer coupling due to the carrier polarization. Electrical electron as well as hole spin injection across a ferromagnetic/nonmagnetic junction and into an InGaAs quantum well has been demonstrated using a ferromagnetic III-V semiconductor as a source of spin polarized holes. We are thus beginning to learn and understand how to control and utilize the spin degree of freedom in semiconductors.[2]

REFERENCES

1. H. Ohno, Science, 281, 951 (1998); J. Mag. Mag. Materials, 200, 110 (1999); Solid State Commun., **117**, 179 (2001)
2. H. Ohno, F. Matsukura, and Y. Ohno, JSAP International, No. 5, January 2002, pp. 4 - 13 (available at http://www.jsapi.jsap.or.jp/)

MAGNETIC RECORDING TECHNOLOGY

Aric Menon (MIC – Micro and Nanotechnology Research Centre, Denmark, Technical University of Denmark)

Digital Magnetic data recording on hard disk devices continue to be the primary archival mass storage device in a computer. Today a 3.5″ device are capable of storage capacity of 160 GB with transfer rates approaching 1 Gbit/sec. Recent areal density demonstrations have shown recording densities as high as 150 Gb/ in^2. Fig 1 shows the increases in areal density and shipped capacity of magnetic storage over time. Fueled by the development of anisotropic magnetoresistance (AMR) and Giant MR sensors, in recent years the compounded growth rate of areal density has exceeded 100 %. Developments in the recording media has kept pace with those of the read sensor and write head. For example, antiferromagnetically coupled (AFC) recording media allow the writing of narrower tracks on the media, which would otherwise be susceptible to super paramagnetic effect. In this paper the current research in advancing the areal density of rigid magnetic recording systems is surveyed with an emphasis on magnetic, mechanical and processing challenges. The challenges of a terabit/in^2 system are identified and some of the key future research directions will also be presented.

Stuart Parkin et al (Proceedings of the IEEE, May 2003)

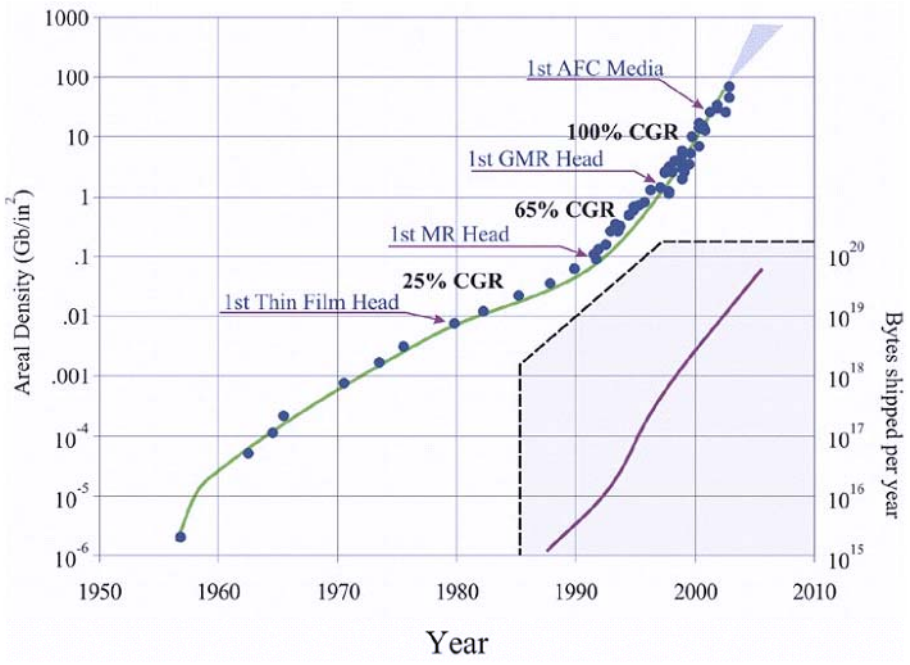

Fig. 1. Areal Density and Shipped Capacity of Magnetic storage over time.

The concept of heat assisted magnetic recording (HAMR) and initial results of its feasibility are shown as potential techniques for writing on ultra high coercivity media. Read sensor concepts beyond the current spin valves where the current flows in the plane across the track width will be explored. In this case the signal voltage amplitude is proportional to the track width for a constant sensor stack height. If the sense current can flow perpendicular to the film, known as current perpendicular to the plane (CPP) mode, reduction of track width will produce no change in the signal voltage amplitude for constant current density. A schematic of such a design is shown in Fig. 2. Here the signal field produces a scissoring motion of the magnetic moment in the alternate layers resulting in a MR signal. The GMR ratio of a CPP multiplayer stack can be significantly higher than that of a spin valve. Such designs could be a potential replacement for spin valves in the future high areal density recording applications.

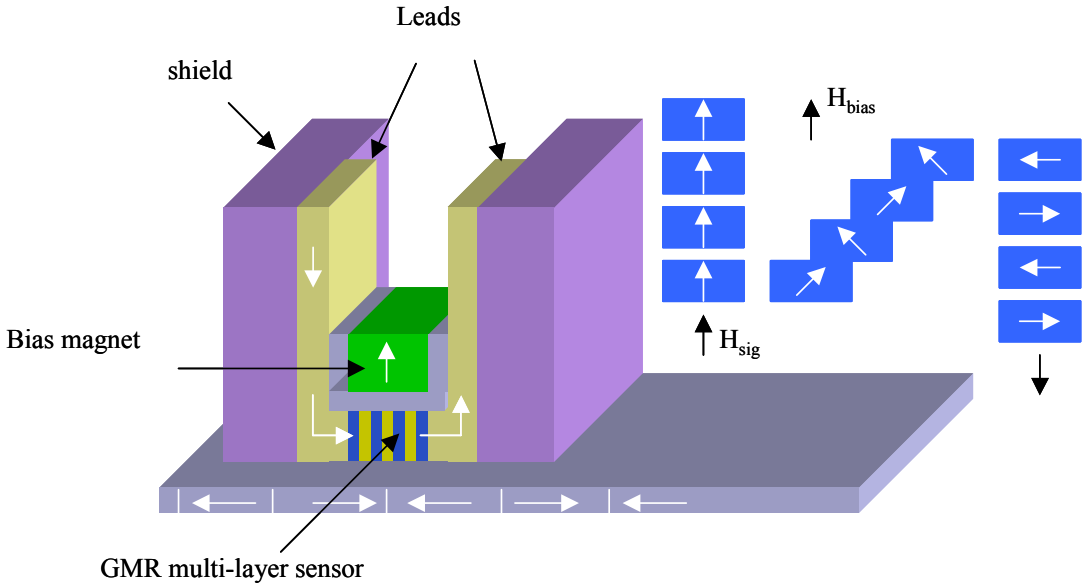

Fig. 2. A CPP/GMR Read Head Design.

REFERENCES

1. Stuart Parkin et al, “Magnetically Engineered Spintronic Sensors and Memory”, Proceedings of the IEEE, VOL. 91. NO.5, May 2003
2. Zhu Jian-Gang (Jimmy), “New heights for hard disk drives”, Materials Today, July/August 2003

SPECTRAL WEIGHT DISTRIBUTION AND SPIN SUSCEPTIBILITY IN A STRIPED MODEL

Brian Møller Andersen and Per Hedegård (Niels Bohr Institute fAPG, Ørsted Laboratory, University of Copenhagen, Denmark)

Many recent theoretical and experimental studies have indicated the existence of stripes in the cupper oxide superconductors.[1, 2] However, it is still highly controversial whether the stripes are ubiquitous to the cuprates and perhaps even involved in the superconducting pairing mechanism or simply a low energy competing state in a restricted part of the phase diagram of some of the cuprate materials.

Starting from a real-space mean-field model that contains both antiferromagnetic and d-wave superconducting order, we study the spectral function and the spin susceptibility in a striped environment. This approach allows us to test the relevance of various proposed symmetry broken states; site or bond centred incommensurate spin order, antiphase or inphase domains, hopping dimerisation, effects of pairing correlations etc.
The spectral function can be measured by angular resolved photoemission spectroscopy (ARPES), and several publications have indicated stripe order.[3, 4] In particular when accounting for the disordering of the stripes, our model calculation agrees with the spectral weight distribution as measured by the ARPES experiments.[5]

The imaginary part of spin susceptibility can be probed by the powerful technique of neutron scattering. In an ordered stripe array we investigate the incommensurable spin waves and their possible relation with the notorious commensurate resonance peak. Also we study the effect of stripe disorder on the measured response.

REFERENCES

1. Tranquada *et al,* Nature **375**, 561 (1995)
2. Mook *et al,* Phys. Rev. Lett. **88**, 097004 (2002)
3. Zhou *et al*, Phys. Rev. Lett. **86**, 5578 (2001)
4. Zhou *et al*, Science 2**86**, 268 (1999)
5. M. Granath, V. Oganesyan, D. Orgad and S. A. Kivelson, Physical Review B **65**, 184501 (2002)

MAGNETIC NANOPARTICLES FOR BIOTECHNOLOGY AND BIOMEDICINE

Quentin Pankhurst (London Centre for Nanotechnology, University College London, London WC1E 6BT, UK)

The physical principles underlying some current biotechnological and biomedical applications of magnetic nanoparticles will be reviewed. Starting from well known basic concepts, and drawing on examples from biotechnology and biomedicine, the relevant physics of magnetic materials and their responses to applied magnetic fields will be surveyed.

The way these properties are controlled and used will illustrated with reference to:

(1) magnetic separation of labelled cells and other biological entities;

(2) therapeutic drug, gene and radionuclide delivery;

(3) radio frequency methods for the catabolism of tumours via hyperthermia;

(4) contrast enhancement agents for magnetic resonance imaging applications; and

(5) the role of biogenic magnetic iron compounds in neurodegenerative diseases such as Alzheimer's disease and Huntington's disease.

Future prospects for applications involving the use of magnetic nanoparticles will also be discussed.

NOVEL INSIGHT INTO NANOMAGNETISM BY SPIN-POLARIZED SCANNING TUNNELING MICROSCOPY

Roland Wiesendanger (Microstructure Advanced Research Center Hamburg (MARCH), University of Hamburg, Jungiusstr. 11, D-20355 Hamburg, Germany)

In order to probe and tailor magnetic properties at the spatial limit we have combined the scanning tunneling microscope (STM) with spin-sensitivity. This is achieved by the use of ferro- and antiferromagnetically coated probe tips offering a high degree of spin-polarization of the electronic states involved in the tunneling process. Magnetic domain imaging with sub-nanometer-scale spatial resolution has been demonstrated for magnetic transition metal as well as rare earth metal films. Ultra-sharp domain walls were discovered in ultra-thin iron films while for antiferromagnetic samples, the different orientation of magnetic moments could directly be made visible at the atomic level. The phenomenon of magnetic hysteresis was observed for the first time at the single-digit nanometer length scale and has directly been correlated with microscopic processes of domain nucleation and domain wall motion.

We also studied magnetic vortex structures in mesoscopic-scale ferromagnetic systems, which are of relevance for current developments in MRAM technology.

Magnetic switching phenomena of nano-scale magnetic islands and nanoparticles were studied by time-dependent spin-sensitive STM imaging. It will be shown that granular thin films exhibit a complex magnetic switching behaviour due to the statistical distribution of grain sizes, grain shapes and inter-grain spacings.

Finally, we will discuss the application of spin-sensitive STM measurements to individual atoms and molecules on magnetic substrates.

REFERENCES

1. R. Wiesendanger et al., Phys. Rev. Lett. **65**, 247 (1990)
2. R. Wiesendanger et al., Science **255**, 583 (1992)
3. M. Bode et al., Phys. Rev. Lett. **81**, 4256 (1998)
4. M. Kleiber et al., Phys. Rev. Lett. **85**,4606 (2000)
5. O. Pietzsch et al., Phys. Rev. Lett. **84**, 5212 (2000)
6. A. Kubetzka et al., Phys. Rev. Lett. **88**, 057291 (2002)
7. M. Bode et al., Phys. Rev. Lett. **86**, 2142 (2001)
8. O. Pietzsch et al., Science **292**, 2053 (2001)
9. A. Wachowiak et al., Science **298**, 577 (2002)
10.M. Pratzer et al., Phys. Rev. Lett. **87**, 127201 (2001)
11.S. Heinze et al., Science **288**, 1805 (2000)

SUPERCONDUCTING CONDUCTORS DEVELOPMENT AND PROSPECTS

Bartek A Glowacki (Department of Materials Science and Metallurgy, University of Cambridge, Pebroke Street, Cambridge CB2 3QZ, IRC in Superconductivity, Cavendish Laboratory, University of Cambridge, Madingley Road CB3 OHE, Cambridge, UK)

Sustain development of all type of superconducting materials are of the equal importance for the future of applied superconductivity, Fig 1. Once it was established in 1960 that Nb-Ti posses strong pinning at elevated magnetic field the industrial process

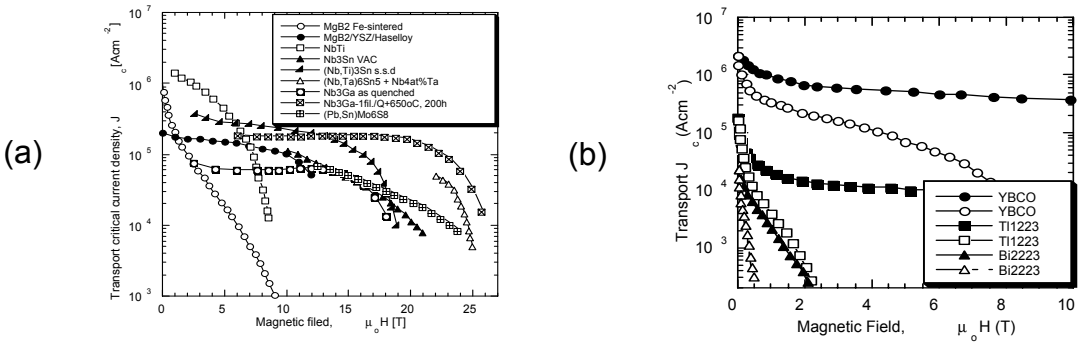

Fig. 1. Transport critical current density vs. magnetic field: (a) low and medium temperature superconductors[1], (b) high temperature superconductors.

was adopted which was originally developed to make filaments for light bulbs. Even so a well establish technology was adopted the price of the first 61 filamentary wire diameter 0.4mm conducting 70 A at 5 T was 400 £/kg during the first year of production, Fig. 2. Today price of the simple Ni-Ti wire for MRI applications is at the level of 1 $/kAm where the price of the sophisticated ITER conductor is currently no more than 2 $/kAm.

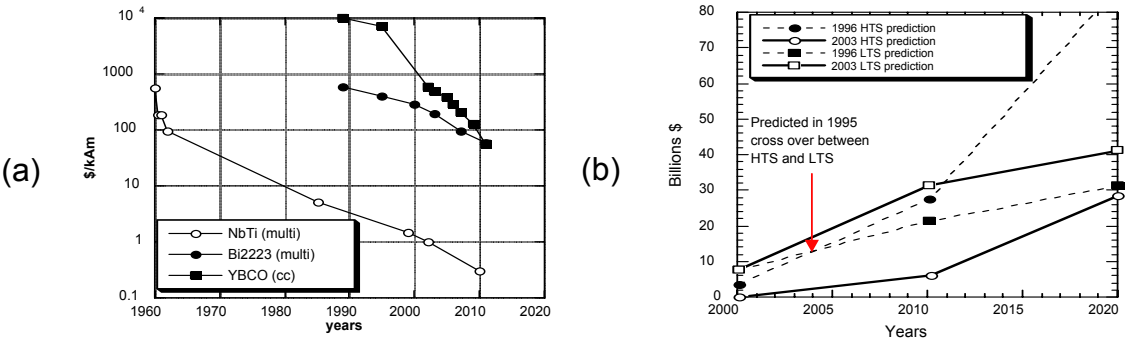

Fig. 2. Market and material projections: (a) Price/performance of NbTi, Bi2223 and YBCO conductors versus years; (b) Projections of the LTS and HTS market which is sheared between electronics, power, industrial processing, medical care and transportation. 1995 estimation conducted at International Superconductivity Industry Summit, Yamanashi 1996, numbers corrected according to data in early

Further reduction of price of Nb-Ti, Nb_3Sn and Nb_3Al conductors can only be realised by increase of performance by introduction of the Artificial Pinning Centres[2] or alternatively by reduction of the material cost by usage of the new emerging technologies eg. Direct Electrochemical Reduction of Oxides developed in Cambridge.[3] Presence of the magnetic material can have a detrimental and also beneficial influence on the reduction of *ac* losses and increase of J_c of superconductors. This problem is particularly important in case of the coated conductors and multifilamentary wires. The latest research on the multifilamentary conductors surrounded by magnetic material proved that losses can be reduced substantially according to eq.1 by coating individual filaments by magnetic material. By comparing losses in a standard multifilamentary superconductor, Q_{st}, to losses in a multifilamentary superconductor with the magnetic covers around individual filaments, Q_{cov}, at the same reduced current i, one can obtain magnetic decoupling loss reduction coefficient, K_{md}, (eq. 1); where $i = I/I_c$, $I_{c1} = I_c/N$, N number of filaments.[4] The parameters $k(i)$ and α are to be determined from experiment and represent individual filament. The example of the effect of shielding of the filaments by a

$$K_{md} = \frac{Q_{st}}{Q_{cov}} = \frac{\alpha I_c^2 F(i)}{Nk(i) a \alpha^2 I_{c1}^2 F(i)} = \frac{N^2 I_{c1}^2}{Nk(i)\alpha^2 I_{c1}^2} = \frac{N}{k(i)\alpha^2} \qquad \text{eq. 1}$$

ferromagnetic material is illustrated in Fig. 3. The geometrical and material factors concerning LTS, MTS and HTS, superconductors, strongly influencing transport current percolation and *ac* losses are of great importance for the engineering applications of superconductivity.[5] However some of the geometrical solutions are more promising than others it is established that interfilamentary decoupling by use of magnetic screening materials may substantially influence further development of ac conductors for application in self and external fields.

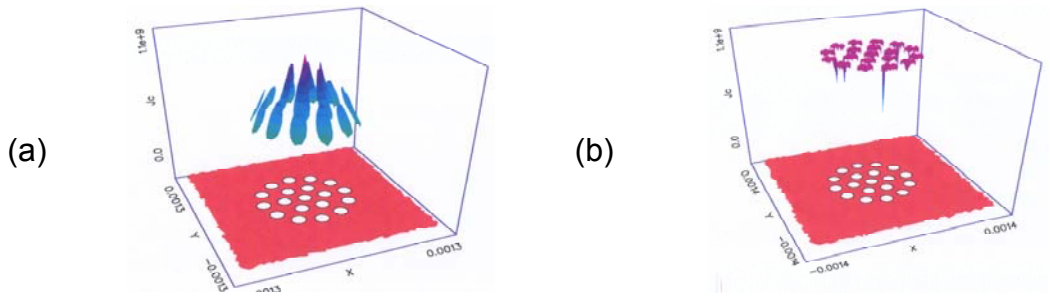

Fig. 3. Spatial distribution of the critical current density in a 19 filament MgB_2 wire cross section in self field, for different values of relative magnetic permeability, μ_r, of the concentric multi-screens[1]: (a) $\mu_r = 1$, $I_c = 442$ A, (b) Non-linear Fe $\mu_{rmax} = 9000$, $I_c = 628$ A.

REFERENCES

1. B. A. Glowacki, M. Majoros, M. Vicker, M. Eisterer, S. Toenies, H. W. Weber, M. Fukutomi, K. Komori, and K. Togano, Supercond. Sci. Technol. **16**, 297 (2003)
2. K. Tchikawa, K. Sakinada, and M. Kobayashi, Cryogenics **33**, 1091 (1993)
3. B. A. Glowacki, X.-Y. Yan, D. J. Fray, G. Chen, M. Majoros and Y. Shi, Physica C **372-376**, 1315 (2002)
4. B. A. Glowacki, M. Majoros, Superconductor Science and Technology **13**, 483 (1999)
5. B. A. Glowacki, In: *Studies of HTS Materials and Applications* (Ed. A. Narlikar, Springer-Verlag, v. 1-Materials 2003 p.239

SPECIFIC HEAT OF $Mg^{11}B_2$, A MULTI-BAND, MULTI-GAP SUPERCONDUCTOR

N. E. Phillips (Lawrence Berkeley National Laboratory, USA), R. A. Fisher, F. Bouquet (Lawrence Berkeley National Laboratory, USA), D. G. Hinks, J. D. Jorgensen (Argonne National Labo*ratory,* USA) and J. C. Lashley (Los Alamos National Laboratory, USA)

The recent discovery[1] of superconductivity in MgB_2 has reopened the question of the maximum critical temperature, T_c, that is possible with the BCS, phonon-mediated mechanism[2] for the electron pairing: Although the isotope effect[3] suggests that the pairing is phonon-mediated, T_c, ~ 40 K, is remarkably high for that mechanism. We have measured the specific heat of $Mg^{11}B_2$ from 1 to 50 K and in magnetic fields to 9 T. The results give information relevant to the magnitude of T_c and the details of the mechanism of the electron pairing.

The temperature dependence of the superconducting-state electron contribution to the specific heat, C_{es}, is dramatically different from that of all other superconductors: At low temperatures it shows an exponential dependence on temperature, as expected, but the parameters correspond to an energy gap that is ~ ¼ of that expected for the value of T_c and a normal-state density of electron states that is ~ ½ of the measured value. At intermediate temperatures a graph of C_{es}/T vs T shows a distinct "hump". Near T_c the general shape of C_{es}/T is typical of strong-coupled superconductors, but the discontinuity at T_c, which would be *greater* than the BCS value for a strong-coupled superconductor, is actually *less*. Over the whole range of temperature C_{es} can be *quantitatively* represented by BCS thermodynamics applied to a model that is generalized to the case of *two* sheets of the Fermi surface with *different* energy gaps. Parameters characterizing the gaps derived from the two-gap fit to the data are in good agreement with theoretical calculations.[4, 5] The calculations give *four* Fermi-surface sheets with two narrow distributions of gap energy centered near the values determined from the specific heat[5], but the effect of those details on the specific heat are too fine to be resolved by the experimental data.). The theoretical work[5, 6] also accounts for the general form of the specific heat and shows that the high value of T_c is intimately related to the existence of multiple gaps.

General features of the superconducting-state specific heat, including, e.g., the discontinuity at T_c, and the amplitudes and apparent temperature dependence of the gaps, are consistent with predictions of the properties of a two-gap superconductor with gap parameters similar to those deduced from the fit. An unusually strong magnetic field dependence of the temperature-proportional term in the electron contribution to the vortex-state specific heat is another manifestation of the two gaps, but the agreement with existing theory is only qualitative. The data give the Debye temperature, Θ = 965 K, the coefficient of the normal–state electron contribution, γ_n= 2.6 mJ mol^{-1} K^{-2}, a

discontinuity in the zero field specific heat of 133 mJ mol^{-1} K^{-1} at T_c = 38.7 K, and the value of the electron–phonon coupling parameter, $\lambda = 0.62$. In single-band extensions of the BCS theory[7, 8] that give more precise relations between these parameters, the value of λ could account for the observed T_c only if the important phonon frequencies were unusually high relative to Θ, but that apparent discrepancy is resolved by the detailed theoretical calculations.

REFERENCES

1. Nagamatsu, N. Nakagawa, T. Muranaka, Y. Zenitani, and J. Akimitsu, Nature **410**, 63 (2001)
2. J. Bardeen, L. N. Cooper, and J. R. Schrieffer, Phys. Rev. **108**,1175 (1957)
3. S. L. Bud'ko et al., Phys. Rev. Lett. **86**, 1877 (2001); D. G. Hinks, H. Claus, and J. D. Jorgensen, Nature **411**, 457 (2001)
4. A. Y. Liu, I. I. Mazin, and J. Kortus, Phys. Rev. Lett. **87**, 87005 (2001)
5. H. J. Choi et al., Nature **418**, 758 (2002)
6. A. Golubov et al., J. Phys. Cond. Mat. **14**, 1353 (2002)
7. W. L. McMillan, Phys. Rev. **167**, 331 (1968)
8. P. B. Allen and R. C. Dynes, Phys. Rev. B **12**, 905 (1975)

SUPERCONDUCTIVITY IN PLUTONIUM BASED COMPOUNDS

F. Wastin, P. Boulet, E. Colineau, J. Rebizant, G. H. Lander (Institute for Transuranium Elements, Germany), J. D. Thompson, J. L. Sarrao and L.A. Morales (Los Alamos National Laboratory, USA)

In 2002, Sarrao *et al.* announced the discovery of superconductivity in $PuCoGa_5$[1]. This new superconductor, the first one to be reported with a transuranium element, displays an astonishing high critical temperature above 18K. $PuCoGa_5$ is thus one of the highest temperature superconductors outside the so-called high-T_c copper oxides. Moreover, it has been found also that the superconductivity is very robust and survives in an applied magnetic field of at least 9 T. The orbital upper critical field was estimated in the WHH[2] approximation to be above 700 kOe, a value exceeding the Pauli limit. Low field values of the critical current ($J_c > 10^4 Acm^{-2}$ for $T > 0.9\ T_c$) compete with the best available superconductors. Recent calculated densities of state (DOS) of $PuCoGa_5$ in the paramagnetic phase reveal that there is a narrow peak due to the Pu $5f_{5/2}$ states close to the Fermi energy E_F, while the Co 3d states lie deeper below E_F. Thus, the electrons at E_F have dominantly Pu *5f* character, and it was concluded that the Cooper pairs are formed by the pairing of Pu *5f*-electrons.[3, 4] Further investigations of Pu compounds have revealed that the isostructural $PuRhGa_5$ compound is also a superconductor[5] as observed by magnetisation and resistivity measurements (Fig. 1) with a critical temperature of ~ 8.7 K and an upper critical field estimated to be above 200 kOe.

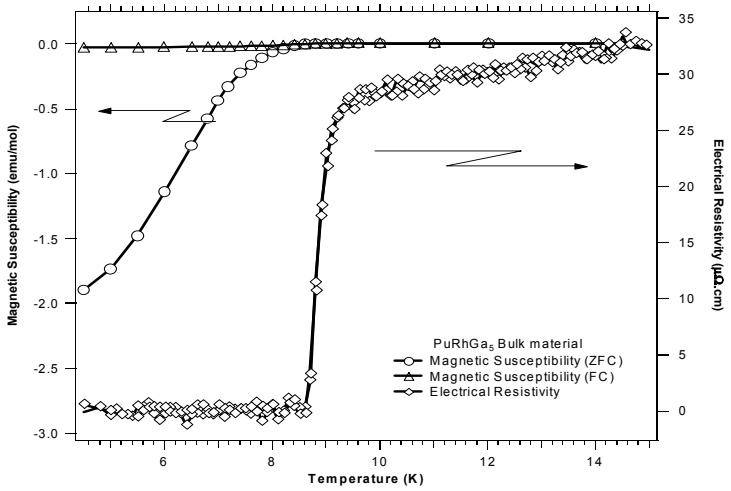

Fig. 1. Zero-Field cooled (ZFC) and Field-cooled (FC) magnetic susceptibility of $PuRhGa_5$ measured in 0.5 kOe on bulk material (left hand-side) and electrical resistivity at zero field on material of the same batch (right hand-side).

A crucial question is, in which framework should the superconductivity of this system be placed?

These new compounds can be viewed as being built from layers of δ-like Pu separated by a layer of 'TGa$_2$'. They crystallizes in a layered structure identical to that of $CeCoIn_5$[6], which is an unconventional, heavy-fermion superconductor but with nearly an order of magnitude lower T_c than the Pu analogues. Interestingly, the Ce and Pu systems share even stronger similarities. Within the series $CeM_{1-x}M'_xIn_5$, where M=Rh, Co and Ir, T_c appears to be a linear function of c/a, with c and a being the tetragonal lattice constants. Figure 2 shows that, within experimental uncertainty, both the Ce and Pu compounds have the same large slope $dT_c/d(c/a) \approx 80$ K, suggesting similar underlying physics.[7]

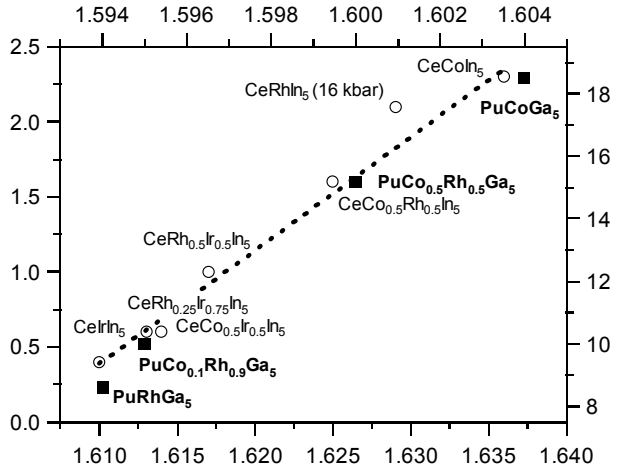

Fig. 2. T_c versus c/a for $CeM_{1-x}M'_xIn_5$ (○), left and bottom axes, and for $PuCo_{1-x}Rh_xGa_5$ (■), top and right axes.

Electronic structure calculations[3, 4] of $PuCoGa_5$ predict magnetic moments on the Pu atoms. Although no long-range magnetic order was observed, in the paramagnetic state, the temperature dependence of the susceptibility for both Pu-compounds follows a modified Curie-Weiss law with an effective moment close to the Pu^{3+} value ($\mu_{eff} \sim 0.70$ μ_B and 0.60 μ_B for the Co and Rh compound, respectively). Since Pu^{3+} is a magnetic ion ($5f^5$ configuration) magnetic interactions must be present. Assuming that superconductivity in $PuCoGa_5$, as in $CeCoIn_5$, is mediated by antiferromagnetic spin fluctuations, the difference between the Ce and Pu f-electron configurations provides a higher spin-fluctuation temperature and thus a potential explanation for the much higher T_c in Pu compounds.

REFERENCES

1. J. L. Sarrao et al., Nature **420**, 297 (2002)
2. N. R. Werthamer et al., Phys. Rev. Lett. **9**, 266 (1962)
3. I. Opahle and P.M. Oppeneer, Phys. Rev. Lett. **90**, 157001 (2003)
4. T. Maehira et al., Phys. Rev. Lett. **90**, 207007 (2003)
5. F. Wastin et al., J. Phys. Condens Matter, in the press
6. C. Petrovic et al., J. Phys. Condens. Matter **13,** L337 (2001)
7. J. D. Thompson et al., 33ièmes Journées des Actinides, Prague 27-29 April, 2003

SPIN DYNAMICS IN HIGH-T_c CUPRATES

*S. M. Hayden** (H. H. Wills Physics Laboratory, University of Bristol, Tyndall Ave, Bristol, BS8 1TL*, UK*)

The advent of chopper spectrometers with PSD detectors based at spallation neutron sources has opened up many new possibilities for studying magnetic excitations. New instruments such as the MAPS spectrometer at ISIS allow measurements to be carried out over a wide energy range with good wave vector resolution and low background. I will show how these techniques have been applied to the study of the high temperature superconductors and their parent compounds. In particular, our recent measurements have demonstrated the existence of higher order exchange couplings and mapped out the incommensurate magnetic excitations for superconducting compositions.

If magnetic excitations contribute significantly to the superconductive pairing, they must be present at the transition temperature - I will discuss the nature of the magnetic excitations at high temperatures.

*Work done in collaboration with G. Aeppli, S.-W. Cheong, N. B. Christensen, R. Coldea, Pengcheng Dai, F. Dogan, C. D. Frost, B. Lake, T. E. Mason, D. F. McMorrow, H. A. Mook, T. G. Perring, H. M. Rønnow, H. Tagaki, and Z. Fisk.

MAGNETIC HETEROSTRUCTURES

W. Keune (Institute of Physics, University of Duisburg-Essen, Lotharstr. 65, D-47048 Duisburg, Germany)

Metallic artificial magnetic heterostructures and superlattices have attracted much attention for many years, because of their scientific and technological significance. Heterostructures consist of alternating layers of different materials on a nanometer or even atomic scale, which show properties not present in a single layer. A famous example is the classical Fe/Cr(001) heterostructure for which antiferromagnetic interlayer exchange-coupling[1] and giant magnetoresistance (GMR)[2,3] were observed for the first time. Although these phenomena are now rather well understood, the correlation of chemical and magnetic interface roughness with GMR is still a matter of debate[4-6], in particular when buried interfaces are involved which are not directly accessible for many experimental techniques. Another example are alternating monoatomic layers in Fe/Pt(001) or Fe/Pd(001) heterostructures[7] (equivalent to $L1_0$ chemical ordering) which exhibit a large perpendicular magnetic anisotropy, making these materials potentially useful as a perpendicular magnetic recording or bias-magnet medium. In this presentation we will concentrate mainly on the two molecular-beam grown superlattice systems Fe/Cr(001) and Fe/Pt($L1_0$).

Fe/Cr:

The correlation between chemical and magnetic local structures at buried interfaces was investigated using ^{57}Fe conversion electron Mössbauer spectroscopy (CEMS)[8] in combination with self-consistent calculations of Fe and Cr magnetic moments in the interface region[9,10]. Depth-selective information about the distribution $P(B_{hf})$ of magnetic hyperfine fields (hff) was obtained by deposition of about monolayer (ML) thick ^{57}Fe probe layers at and near the interfaces. The superlattices were grown at different substrate temperatures up to ~ 500 K in order to modify their interface roughness. ^{57}Fe atoms near the interface with various magnetic moments and with different local atomic environments lead to distinct satellite lines in CEMS spectra, equivalent to distinct hff. A model for various degrees of interface alloying presupposing exchange of adatoms with underlying atoms and floating of adatoms on upper layers was used in the magnetic moment calculations. A linear correlation between positions of maxima in the calculated Fe moment distribution and distinct hff peaks was obtained. Different scenarios of epitaxial growth/intermixing were considered, and the corresponding distributions of magnetic moments for interfacial Fe atoms with a given number of nearest and next-nearest Cr neighbours are compared with experimental hff distributions. Our experimental samples exhibit larger intermixing than the simplified theoretical models used. The measured GMR ratio was observed to increase with the experimental fraction of floated ^{57}Fe atoms.

Fe/Pt ($L1_0$):

The growth and structure of epitaxial $[Fe(1ML)/Pt(1ML)]_n$ superlattices, grown at different temperatures T_s by alternating deposition of Fe and Pt atomic layers on buffer-Pt/seed-Fe/GaAs(001) substrates, were studied in-situ by RHEED and ex-situ by X-ray scattering of synchrotron radiation as a function of growth conditions[11]. RHEED intensity oscillations during growth provide evidence for island growth at T_s = 200 °C and quasi layer-by-layer growth at T_s = 350 °C. The degree of epitaxy depends critically on the morphology of the seed layer and substrate roughness. The long range $L1_0$-order parameter S increases from near zero at T_s = 200 °C to 0.65 at T_s = 350 °C. This confirms the fact that S is mainly determined by the surface mobility of the atoms, which is controlled by T_s. The CEM spectra exhibit a distribution of magnetic hyperfine splittings, which were decomposed into two components originating from a chemically disordered local environment and the $L1_0$-ordered local environment around ^{57}Fe atoms. The fraction of $L1_0$-order environments increases with T_s and correlates with S. The relative Mössbauer line intensities indicate preferred perpendicular Fe spin orientation at $T_s \geq 300$ °C for both the $L1_0$-order *and* the disordered environment. These findings agree qualitatively with results from polar MOKE and MFM[12]. For $T_s \geq 300$ °C, polar MOKE loops are nearly square shaped with $M_{rem}/M_{sat} \approx 1$ and high coercivity > 2kOe. MFM images of these samples show strong contrast from perpendicular domains and nearly no in-plane contribution. For potential applications in magnetoelectronics the challenge remains to further lower the $L1_0$-ordering temperature.

Work supported by Deutsche Forschungsgemeinschaft (SFB491)

REFERENCES

1. P. Grünberg et al., Phys. Rev. Lett. **57**, 2442 (1986)
2. M. N. Baibich et al., Phys. Rev. Lett. **61**, 2472 (1988)
3. G. Binasch et al., Phys. Rev. B **39**, 4828 (1989)
4. R. Schad et al., Phys. Rev. B **59**, 1242 (1999)
5. R. Schad et al., Europhys. Lett. **44**, 379 (1998)
6. D. Olligs et al., Europhys. Lett. **59**, 458 (2002).
7. J. U. Thiele et al., J. Appl. Phys. **84**, 5686 (1998) and references therein
8. T. Shinjo and W. Keune, J. Magn. Magn. Mater. **200**, 598 (1999)
9. V. M. Uzdin et al., Phys. Rev. B. **63**, 1044071 (2001)
10. V. Uzdin and W. Keune, Phys. Met. Metall. **91**, Suppl.**1**, 82 (2001)
11. A. Nefedov et al., J. Phys. : Condens. Matter **14**, 12273 (2002)
12. E. Schuster, W. Keune, T. Schmitte, S. Goek, A. Nefedov, K. Theis-Bröhl and H. Zabel (in preparation)

INHOMOGENEOUS MAGNETIC AND ELECTRONIC STATE IN UNDERDOPED HIGH-T_c OXIDES

Christof Niedermayer (Laboratory for Neutron Scattering, ETH Zurich & Paul Scherrer Institute, CH-5232 Villigen, Switzerland), C. Bernhard (Max-Planck-Institut für Festkörperforschung, D-70569 Stuttgart, Germany), J. I. Budnick (Physics Department, University of Connecticut, 06268 Storrs CT, USA)

The technique of muon spin rotation or relaxation (μSR) is a powerful tool for studying the internal distribution of magnetic fields within solids. In the context of high temperature superconducting cuprates μSR experiments have provided important contributions to a better understanding of the physics of the vortex state[1], superfluid density[2, 3] and the complex interplay between magnetism and superconductivity[4] that distinguishes the high temperature superconducting cuprates.

The basic idea of a μSR experiment is very similar to that of the NMR technique. Positive muons are incorporated as local probes in the host lattice of the sample to be studied. The spin of the muon and the related magnetic moment act as a sensitive probe for the local magnetic field through its precession in the field with a frequency of $\omega_\mu = \gamma_\mu B_{loc}$ where γ_μ = 851.4 MHz/T is the gyromagnetic ratio of the muon and B_{loc} is the local field. The time evolution of the muon spin polarization can be conveniently monitored due to the fact that when a muon decays (half life 2.2 μs) the resulting positron is emitted preferentially in the direction of the muon spin at the time of decay. A fascinating aspect of the μSR technique compared to other microscopic techniques is the possibility of measuring internal magnetic fields in zero external field. The observation of a muon spin precession signal in zero field is an unambiguous indication for the existence of a magnetic hyperfine field at the muon site, which is produced by the magnetic moments of the surrounding atoms and has to be static or slowly fluctuating on a timescale of microseconds in order to be seen by the muon. In the high-T_c cuprates the internal field at the muon site is dominated by dipolar contributions from the surrounding moments and due to the r^{-3} dependence of the dipolar coupling the dominant contributions come from dipoles within the first and second coordination shells. Thus another advantage of the experiment is the sensitivity of the muon probe to extremely short ranged magnetic correlations on a nanometer scale.

A summary of results is presented describing studies carried out over a broad concentration range for Sr doped La_2CuO_4 and Ca doped $YBa_2Cu_3O_6$ In the underdoped superconducting region for both systems clear evidence for concentration dependent spin freezing of strongly correlated antiferromagnetic regions is found. The persistence of these strong static antiferromagnetic correlations in the superconducting state is evidence for an inhomogeneous hole distribution possibly relatable to the stripe phase deduced from the neutron experiments of Tranquada et al.[5]

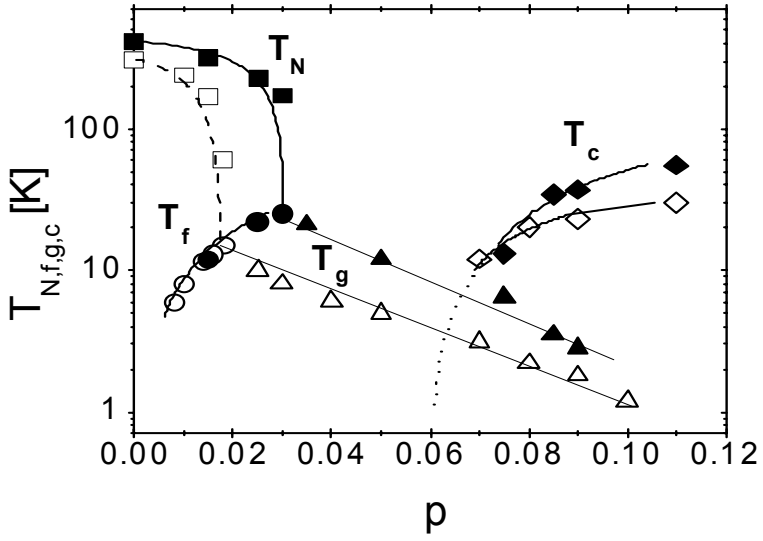

Fig. 1. Magnetic phase diagram for $La_{2-x}Sr_xCuO_4$ (open symbols) and high temperature superconducting $Y_{1-x}Ca_xBa_2Cu_3O_6$ (full symbols). Squares represent the Néel temperatures T_N, at which the Cu^{2+} spins order into a three dimensional antiferromagnetic state. T_g indicates a transition into a spin-glass like state (cluster glass, triangles) with strong magnetic correlations which coexist with superconductivity for $p >$ 0.06.

REFERENCES

1. S. L. Lee et al., Phys. Rev. Lett. **71**, 3862 (1993)
2. Y. J. Uemura et al., Phys. Rev. Lett. **66**, 2665 (1991), Y. J. Uemura et al, Nature **364**, (1993) 605
3. C. Bernhard et al., Phys. Rev. Lett. **86**, 1617 (2001)
4. Ch. Niedermayer et al., Phys. Rev. Lett. **80**, 3843 (1998)
5. J. M. Tranquada et al., Nature **375**, 561 (1995)

ADVANCED OXIDE THIN FILM RESISTIVE MEMORY DEVICES

Alex Ignatiev (Texas Center for Superconductivity and Advanced Materials, University of Houston, Houston, Texas, USA)

A novel electric pulse-induced resistive change (EPIR) effect has been found in thin film oxides with focus on the colossal magneto resistive (CMR) materials system. This EPIR effect manifests itself as a rapid and reversible change of resistance of an oxide film under short (~10 ns), low voltage (~4 V) pulsing, and thus has shown promise for the development of resistive, non-volatile memory. The electrical pulses are applied across a thin film oxide sample at room temperature and under no applied magnetic field. A pulse can directly either increase or decrease the resistance of the thin film sample depending on pulse polarity. The sample resistance change has been shown to be over two orders of magnitude, and is non-volatile after pulsing. The operating temperature range for a single cell device has been shown to be from -100^{o}C to 200^{o}C. The cell resistance change ratio remains constant in the temperature range of -100^{o}C to 100^{o}C, but shows a decrease above 120^{o}C with major changes in resistance ratio above 200^{o}C. In addition, the resistive state of a cell is highly immune to radiation exposure. The physical mechanism for the effect is not fully clear but may involve defect formation/migration with both bulk and interface contributions. It has also been shown that the sample resistance can be changed through multiple levels - as many as 50 have been shown. Such a programmable resistance device can provide a way for the development of a new kind of non-volatile memory with high density, fast write/read speed, low power-consumption and potential high radiation-hardness. When these memory characteristics are coupled with the prospect of multiple valued memory, the applications possibilities are significantly enhanced.

FERROMAGNETIC METAL – SUPERCONDUCTOR SUPERLATTICES: PROXIMITY EFFECT, π-PHASE MAGNETISM AND LOGICAL DEVICES

Yurii N. Proshin, *Mansur G. Khusainov* (*Kazan State University, Kazan, Russia*) *and Yuri A. Izyumov* (*Institute of Metal Physics, Ekaterinburg, Russia*)

We study the coexistence and mutual influence of magnetism and superconductivity in the artificial layered ferromagnetic metal/superconductor (FM/S) nanostructures. The review of experimental situation, critical analysis of existing theories of proximity effect in these systems, and schematic diagram of new type logical device are given.[1-5]

It is shown that the superconducting state of an FM/S system is a superposition of two pairing mechanisms, Bardin-Cooper-Schrieffer's in the S layers and Fulde-Ferrell-Larkin-Ovchinnikov 's in the FM ones. We propose the original theory of the proximity effect in the dirty limit based on the microscopically derived Usadel equations with original boundary conditions. We give an explanation for the qualitatively different behavior of T_c versus thickness of the FM layer d_f which observed by various experimental groups on identical FM/S structures. A detailed analysis of a large amount of experimental data amply confirms the proposed theory.

For the FM/S superlattice we take into account π phase magnetism[3, 5] along with known π phase superconductivity.[6-7] We derive the new classification of the FM/S superlattice states and predict new 0π and ππ states characterized by an antiferromagnetic ordering of the adjacent FM layer magnetizations[3]. If the S layers thickness is less than threshold value d_s^{π}, these π magnetic states have higher critical temperature than earlier known 0 magnetic states (00 and π0) having a ferromagnetic ordering of the FM layer magnetizations. The recent theoretical works investigate the part of this problem only for the trilayer FM/S/FM[8] structures, in which the π phase superconductivity is impossible in principle.

The FM/S superlattices have more logically different variants of recording than the early-discussed spin switch device based on the FM/S/FM trilayer[8]. Therefore on the FM/S superlattice base we propose the principal scheme of the new logical device that combines in one sample the advantages of two different recording channels. These superconducting and magnetic channels can be *separately* managed by the external magnetic field.[4, 5] We found a physically interesting region of the theory parameters, which should help experimentalists in the preparation of the FM/S superlattices with the new π magnetic properties.

This work is supported in part by RFBR (01-02-17534, 01-02-17822) and CRDF (REC-007).

REFERENCES

1. M.G. Khusainov and Yu.N. Proshin, Phys. Rev. B **56,** 14283 (1997)
2. Yu.N. Proshin and M.G. Khusainov, JETP **86**, 930 (1998)
3. Yu.N. Proshin, Yu.A. Izyumov, and M.G. Khusainov, Phys. Rev B, **64**, 064522 (2001)
4. Yu.N. Proshin, Yu.A. Izyumov, and M.G. Khusainov, Physica C **367**, 181 (2002)
5. Yu.A. Izyumov, Yu.N. Proshin, and M.G. Khusainov, Physics-Uspekhi **45**, 109 (2002)
7. Z. Radović *et al*. Phys. Rev. B **44**, 759 (1991)
8. A.I. Buzdin *et al.* Sov. Phys. JETP **74**, 124 (1992)
9. A.I. Buzdin, A.V. Vedyayev, and N.V. Ryzhanova, Europhys. Lett. **48**, 686 (1999); L.R. Tagirov, Phys. Rev. Lett. **83**, 2058 (1999)

MAGNETOCALORIC PROPERTIES OF $La_{0.67}Ca_{0.33-x}Sr_xMnO_{3\pm\delta}$ ($x \in [0;0.33]$)

Anders Reves Dinesen, Søren Linderoth (Materials Research Department, Risø National Laboratory, Denmark), Steen Mørup (Department of Physics, Technical

University of Denmark, Denmark) and Nini H. Pryds (Materials Research Department, Risø National Laboratory, Denmark)

The magnetocaloric properties of a series of Ca- and Sr-doped lanthanum manganites, $La_{0.67}Ca_{0.33-x}Sr_xMnO_{3\pm\delta}$ ($0 \le x \le 0.33$), have been investigated and selected results will be presented. The samples showed a substantial magnetocaloric effect in a temperature range around their respective Curie temperature. By varying the composition parameter x the Curie temperature could be adjusted between 267 K ($x = 0$) and 369 K ($x = 0.33$). The possibility of tailoring a working substance for magnetic refrigeration near room temperature was thereby demonstrated.

Seven $La_{0.67}Ca_{0.33-x}Sr_xMnO_{3\pm\delta}$ samples (with a variation of x corresponding to an equidistant exchange of Ca with Sr) were synthesized using the glycine-nitrate combustion technique. By x-ray diffraction the samples were found to be single-phase perovskites. The magnetocaloric effect was measured both directly, providing the adiabatic temperature change ΔT_{ad}, and indirectly, providing the isothermal magnetic entropy change ΔS_M (the entropy change was derived from magnetization measurements).

Figure 1 shows an example of raw data obtained from a direct measurement of the adiabatic temperature change in $La_{0.67}Ca_{0.33}MnO_{3\pm\delta}$ (i.e. the sample with $x = 0$). Each step on the temperature curve in Fig. 1a is associated with magnetization and subsequent demagnetization of the sample. Fig. 1b shows an enlarged view of a single magnetization cycle, where the applied field (0.7 T) gives rise to an adiabatic temperature change of about 1.5 K.

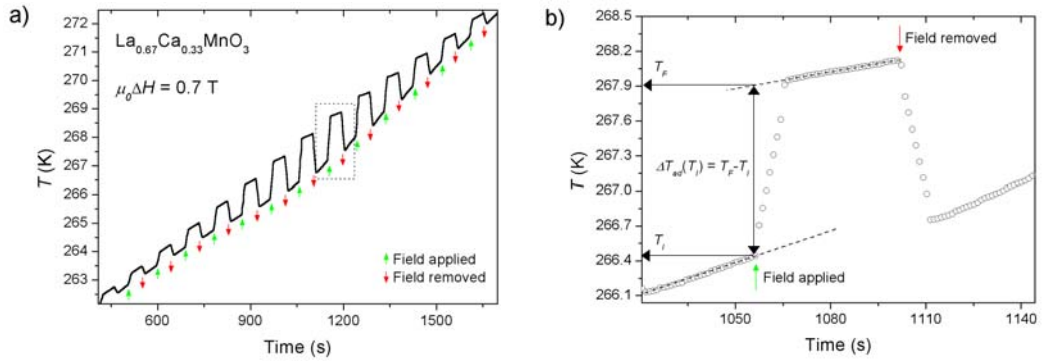

Fig. 1. (a) Temperature profile for the $La_{0.67}Ca_{0.33}MnO_3$ sample obtained during a direct measurement of the adiabatic temperature change. (b) Enlarged view of the magnetization cycle outlined in panel (a).

Figure 2 shows the temperature dependence of the magnetic entropy change of the manganite samples due to a field change of 1.2 T. The samples show caret-shaped magnetocaloric peaks with a maximum $|-\Delta S_M|$ value at the Curie temperature. The figure thus illustrates the close relationship between the substitution parameter x and the Curie temperature (and thereby the magnetocaloric temperature working range of the compounds). For comparison the entropy change of Gd (the prototypical working substance for magnetic refrigeration at room temperature[1]) is shown in the same figure. Considering the maximum magnetic entropy changes, the values obtained for the $La_{0.67}Ca_{0.33-x}Sr_xMnO_{3\pm\delta}$ samples with low Ca content are comparable to that of Gd. For the $x = 0$ sample the maximum $|-\Delta S_M|$ value exceeds the maximum $|-\Delta S_M|$ value of Gd by a factor of 1.7.

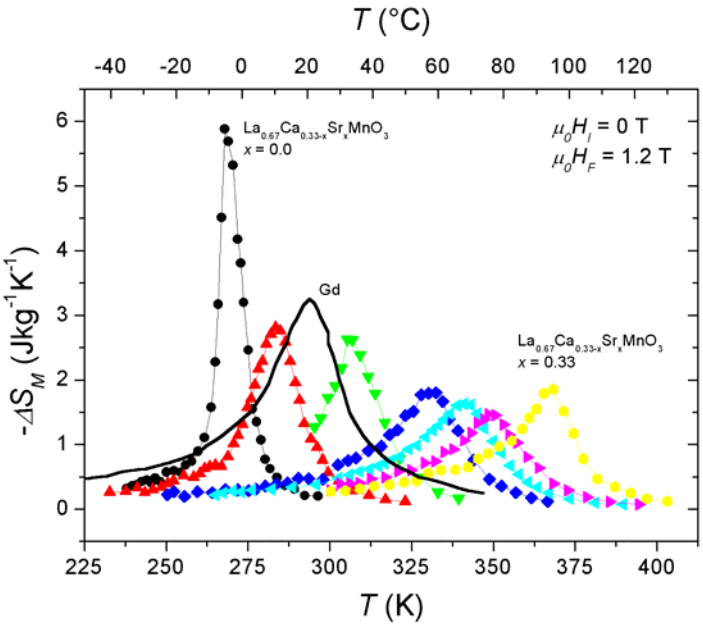

Fig. 2. Temperature dependence of the magnetic entropy changes in the $La_{0.67}Ca_{0.33-x}Sr_xMnO_3$ samples due to a field change of 1.2 T. Magnetic entropy change of Gd is shown for comparison (data obtained from reference 2).

The combination of a quite large magnetocaloric effect, excellent chemical stability, and adjustable temperature working range makes $La_{0.67}Ca_{0.33-x}Sr_xMnO_{3\pm\delta}$ an interesting candidate as refrigerant in future cooling technology based on the magnetocaloric effect.

REFERENCES

1. V. K. Pecharsky and K. A. Gschneidner, Jr., J. Magn. Magn. Mater. 200, 44 (1999)
2. T. Z. Zhou *et al*. J. Appl. Phys. **85**, 7975 (1999)

TWO-DIMENSIONAL MAGNETIC STRUCTURES AND THE MULTI-STEP METAMAGNETIC PHASES IN $TbRu_2Si_2$

S. Kawano (Research Reactor Institute, Kyoto University, Japan), M. Takahashi (Institute of Materials Science, University of Tsukuba, Japan), T. Shigeoka, N. Iwata, M. Shiimoto (Faculty of Science, Yamaguchi University, Japan), B. Lebech (Materials Research Department, Risø National Laboratory, Denmark)

The rare-earth compound $TbRu_2Si_2$ crystallizes in the $ThCr_2Si_2$-type structure (space group: *I*4/*mmm*), with the Tb ions, which are carrying the magnetic moment, arranged in the tetragonal body centred lattice. The magnetic behaviour is characterized by successive temperature induced transitions at T_N = 57 K, T_t = 5 K and T_t' = 4.2 K, and a multi-step metamagnetic transition (probably six steps up to a fully induced ferromagnetic phase) at low temperatures.[1] Figure 1 shows the field-temperature (*H*, *T*) magnetic phase diagram for $TbRu_2Si_2$, which is slightly modified when compared to the original one.[1] From single crystal neutron diffraction studies we have found that the high and intermediate temperature phases (phase I and phase II) at zero-field are, respectively, a one-dimensional spin arrangement with frustrated (2 0 0)/(1 0 0) Tb planes and a two-dimensional one with frustrated Tb sites[3] embedded in regular arrangements of antiferromagnetically coupled ferromagnetic (2 0 0)/(1 0 0) planes. The low temperature phase (phase III) is still unsolved.

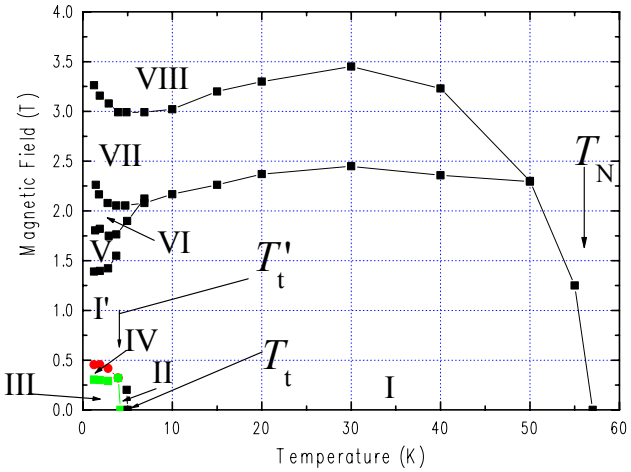

Fig. 1. Magnetic field versus temperature (H, T) Phase diagram for $TbRu_2Si_2$.

In the present note we report the results of pulsed and reactor-based neutron diffraction investigations of $TbRu_2Si_2$ revealing not only magnetic modulations of three ordered phases at zero-field but also those of the field-induced phases (phase IV to VIII) at 1.6 K. All the diffraction measurements were performed on the same $TbRu_2Si_2$ single crystal with the ***a*b**** reciprocal plane in the scattering plane. The reactor-based data were collected using the TAS3 neutron spectrometer at the Risø National Laboratory, Denmark. The pulsed neutron data were collected by use of the FOX diffractometer at the Neutron Scattering Facilities of the High Energy Accelerator Research Organization (KENS),

Japan. The magnetic field was applied along the easy *c*-axis, i.e. the Bragg reflections, were collected only for (*h k* 0)-type reflections.

At zero-field we have modelled the magnetic order of phase I with a one-dimensional pattern which contains two frustrated (2 0 0)/(1 0 0) planes. The magnetic unit cell is 13*a*×*a*×*c*, where *a* and *c* are the lattice constants of the original chemical cell and the order may be described by a propagation vector $\boldsymbol{Q}$ = (3/13 0 0). For phase II, the modelled magnetic order is two-dimensional (13*a*×13*a*×*c*) and consists of a regular sequence of two antiferromagnetic/frustrated and 24 ferromagnetic (2 0 0)/(1 0 0) planes [3]. The low temperature phase III indicates also a two-dimensional arrangement with a smaller magnetic cell (13*a*×4*a*×*c*) containing no frustrated Tb sites but two pure antiferromagnetic and 24 ferromagnetic (2 0 0)/(1 0 0) planes.

When an external magnetic field is applied at 1.6 K along the easy *c*-axis the predominant changes in the model magnetic order occur in the two antiferromagnetic/frustrated (2 0 0)/(1 0 0) planes. Phase IV appears at the first step in the magnetisation. This phase is also considered to be two-dimensional and is only slightly different from that of the zero-field phase II. The antiferromagnetic/frustrated Tb sites disappear and is replaced by one ferrimagnetic (2 0 0)/(1 0 0) plane in the 13*a*×13*a*×*c* magnetic unit cell. In contrast, the following phase I' is again one-dimensional with a magnetic unit cell of 13*a*×*a*×*c* and contains 26 ferromagnetic (2 0 0)/(1 0 0) planes of Tb spins parallel or anti-parallel to the *c*-axis. Phase V is again two-dimensional (13*a*×13*a*×*c*) and only slightly different from phase IV with one (2 0 0)/(1 0 0) ferromagnetic plane. The same is the case for phase VI but it contains two (2 0 0)/(1 0 0) ferrimagnetic planes. Also phase VII is two-dimensional, with regions of spins anti-parallel to the field direction regularly distributed in the sea of spins parallel to the field direction. Finally the spin structure becomes fully ferromagnetic. Each model phase results in a jump in the magnetization. The values of these jumps are in fair agreement with the observed value.

REFERENCES

1. A. Garnier, D. Gignoux, D. Schmitt and T. Shigeoka, Physica B **212**, 343 (1995)
2. T. Kawae, H. Sakita, M. Hitaka, K. Takeda, T. Shigeoka and N. Iwata, J. Magn. Magn. Mater. **177-181**, 795 (1998)
3. S. Kawano, B. Lebech, T. Shigeoka and N. Iwata, Appl. Phys. A **74** (Suppl.), S643 (2002)

THEORY AND SIMULATION OF INTERACTING FERRO- AND ANTIFERROMAGNETIC NANO-PARTICLES

Per-Anker Lindgård (*Materials Research Department, Risø National Laboratory, Denmark)*

The understanding of the interplay between ferro(FM)- and antiferromagnetic (AFM) materials is still incomplete, in spite of the great interest in 'exchange-bias' devices. In order to minimize the problem with domain wall mechanisms we have studied a model system consisting of nano-sized spheres that are half an fcc structured AFM in contact with an F-hemisphere. For the AFM part, parameters corresponding to NiO or CoO are used. It has previously been found[1,2] that fcc AFM nano-particles have a multi-q structure. In the interacting model system the AFM ground state is, however, at low temperatures the simple single-$\boldsymbol{q}$ state with the moments parallel to the ferromagnet at the interface as expected by Miklejohn and Bean[3]. At low temperatures the switching does not follow the rotating uniform mode model. Although the system has different energy barriers for the FM and AFM hemispheres, the switching occurs simultaneously (even for small couplings). Hence no exchange bias effect is observed when the FM and AFM have similar axial anisotropies, even at low temperatures. A small exchange bias effect is observed when the AFM has a large axial anisotropy. However, it is very much reduced due to fluctuations among the various multi-$\boldsymbol{q}$ states, which facilitates the switching of the antiferromagnetic hemisphere. This study was undertaken for the present model system in order to avoid any complications from possible domain switching mechanisms. However, the switching is found to be replaced by the mechanism of transitions between the superposition of various domain states. The possibility of having multi-$\boldsymbol{q}$ structure for AFM's may be a contributing reason (and a new model) for the observed, much reduced, exchange bias also in other more realistic systems.

REFERENCES

1. R.H. Kodoma and A.E. Berkowitz, Phys. Rev. B **59**, 6321 (1999)
2. P.-A. Lindgård, J. Magn. Magn. Mat. (to be published)
3. W.H. Meiklejohn and C.P. Bean, Phys. Rev. **102**, 1413 (1956) and **105**, 904 (1957)

LOCALISED MAGNETIC EXCITATION MODE IN HEMATITE NANOPARTICLES

Stine Nyborg Klausen, Kim Lefmann, Per-Anker Lindgård, and Luise Theil Kuhn (Materials Research Department, Risø National Laboratory, Denmark), Cathrine Frandsen and Steen Mørup (Department of Physics, Technical University of Denmark), Bertrand Roessli and Nordal Cavadini (Laboratory for Neutron Scattering, Paul Scherrer Institute, Switzerland)

The magnetic dynamics of nanoparticles is a challenging field both technologically and scientifically. As the size of a particle decreases and enters the nanometer scale the magnetic properties change and new dynamical phenomena appear. An example is superparamagnetic relaxation, in which the direction of the total magnetic moment of the particle performs a spontaneous reversal due to thermal fluctuations. Superparamagnetism is seen in antiferromagnetic particles as well – here each sublattice reverses it magnetisation. Another example of magnetic nanoparticle dynamics is collective magnetic excitations. Here the magnetic (sublattice) moments move coherently around its ground state position, performing a precession. These excitations correspond to spin waves with $q = 0$.

Nanoparticles of the canted antiferromagnet hematite (α-Fe_2O_3) are particularly interesting due to the complicated magnetic structure of the bulk material.[1] Using high-resolution neutron scattering we have earlier observed both superparamagnetic relaxation and collective magnetic excitations in nanoparticles of hematite.[2, 3] Superparamagnetism was seen as a broadening of the elastic peak in a quasielastic scan at the antiferromagnetic (1 1 1) scattering vector, whereas the collective magnetic excitations appears as broad side peaks centred at ±0.26 meV. At temperatures above 150 K the superparamagnetic relaxation time was found to agree with the (Arrhenius type) Néel-Brown law, but small deviations - at the limit of the experimental resolution - were found at lower temperatures.[3]

Recently, we have discovered a new mode of magnetic dynamics in hematite nanoparticles.[4] The signal is visible as an inelastic peak around 1.0 – 1.3 meV at the antiferromagnetic (100) scattering vector, and the peak is localized in both q and ω, see Fig. 1. Our neutron scattering studies of this mode includes measurements in applied fields up to 9 T as well as polarisation analysis. We present a detailed model for the mode and its field dependence.

Our results show that two collective excitation modes exist in hematite nanoparticles, a low-frequency mode and a high frequency mode. In the previously observed low-frequency mode, the (elliptical) precession is mainly in the easy plane. The newly observed high-frequency mode is found to have mainly out-of-plane precession. The modes correspond to two $q = 0$ spin waves with (different) anisotropy gaps. Whereas the existence of two anisotropy gaps are known from bulk hematite[1], the localisation of the nanoparticle modes provides direct evidence for the predicted discrete spin wave spectrum in magnetic nanoparticles.[5]

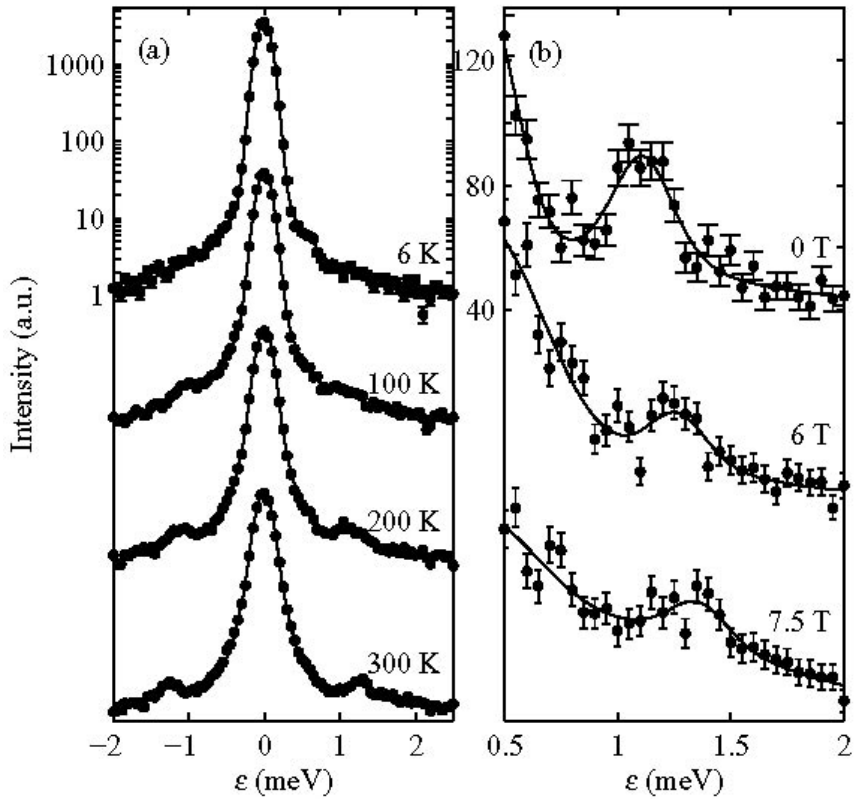

Fig. 1. Inelastic neutron data on 16 nm hematite nanoparticles taken at the (1 0 0) antiferromagnetic scattering vector. The left panel shows the temperature dependence of the elastic peak and the side peaks, shown on a logarithmic scale. These data were taken at the RITA-2 spectrometer at PSI. The right panel shows a zoom-in on one side peak as a function of applied field, shown on a linear scale. These data were taken at the TASP spectrometer at PSI.

We have varied the temperature in the range 6 - 300 K. The energy of the newly observed mode is found to increase with increasing temperature, reflecting the changes in the out-of-plane anisotropy. In hematite nanoparticles, this anisotropy differs from the bulk material resulting in a suppression of the Morin (spin-flip) transition for nanoparticles of diameters less than 20 nm. Our results give direct access to measuring the anisotropy, thereby shedding more light on the suppression of the Morin transition in nanoparticles.

REFERENCES

1. A. H. Morrish, *Canted Antiferromagnetism: Hematite* (World Scientific, Singapore, New Jersey, London, Hong Kong, 1994)
2. M. F. Hansen, F. Bødker, S. Mørup, K. Lefmann, K. N. Clausen, and P.-A. Lindgård, Phys. Rev. Lett. **79**, 4910 (1997)
3. S. N. Klausen, K. Lefmann, P.-A. Lindgård, K. N. Clausen, M. F. Hansen, F. Bødker, S. Mørup, and M. Telling, to appear in J. Magn. Magn. Mater. (2003)
4. S. N. Klausen, K. Lefmann, P.-A. Lindgård, L. T. Kuhn, C. Frandsen, S. Mørup, B. Roessli, and N. Cavadini., submitted to Phys. Rev. Lett. (2003)
5. P. V. Hendriksen, S. Linderoth, and P.-A. Lindgård, Phys. Rev. B **48**, 7259 (1993)

SYMMETRY ANALYSIS OF THE 4*c* SITES IN THE RHOMBOHEDRAL SPACE GROUP $R\bar{3}c$ AND THE MAGNETIC ORDERING OF HEMATITE

B. Lebech (Materials Research Department, Risø National Laboratory, Denmark) and W. Sikora (Faculty of Physics and Nuclear Techniques, University of Mining and Metallurgy, Kraków, Poland)

The models used for description of magnetic structures determined from neutron diffraction data are usually presented as sets of Fourier coefficients of a particular propagation vector ***k*** describing the magnetic moment components on the magnetic atoms in the compound. The propagation vector and the moment directions are most often determined directly from the experimental data and often the model of the magnetic structure is guessed from the absence of certain reflections in the diffraction pattern in combination with experimental results from other techniques (Mössbauer, magnetisation, susceptibility etc.). We have made a symmetry analysis for the 4*c* sites of the rhombohedral space group $R\bar{3}c$ (D_{3d}^6, no. 167), i.e. the space group of hematite (α-Fe_2O_3), a compound that has been studied extensively in recent years as an example of a nano-magnetic material.[1-5] The analysis has been made by means of the PC-programme MODY[6], which is based on the theory of groups and representations proposed by Bertaut[7] and Izymov[8] and predicts possible magnetic structures for particular sites in the considered space group.

In the rhombohedral description of the $R\bar{3}c$ space group for α-Fe_2O_3 the magnetic Fe-atoms occupy the 4*c* positions while the non-magnetic O-atoms occupy 6*e*. In the corresponding hexagonal cell the site positions for the Fe-atoms are 12*c* and 18*e* for the O-atoms. Only the Fe-atoms are important for the symmetry analysis leading to the magnetic structure. Neutron diffraction data indicate that the magnetic structure of hematite should be an antiferromagnetic structure, commensurate with the crystal lattice and with a propagation vector ***k*** along the ***c***-axis of the hexagonal unit cell (body diagonal for the rhombohedral unit cell). According to the symmetry analysis, the only commensurate ***k***-vectors along to ***c***-axis that are compatible with the crystal symmetry are ***k*** = (0 0 0) and ***k'*** = (0 0 3/2) which is equivalent to a cell doubling of the rhombohedral cell along the body diagonal. For ***k*** = (0 0 0) the MODY calculation shows that there are four one-dimensional representations and two two-dimensional representations. Each representation may be a component of the resulting magnetic structure. The one-dimensional representations of ***k*** = (0 0 0) have magnetic moments parallel or antiparallel to the hexagonal ***c***-axis while the two-dimensional ones have magnetic moments in the basal plane of the hexagonal unit cell. For ***k'*** = (0 0 3/2) the MODY results show that there are three two-dimensional representations each of which may be a component of the resulting magnetic structure. In this case one of the two-dimensional representation has magnetic moments parallel or antiparallel to the hexagonal ***c***-axis while the two others have magnetic moments in the basal plane of the hexagonal unit cell.

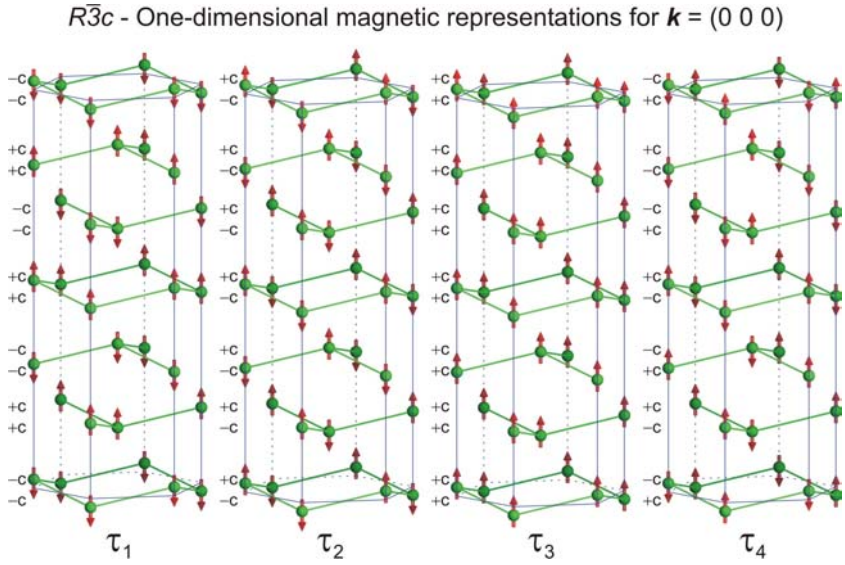

Fig. 1. Illustration of the one-dimensional magnetic representations compatible with the $R\bar{3}c$ space group and derived by MODY for propagation vector ***k*** = (0 0 0). Note that the magnetic structure given by τ_3 is ferromagnetic.

The magnetic structures predicted by the irreducible representations as derived by MODY are possible magnetic structures for the magnetic atoms placed at the 12*c* sites of the hexagonal cell of the $R\bar{3}c$ space group (Fe-atoms in hematite). The real magnetic structures may be linear combinations of these, i.e. the Fe-sites in hematite may order magnetically with moment parallel or perpendicular to the hexagonal ***c***-axis, moments in the hexagonal basal plane or even into a canted magnetic structure having moment components parallel and perpendicular to the hexagonal ***c***-axis.

The relation between the predicted possible magnetic structures and the experimental findings from neutron diffraction, Mössbauer and related techniques will be discussed.

REFERENCES

1. A. H. Morrish, *Canted Antiferromagnetism: Hematite* (World Scientific, Singapore, New Jersey, London, Hong Kong, 1994)
2. M. Catti, G. Valerio and R. Dovesi, Phys. Rev. B **51,** 7441 (1995)
3. F. Bødker, M. F. Hansen, C. B. Koch, K. Lefmann and S. Mørup, Phys. Rev. B **61,** 6826 (2000) and references therein
4. M. F. Hansen, C. B. Koch and S. Mørup, Phys. Rev. B **62**, 1124 (2000)
5. M. F. Hansen, F. Bødker, S. Mørup, K. Lefmann, K. N. Clausen and P.-A. Lindgård, J. Magn. Magn. Mat. **221,** 10 (2000)
6. W. Sikora, In: *Proceedings of Symmetry and Structural Properties of Condensed Matter*, Zajączkowo, Poland, p.484. (1994), the MODY program may be made available by contacting W. Sikora
7. E. F. Bertaut, Acta Crystallogr. Section A **24,** 217 (1968)
8. Y. A. Iyumov, *Phase Transitions and Crystal Symmetry* (Kluwer Academic Publishers, Dordrecht, 1990)

SPIN-POLARIZED TUNNELING STUDY OF (Ga,Mn)As/SUPERCONDUCTOR JUNCTIONS

B. S. Sørensen, J. Sadowski (Niels Bohr Institute fAPG, Ørsted Laboratory, University of Copenhagen, Denmark), A. Jensen, (Department of Physics, Technical University of Denmark, Denmark) and P. E. Lindelof (Niels Bohr Institute fAPG, Ørsted Laboratory, University of Copenhagen, Denmark)

The discovery of ferromagnetism in the dilute magnetic semiconductor (Ga,Mn)As initiated a rapid expansion in both the experimental and theoretical investigation of this material. Ferromagnetism in (Ga,Mn)As is commonly related to the magnetic exchange interaction between the conduction holes and the magnetic moment of the localised substitutional Mn^{2+}-ions[1]. In view of the ongoing experiments on spintronics devices, the degree of spin-polarization of the charge carriers in (Ga,Mn)As is a very important question. It has been predicted to be as high as 80 %[1], but to our knowledge no experimental results has been published on this subject. Using the approach of a ferromagnet/superconductor tunnel junction in a magnetic field, first used by Tedrow and Meservey[2], we have determined the spin polarization of a 30 nm thick $Ga_{0.94}Mn_{0.06}As$ film by electrical transport measurements at ^{3}He temperatures. We have also observed the effect of Zeeman splitting in a superconducting layer induced by the ferromagnet.

A thin layer of Al is evaporated on epitaxially grown $Ga_{0.94}Mn_{0.06}As$ imbedded in low temperature GaAs. The Al thickness was determined using a quartz-crystal monitor and set to 1.5 nm. The sample was then exposed to ambient air for 24 hours. Afterwards a second Al layer with thickness of 50 nm was evaporated followed by a gold layer. The $Ga_{0.94}Mn_{0.06}As$ was contacted using Cr/Au. The Curie temperature of the $Ga_{0.94}Mn_{0.06}As$ layer has been determined from resistance vs. temperature measurements to be 65 K. Two-point measurements of the differential conductance of the tunnel devices as a function of voltage have been made. The devices were placed in a ^{3}He-cryostat with the applied magnetic field in plane of the Al-film. This configuration ensures high enough breakdown fields of the superconducting state, to observe relatively large Zeemann splitting before the superconducting state is destroyed. Furthermore the (Ga,Mn)As film has in-plane magnetic easy axis. Results from one tunnel junction at different values of the applied magnetic field are shown in Fig. 1a. With increasing magnetic field, the increasing Zeemann splitting of the levels on each side of the superconducting gap in the Al-film, results in four peaks in the conductance. The innermost peaks correspond to conduction across the tunnel junction of one spin-direction only, whereas the outermost peaks are a mixture of both spin-directions. Since the spins are unaffected by the Al-oxide tunnel barrier, the relative difference in conduction of the peaks is a direct measure of the spin-polarization of the charge carriers in the ferromagnet[2]. Examination of the results shows that the energy difference between the spin-split peaks equals $2\mu_B B$ in the intermediate magnetic field range. The degree of spin-polarization of the ferromagnet, calculated by use of the relative difference in peak conductance, is seen to depend on the magnitude of the applied magnetic field. The value decreases from about

35 % at B= 1 T to less than 1 % just before the superconducting state is destroyed at above 4 T. It is not clear if this can be attributed to the behaviour of the ferromagnet. The difference in height of the conductance peaks depending on the relative bias between the ferromagnet and the superconductor, reveals that the electrons in the tunnel current is predominantly with spin-direction anti-parallel to the magnetization of the GaMnAs layer.

A result from another device is shown in Fig. 1b. Here four peaks are present at zero field. This effect resembles tunnelling between two superconductors with different energy gaps, where the energy levels of one superconductor are Zeemann split by an exchange field arising from the ferromagnetic layer[3]. We attribute this effect to insufficient oxidation of the tunnel layer, resulting in an $Al/Al_2O_3/Al/GaMnAs$ structure. At B = 4.5 T only one of the Al layers are superconducting, and a low degree of spin-polarization of the ferromagnet, comparable to the other device, can be deduced.

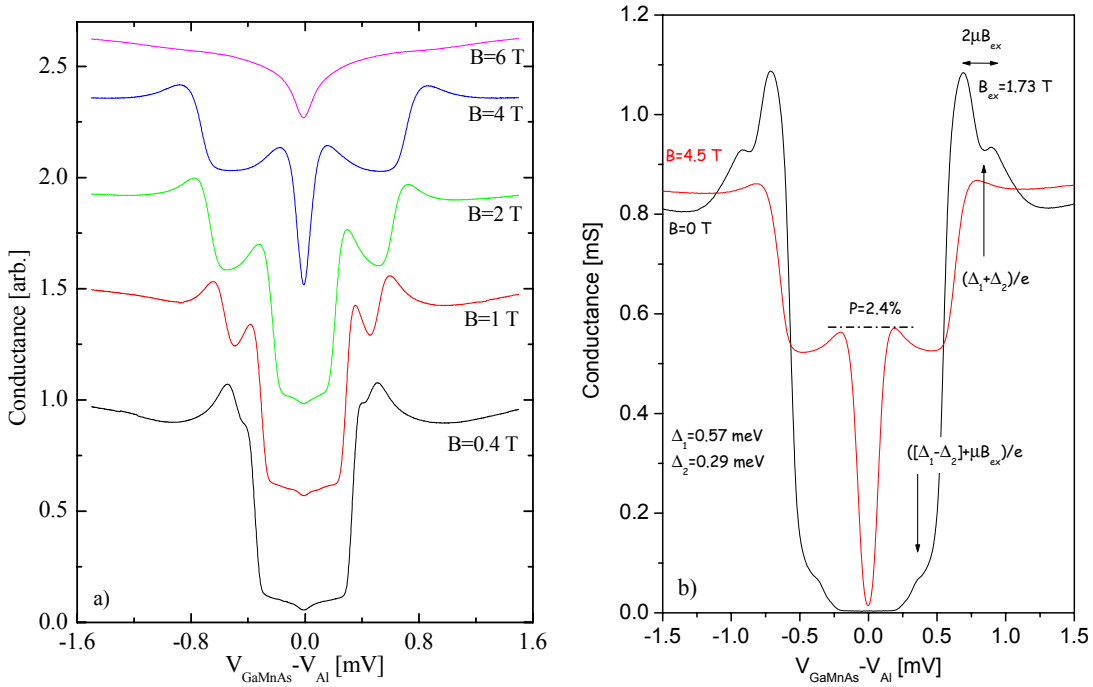

Fig. 1. (a) Differential conductance as a function of bias at different in-plane magnetic fields at T = 60 mK of an $Al/Al_2O_3/GaMnAs$ junction, and (b) of what can be interpreted as an $Al/Al_2O_3/Al/GaMnAs$ junction. Each graph in (a) is offset for clarity.

REFERENCES

1. T. Dietl, H. Ohno, and F. Matsukura, Phys. Rev. B **63**, 195205 (2001)
2. P. M. Tedrow and R. Meservey, Phys. Rev. B **7**, 318 (1973)
3. J. E. Tkaczyk and P. M. Tedrow, Phys. Rev. B **46**, 8344 (1992)

Fe-CONTACTS ON InAs(100) AND InP(100) CHARACTERISED BY CONVERSION ELECTRON MÖSSBAUER SPECTROSCOPY

C. D. Damsgaard (Department of Physics, Technical University of Denmark, Denmark), H. P. Gunnlaugsson, G. Weyer (Department of Physics and Astronomy, Aarhus University, Denmark), T. A. Anhøj, S. Mørup, J. B. Hansen, C. S. Jacobsen, L. Lilleballe, I. Rasmussen, J. L. Skov (Department of Physics, Technical University of Denmark, Denmark)

Ferromagnet-semiconductor heterostructures are currently of high interest because of their potential applications in the field of spintronics[1], which explores the possibilities of using the electronic spin as a control parameter in electronic devices in addition to the charge. Multilayers of ferromagnets and nonmagnetic metals are already widely used as magnetoresistive sensors, and one could hope to consider-ably increase the range of applications by combining ferromagnets with semiconductors thus exploiting their enormous flexibility with respect to carrier concentration, mobility and the ability of creating electronic structures of restricted dimensionality. The concept of the spin field effect transistor[2] has greatly stimulated the interest.

For spintronic devices to work, a spin-polarised current is needed. One way of obtaining that is by injecting a current from an aligned ferromagnetic contact into the semiconductor structure. The first step towards success is to fabricate near perfect epitaxial interfaces between ferromagnets and semiconductors. In this work we have deposited Fe-57 on variously prepared (100) surfaces of InAs and InP and subsequently studied the chemical/magnetic properties by using the surface-sensitive Conversion Electron Mössbauer Spectroscopy (CEMS). This technique was recently used to study Fe films on GaAs.[3]

The Fe-deposition was done by thermal electron-beam evaporation from a small alumina crucible in a metal MBE-system. The substrates were in all cases held at 1^{o}C and the film thicknesses were 4-7 nm. In some cases the Fe-57 layers were subsequently protected by evaporating a 2 nm gold layer. During growth the crystallinity of the surface could by checked using Reflection High Energy Electron Diffraction (RHEED). The following samples were prepared:

SAMPLE	DESCRIPTION
InAs #1	Surface as received. 5 – 7 nm Fe, no Au
InAs #2	Surface as received. 4 nm Fe, no Au
InAs #3	As #1, but sample stored in air for several months
InAs #4	As #3, but sample annealed for 1h @ 450^{o}C, < 10^{-5} mbar
InAs #5	Annealed @ 611^{o}C + 3 min. ion mill (100 eV Ar) 4 nm Fe, 2 nm Au
InAs #6	Surface 3 min. ion milled, 4 nm Fe, 2 nm Au
InAs #7	Photoresist on surface and subsequent ion milling, 4 nm Fe, 2 nm Au
InP	Surface ion milled for 3 min. 4 nm Fe, 2 nm Au

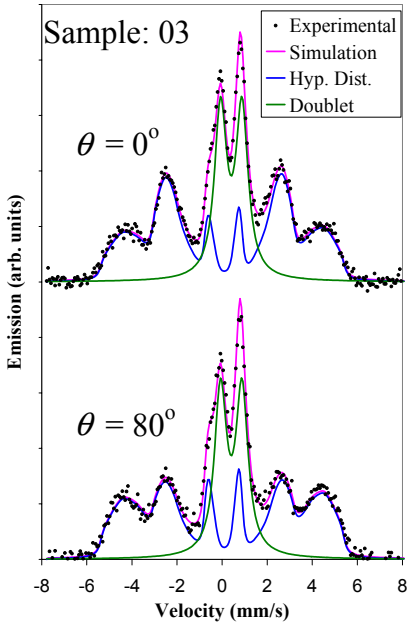

Fig. 1. Mössbauer spectra for Fe-57 thin-film on InP(100) measured for two angles θ between the surface normal and the γ-direction. Dots are experimental points. Solid lines are fits to a magnetic hyperfine field distribution plus a doublet.

A remarkable result is that for InP; CEMS spectra are shown in Fig. 1. The broadened sextet is not consistent with α-Fe, but rather indicates the formation of an amorphous phase. This is consistent with the absence of a RHEED pattern after growing the Fe-57 film, even with a clear pattern before. In contrast, the samples InAs #5 to #7 all show nice sextets indicative of dominant α-Fe and RHEED patterns after growth.

Samples InAs #1 and #2 both have a considerable content of a component, which can be attributed to some Fe-As alloy. This interpretation is supported by the component being strongest in the thinner film (InAs #2). The samples InAs #3 and #4 both show much deteriorated character. These latter results show that it is in no way acceptable to grow iron directly on "as received" substrates. Presumably the surface accommodates an excess of As, which must be removed by annealing and soft ion milling. Actually the study indicates that soft ion milling suffices. Also it is worth noting that sample InA s#7 shows no deterioration. Here typical patterning processes were done prior to deposition of Fe-57.

In conclusion, we have found that epitaxial Fe films may be grown on InAs(100) provided the surface is cleaned by a soft ion milling with 100 eV Ar. Surprisingly we have found signs of amorphous iron on an ion milled InP-substrate.

REFERENCES

1. See, for example, G. A. Prinz, Science **282**, 1660 (1998)
2. S. Datta and B. Das, Appl. Phys. Lett. **56**, 665 (1990)
3. B. R. Cuenya et al. , Appl. phys. Lett. **82**, 1072 (2003)

THE USE OF HEUSLER ALLOYS IN SPINTRONICS

C. D. Damsgaard, J. B. Hansen, C. S. Jacobsen, L. Lilleballe (Department of Physics, Technical University of Denmark, Denmark), P. E. Lindelof (Niels Bohr Institute fAPG, Ørsted Laboratory, University of Copenhagen, Denmark), I. Rasmussen and J. L. Skov (Department of Physics, Technical University of Denmark, Denmark)

Since R. A. de Groot[1] first predicted the Heusler alloys NiMnSb and PtMnSb to exhibit half-metallic behavior, there has been increasing interest in using half-metallic materials in applications such as spin valves, magnetic tunnel junctions and spin injectors for semiconductors. Half-metallic ferromagnets constitute a unique class of materials in which one spin subband has metallic character while the other has semiconducting or insulating behavior.[2] As a result in such a ferromagnet, the conduction electrons are predicted to be 100% spin polarized.

Recently, spin injection have been attempted into a semiconductor by the use of either a ferromagnetic semiconductor (ex. GaMnAs) or a ferromagnetic metal (ex. Fe, Ni, Co etc.). In both cases the efficiency is very low at 300 K, at least in the diffusive limit. Semiconducting ferromagnetic injection due to the low Curie temperature for GaMnAs (approximately 100 K) and ferromagnetic metal injection due to a moderate spin polarization combined with the conductivity mismatch between the ferromagnetic metal and the semiconductor result in very small effects.[3] The solution to the problem may be to use half metals as injectors.

In the poster, an introduction to spintronics and Heusler alloys will be given. Recent results and measurement techniques on epitaxially grown Heusler alloys on semiconducting substrates will be discussed.

REFERENCES

1. R. A. de Groot et al., Phys. Rev. Lett. **50,** 2024 (1983)
2. J. M. D. Coey and M. Venkatesan, J. Appl. Lett. **91,** 8345 (2002)
3. G.Schmidt et al., Phys. Rev. B. **62,** R4790 (2000)

FIELD-DRIVEN HYSTERETIC AND REPEATABLE RESISTIVE SWITCH IN OXIDE INTERFACES

Y. Y. Xue, S. Tsui (Department of Physics and Texas Center for Superconductivity, University of Houston, Houston, Texas, USA) and C. W. Chu (Department of Physics and Texas Center for Superconductivity, University of Houston, Houston, Texas, USA; Lawrence Berkeley National Laboratory, Berkeley, California, USA; Hong Kong University of Science and Technology, Hong Kong)

The resistive polarity-dependent switch driven by electric pulses has been studied in different perovskite oxides, including cuprates, nickelates, manganites, and others. The data demonstrate that this hysteretic and repeatable polarity-dependent switch is a common phenomenon in the highly defective metal-oxide interface with no particular correlation to the detailed magnetic and structural properties of the bulk compounds. It occurs within a layer much thinner than our experimental resolution of 10-50 nm and is accompanied by a capacitance increase associated with charge accumulation accompanied by a relatively slow response time. The interface resistance shows a power-law I-V characteristic and the same temperature dependency in both the low- and high-resistance states. We propose a space-charge limit with carrier trapping as the mechanism responsible for the switch. The electro migration of crystalline defects, therefore, will play a key role in possible device applications. Ways to shorten the response time, which is crucial for applications, will be discussed.

ANTIFERROMAGNETISM IN $YBa_2Cu_3O_{6+x}$ NANOPARTICLES STUDIED BY ELASTIC NEUTRON SCATTERING

L. Theil Kuhn, P. Andersen, K. Lefmann, N. H. Andersen (Materials Research Department, Risø National Laboratory, Denmark), M. Meedom Nielsen (Danish Polymer Centre, Risø National Laboratory, Denmark), P. Paturi, J. Raittila (Wihuri Physical Laboratory, Department of Physics, University of Turku, FIN-20014 Turku, Finland)

The interplay between antiferromagnetism and superconductivity in the compound $YBa_2Cu_3O_{6+x}$ in bulk form has been intensively studied; see for instance.[1] We have initiated a similar study but now focusing on the properties as the size of $YBa_2Cu_3O_{6+x}$ nanoparticles becomes comparable to the coherence length for superconductivity. Here we present the first results on the antiferromagnetic phase of $YBa_2Cu_3O_{6+x}$ (x = 0.15, x = 0.25 and x = 0.37) nanoparticles, i.e. the behaviour of the Neél temperature for the various degrees of oxygen doping, studied by elastic neutron scattering.

The YBCO nanoparticles were prepared by a citrate gel modification of the sol-gel technique as described in[2], and subsequently reduced in a N_2 atmosphere to zero oxygen doping. The YBCO nanoparticle powder were in a controlled manner oxidized in an O_2 atmosphere obtaining different degrees of oxygen doping, i.e. x = 0.15, x = 0.25 and x = 0.37. The composition, crystal structure and the nanoparticle size and shape was characterized by x-ray powder diffraction and high resolution electron microscopy showing that the main part of the nanoparticles are pure tetragonal phase $YBa_2Cu_3O_{6+x}$, however a few percent of the impurity phase $Y_2Cu_2O_5$ is present. The YBCO nanoparticles are disk-shaped with the Cu-O planes perpendicular to the short axis of the disk and have an average diameter of 50 nm.

The elastic neutron scattering was performed at the triple-axis spectrometer RITA-2 at SINQ, Paul Scherrer Institute, Switzerland. The spectrometer was run at 5meV, and the beam was defined by slits at the monochromator, at the sample and at the analyser. A Be-filter with radial collimators was inserted between sample and analyser to reduce higher order scattering. Elastic q-scans were measured on the samples in the temperature range 15 K to 500 K. In the q-range we have studied there are two antiferromagnetic reflections, i.e. (½ ½ 1) and (½ ½ 2), but due to the very low intensity we have focussed our study on the (½ ½ 1) reflection. We have measured the behaviour of this reflection with temperature for x = 0.15, x = 0.25 and x = 0.37 and hereby measured the transition between the paramagnetic and antiferromagnetic phase and obtained the Neél temperature, which decreases with increasing x-value. For this nanoparticle size the Neél temperatures correspond to the bulk values.

REFERENCES

1. J. M. Tranquada et al, Phys. Rev. B **38**, 2477 (1988)
2. E. Blinov et al, Supercond. Sci. Technol. **10**, 818 (1997), J. Raittila et al, Physica C **317**, 90 (2002)

PHASE EQUILIBRIA IN THE SrO – Sc_2O_3 – CuO SYSTEM WITH EMPHASIS ON THE $Sr_{14}Cu_{24}O_{41-\delta}$ PHASE

J.-C. Grivel and N. H. Andersen (Materials Research Department, Risø National Laboratory, Denmark)

The sub-solidus phase relations in the Sc_2O_3 – SrO – CuO system were determined at 900°C in air (see Fig. 1). Like in the case of SRE_2O_3 – SrO – CuO systems with SRE = small rare-earth elements, no ternary compound was formed. However, the Sc_2O_3 – SrO – CuO system is dominated by the Sc_2SrO_4 phase, which is in equilibrium with all other phases. This is not the case in SRE_2O_3 – SrO – CuO systems, where the $SRE_2Cu_2O_5$ phase is in equilibrium with $Sr_{14}Cu_{24}O_{41-\delta}$.[1] We confirm that the $Sr_{14}Cu_{24}O_{41-\delta}$ phase is slightly Cu-deficient[2], its formulation being closer to $Sr_{14}Cu_{23.5}O_{41-\delta}$.

While all rare-earth elements substitute on the Sr sites in the $Sr_{14}Cu_{24}O_{41}$ phase, Sc appears to partially replace Cu instead. This difference can be understood on the basis of ion size considerations. The solubility limit of Sc is low and amounts to about 2 at%. This substitution results in a shrinkage of the c-axis (running along the chains and ladders of the structure) by 0.3%.

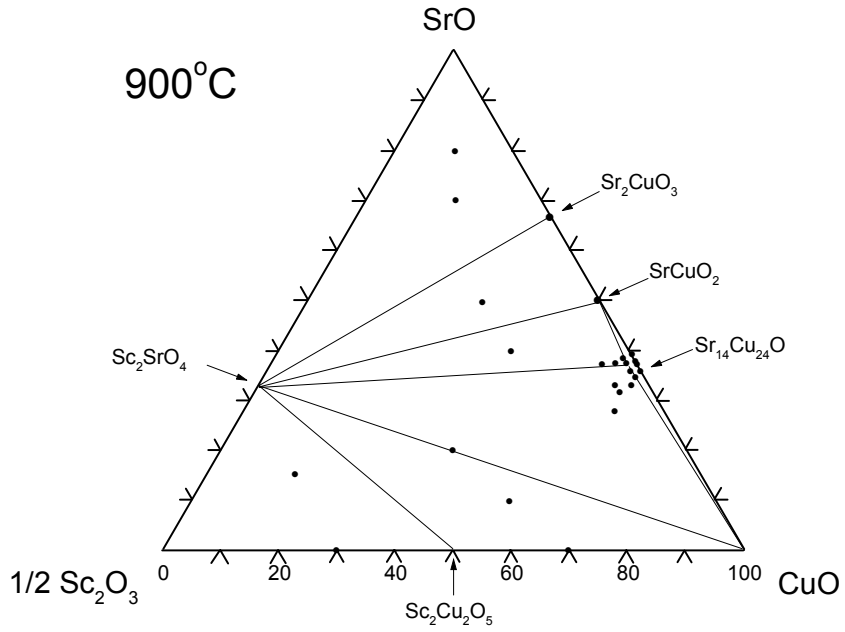

Fig. 1. Phase equilibria in the Sc_2O_3 – SrO – CuO system at 900°C in air

REFERENCES

1. W. Wong-Ng et al., Int. J. Inorg. Mater. **3** (2001) 1283
2. E.M. McCarron et al., Mat. Res. Bull. **23** (1988) 1355

MAGNETIC-FIELD DRIVEN $x \approx 1/8$ ANOMALY OF SUPERCONDUCTIVITY IN $La_{2-x-y}Sr_xMn_yCuO_4$

R. Laiho, J. Salminen and V. Zakhvalinskii (Wihuri Physical Laboratory, University of Turku, FIN - 20014 Turku, Finland)

Craford et al.[1] found in $La_{1.6-x}Nd_{0.4}Sr_xCuO_4$ (LNSCO) and in LSCO a local minimum of the superconducting critical temperature $T_c(x)$ at the concentration of $x \approx 1/8$. Later on Nakamura and Uchida[2] have observed a discontinuous jump in various transport coefficients of LNSCO at $x \approx 1/8$. In layered cuprates the competition between the kinetic energy of charge carriers and the superexchange interactions between neighbouring Cu spins leads to spatial segregation of holes, forming antiphase domain walls between stripes of antiferromagnetically correlated Cu spins. Referring to lattice commensuration effects Tranquada et al.[3] explained the $x = 1/8$ anomaly by freezing of charged domain walls in the low-temperature tetragonal LTT phase of LNSCO. However, nuclear-quadrupole-resonance experiments[4] show no anomaly at $x = 1/8$ and Ichikawa et al.[5] have concluded that it is caused mainly by local antiferromagnetic order.

We have prepared by substituting Mn^{3+} for La^{3+} ceramic $La_{2-x-y}Sr_xMn_yCuO_4$ (LMSCO) samples with $0.08 \le x \le 0.15$, $0 \le y \le 0.05$ and $x + y = 0.15$. The critical temperatures of the samples, $T_c(x, y)$, are determined from onsets of the Meissner susceptibility in measurements with a SQUID magnetometer between 4 and 300 K. The values of $T_c(y)$ show in the field of 8 mT a weak decrease when y is increased between 0 and 0.015 and a valley between 0.015 and 0.03 before total collapse of the superconductivity at $y = 0.05$. Around $y = 0.025$ ($x = 0.125$) the T_c can be suppressed to zero by application of a field of 0.6 mT. A weak drop of T_c at $x = 0.125$ is observed also in LSCO but without any influence of magnetic field at least up to100 mT.

To understand the magnetic interactions brought about by doping with Mn the temperature dependence of the magnetic susceptibility of LMSCO is investigated for different y in the normal state. Analyzing the data in terms of Mn^{3+} ions using a cluster Hamiltonian[6] and the Curie - Weiss law $\chi - \chi_0 = C/(T - \theta)$ a correlation is observed between the minimum of T_c at $y = 0.025$ and the maxima of the number of Mn^{3+}-Mn^{3+} pairs, the effective Bohr magneton number $p_{eff} = 30$ and the Curie temperature $\theta = -$ –240 K. No long-range magnetic correlations neither the LTT phase is observed in our LMSCO samples by neutron diffraction investigations made at LLB, Saclay, France.

Although the charge stripes in LSCO are likely to be disordered and dynamic, a small dip of T_c is observed by magnetization measurements for the sample with $x = 1/8$ as mentioned above. In LMSCO this behaviour is greatly enhanced, obviously as a result of interaction between the superconducting carriers in the CuO_2 plane and the Mn-Mn pairs occupying two nearest neighbour positions of La^{3+} at a mutual distance of 3.668 Å along the *c*-axis. However, it is likely that this distance is too long to support a direct Mn-Mn exchange interaction. On the other hand, the magnetic properties of LMSCO, including the values of θ and $J/k \approx -0.45$, resemble above T_c in many ways those of the diluted magnetic semiconductors $Hg_{1-x}Mn_xTe$ ($J/k = -0.7$)[6] and $Cd_{1-x}Mn_xTe$ (J/k = –0.55)[7] for $x < 0.1$ where the coupling mechanism is ascribed to superexchange interaction by *d-sp* band hybridization in a triangle formed by two Mn ions and one Te ion.[8]

Applying the same three-center-model to LMSCO the canting between the Mn spins S_1 and S_2 can be expressed by the angle $\theta_{12} \sim \pi - |D_{12}/J_{12}|$ where $J_{12} \propto \cos\phi^2$ is the AF superexchange interaction constant and $D_{12} \propto \cos\phi \cdot \sin\phi \cdot z$ is the Dzyaloshinsky-Moriya anisotropic exchange constant. In a usual case $D_{12} << J_{12}$ one gets $\theta_{12} \approx \pi$. Using the Mn-Mn distance of 3.668 Å and the Mn-O distance of 2.63 Å we have $\phi \approx 90^o$. According to the band theory of magnetism in MnO, the nearest-neighbour 90^o Mn-O-Mn coupling is antiferromagnetic due to bonding of t_{2g} orbitals of one Mn ion and e_g orbitals of the other via the oxygen p orbitals.[9]

To conclude, we attribute the strong suppression of T_c by magnetic field in LMSCO (y = 0.025) to interaction between local AF order and mobile charge stripe domains, reducing the density of superconducting pairs by polarization of the carriers due to hybridization of the manganese and oxygen orbitals in the CuO_2 plane. Our results encourage testing of alternating LSCO and LMSCO (x = 1/8) layers where the layer containing Mn^{3+} could be driven with a modest magnetic field from the superconducting to the normal state.

REFERENCES

1. M. K. Crawford et al., Phys. Rev. B **44**, 7749 (1991)
2. Y. Nakamura and S. Uchida, Phys. Rev. B **46**, 5841 (1992)
3. J. M. Tranquada et al., Nature **375**, **561** (1995); Tranquada et al., Phys Rev. Lett. **78**, 338 (1997)
4. A. W. Hunt et al., Phys. Rev. Lett. **82**, 4300 (1999); P. M. Singer, A. W. Hunt et al., Phys. Rev. B **60**, 15345 (1999)
5. N. Ichikawa et al., Phys. Rev. Lett. **85**, 1738 (2000)
6. S. Nagata et al., Phys. Rev. B **22**, 3331 (1980)
7. R. R. Galazka et al., Phys. Rev. B **22**, 3344 (1980)
8. B. E. Larson and H. Ehrenreich, J. Appl. Phys. **67**, 5084 (1990)
9. T. Oguchi et al., Phys. Rev. B **56**, 6120 (1997)

FIELD-INDUCED ANTIFERROMAGNETISM IN THE CUPRATE HIGH-T_c SUPERCONDUCTOR $La_{2-x}Sr_xCuO_4$

B. Lake (Oxford University, U.K.), G. Aeppli (University College London, U.K.), N. B. Christensen, K. Lefmann, D. F. McMorrow, K. N. Clausen, (Risø National Laboratory, Denmark), H. M. Rønnow, (N.E.C. Research Institute, U.S.A.), N. E. Hussey, (University of Bristol, U.K.), P. Vorderwisch, P. Smeibidl, (Hahn-Meitner Institut, Germany), N. Mangkorntong, T. Sasagawa, M. Nohara, H. Takagi, (University of Tokyo, Japan)

The cuprate high-transition temperature superconductor $La_{2-x}Sr_xCuO_4$ (LSCO) is structurally the most simple of the cuprate superconductors, making this system attractive for seeking the fundamental mechanisms behind high-temperature superconductivity. One class of theories connects the superconducting mechanism with the magnetic properties of the material[1], calling for detailed investigations of cuprate magnetism.

We have performed neutron scattering measurements on LSCO in zero and applied magnetic fields. In the superconducting phase, $T < T_c$ and $H < H_{c2}$, magnetic flux penetrates the superconductor via vortices while phase coherent superconductivity is suppressed to the lower field-dependent irreversibility temperature, $T_{irr}(H)$. We show that both optimally doped LSCO (x = 0.16, T_c = 38.5 K) and underdoped LSCO (x = 0.10, T_c = 29 K) have an enhanced antiferromagnetic response in a field.

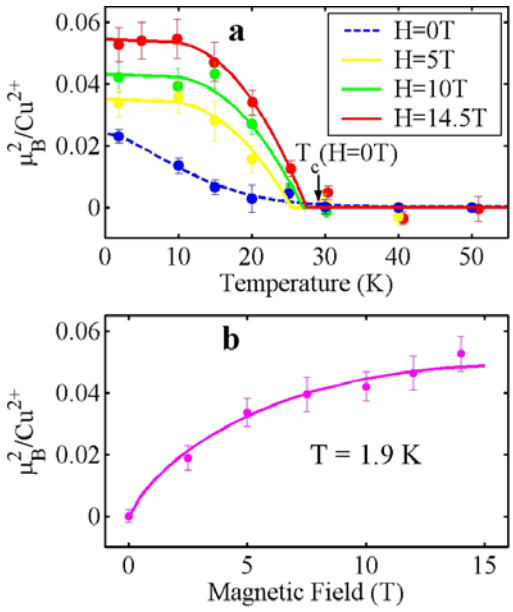

Fig. 1. (Upper panel) Zero field and field-induced elastic neutron signals at LSCO (x = 0.10) as a function of temperature. The superconducting transition temperature in zero field is marked with an arrow. Data were taken at the V2 spectrometer at HMI, Berlin. (Lower panel) Field induced ordered moment at T = 2 K shown as a function of applied magnetic field. The curve shows the theoretical prediction by Demler et al.[4], scaled by an overall factor.

Measurements of the optimally doped system in zero field show incommensurate short-range fluctuations at all energies above T_c while an energy gap opens up in the superconducting phase.[2] In an applied field of H = 7.5 T we observe incommensurate sub-gap spin fluctuations, which upon cooling disappear with the loss of finite resistivity at T_{irr}, but then reappear at a lower temperature.[3]

In the underdoped system, x = 0.10, long-range (>400 Å) antiferromagnetic order develops in zero field, and the order is significantly enhanced by application of a magnetic field. The field-induced signal vanish at the zero-field value of T_c. Phase coherent superconductivity is then established within the antiferromagnetic phase at the lower $T_{irr}(H)$. The strength of the field-induced signal is modelled perfectly by a theoretical prediction by Demler et al.[4], as shown in Fig. 1.

Our results imply that for optimally doped LSCO the vortices nucleate large antiferromagnetic regions extending beyond the vortex cores. For underdoped LSCO, the vortices link pre-existing regions of antiferromagnetic order, possibly nucleated by impurities. Our recent results indicate a field-induced correlation between antiferromagnetic regions in the direction perpendicular to the superconducting planes.

REFERENCES

1. M. R. Norman and C. Pépin, cond-mat/0302347, (2003)
2. B. Lake, G. Aeppli, K. N. Clausen, D. F. McMorrow, K. Lefmann, N. E. Hussey, N. Mangkorntong, M. Nohara, H. Takagi, T. E. Mason, and A. Schröder, Science **291**, 832 (2001)
3. B. Lake, H. M. Rønnow, N. B. Christensen, G. Aeppli, K. Lefmann, D. F. McMorrow, P. Vorderwisch, P. Smeibidl, N. Mangkorntong, T. Sasagawa, M. Nohara, H. Takagi, and T. E. Mason, Nature **415**, 299 (2002)
4. E. Demler, S. Sachdev, and Y. Zhang, Phys. Rev. Lett. **87**, 067202 (2001)

A COMPARISON BETWEEN THE SPIN FLUCTUATION SPECTRA OF UNDERDOPED AND OPTIMALLY DOPED $La_{2-x}Sr_xCuO_4$

N. B. Christensen and D. F. McMorrow (Materials Research Department, Risø National Laboratory, Denmark), B. Lake (Clarendon Laboratory, University of Oxford, UK), H. M. Rønnow (CEA Grenoble, France), S. M. Hayden (H. H. Wills Physics Laboratory, University of Bristol, UK), G. Aeppli (NEC Research Institute, New Jersey, USA), T. G. Perring (ISIS Facility, Rutherford Appleton Laboratory, UK), H. Tagaki (Institute of Solid State Physics, University of Tokyo, Japan)

Time-of-flight neutron spectrometry has been used to study the spin excitation spectra of under doped (x = 0.10) and optimally doped (x = 0.163) $La_{2-x}Sr_xCuO_4$ (LSCO) over the full Brillouin zone at energies up to 40 meV, while retaining good resolution in both energy and wave vector. Each sample is studied in both normal and superconducting states. Our analysis allows us to obtain and compare "global views" of $\chi''(q, \omega)$, the imaginary part of the dynamic susceptibility, at the two doping levels. While the overall intensity distributions and absolute magnitudes of $\chi''(q, \omega)$ are similar, there are important differences in the spectral weight redistribution upon entering the superconducting state.

When compared with results on $YBa_2Cu_3O_{7-x}$, (YBCO) our data reveals striking similarities in $\chi''(q, \omega)$ for these two families of superconductors. These results challenge the commonly held view that the spin excitations of LSCO systems should be thought of in terms of stripe fluctuations[1-2] while those of YBCO can be most easily understood as arising from Fermi surface nesting.[3]

We discuss our results in the light of recent theories within the stripe[4] and Fermi surface nesting[5] schools of thought.

REFERENCES

1. J. M. Tranquada et al, Nature **375**, 561 (1995)
2. J. Zaanen and O. Gunnarsson, Phys. Rev. B **40**, 7391 (1989)
3. Q. Si et al, Phys. Rev. B **47**, 9055 (1993)
4. C. D. Batista, G. Ortiz and A. V. Balatsky, Phys. Rev. B **64**, 172508 (2001)
5. M. R. Norman, Phys. Rev. B **61**, 14751 (2000)

EVIDENCE FOR THERMALLY INDUCED VORTEX FLUCTUATIONS ABOVE T_c IN HIGH TEMPERATURE SUPERCONDUCTORS

Ulrik Thisted, Jørgen Nyhus (Norwegian University of Science and Technology, Norway), Takashi Suzuki, Junya Hori (ADSM, Hiroshima University, Japan) and Kristian Fossheim (Norwegian University of Science and Technology, Norway)

There has been increasing interest in the properties of the so called pseudogap (PG) phase of high temperature superconductors (HTSC).[1] This phase is characterised by a PG in the single particle spectrum as measured by tunneling spectroscopy[2]. Recently, the presence of vortices in this phase has been suggested due to the observation of an anomalous Nernst signal.[3] Furthermore, the discovery of diamagnetic domains in the PG phase by scanning SQUID microscopy[4], has supported the assumption that the nature of the PG phase is closely connected with superconductivity.

We have performed ac susceptibility (χ_{ac}) and elastic constant measurements on a single crystal of $La_{1.85}Sr_{0.15}CuO_4$. We found that if the amplitude of the ac field used to probe the magnetic behaviour is very small (~1 mG), the sample shows a diamagnetic response in a temperature region above T_c, T_c (37 K) < T < T* (41 K), as can be seen in Fig. 1.

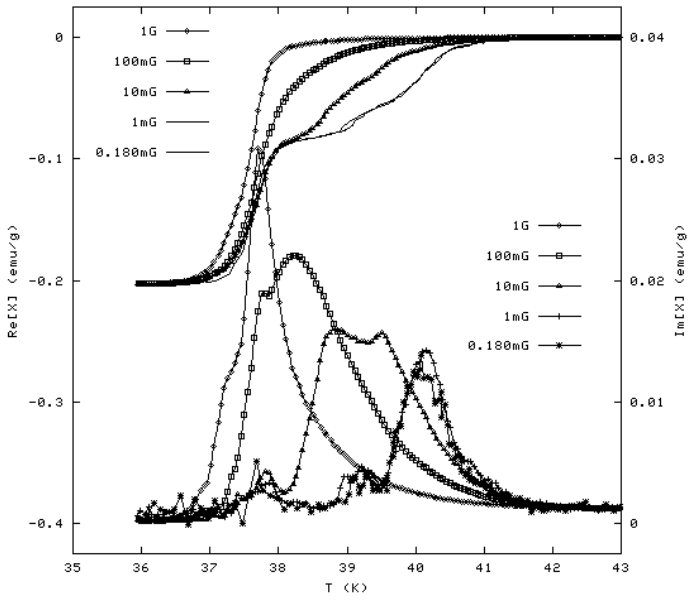

Fig. 1. Real (filled symbols) and imaginary (open symbols) part of ac susceptibility in $La_{1.85}Sr_{0.15}CuO_4$ when measured with different ac field amplitudes. Measurements are performed at f = 10 kHz and with the field along the c-axis. The 1 mG and 180 μG curves almost coincide and are shown without data markers for clarity. The solid curves are guides to the eye.

The observed diamagnetic response is only detected for fields along the *c*-axis, this corresponds well with the anomalous Nernst signal, which has also only been observed for fields along the *c*-axis.[5] The diamagnetic response is almost frequency independent and is observable in bias fields as high as 1 T.

We have found an interesting correlation with other measurements on the same sample: In Fig. 2 we show the temperature dependence of the elastic constant c_{33} in zero magnetic field. It has been shown by thermodynamic analysis, that a change in c_{33} at phase transitions is proportional to the change in specific heat C_p but with opposite sign.

In fig. 2 we see two anomalies in c_{33}. The one at T_c resembles C_p at the lambda point in ^{4}He whereas the one at T^* resembles more the step-like anomaly in C_p of a BCS superconductor. We therefore suggest that the anomaly at T^* is caused by formation of Cooper pairs, and the transition at T_c is caused by these Cooper pairs attaining phase-coherence. Between T_c and T^* we have a densely packed vortex tangle of thermally induced vortex loops and field induced vortex lines.[6, 7] The measurements of c_{33} and χ_{ac} show the same characteristic temperatures T_c and T^*.

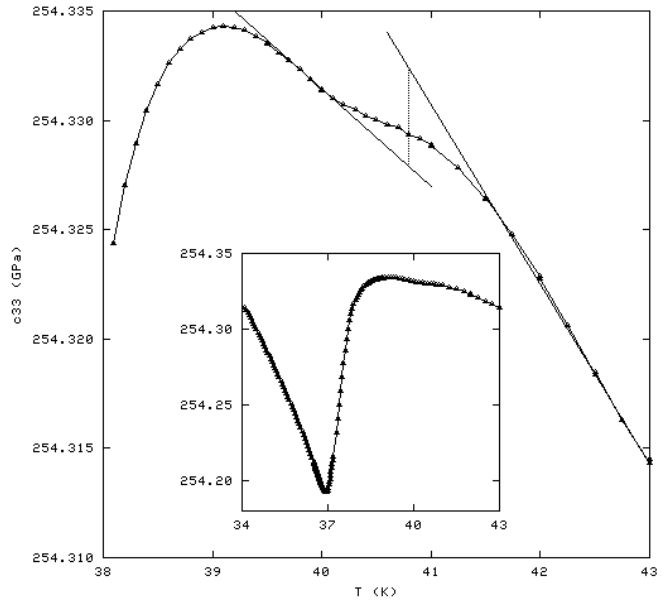

Fig. 2. Elastic constant c_{33} of $La_{1.85}Sr_{0.15}CuO_4$ measured by ultrasound in zero field. There is a small but significant step feature at T^* between 40 K and 41 K, resembling that observed in BCS superconductors. The large cusp anomaly at T_c is shown in the insert and resembles the lambda curve in ^{4}He. Lines are guides to the eye.

We suggest, that the diamagnetic response in the PG phase is caused by a surface barrier against vortex penetration due to the presence of a high density of Cooper pairs, i.e. a superfluid component above T_c.

REFERENCES

1. T. Timusk and B. Statt, Rep. Prog. Phys. **62**, 61 (1999)
2. C. Renner, B Revaz, J.-Y. Genoud, K. Kadowaki and Ø. Fischer, Phys. Rev. Lett. **80**, 149 (1998)
3. Z. A. Xu, N. P. Ong, Y. Wang, T. Kakeshita, and S. Uchida, Nature (London) **406**, 486 (2000)
4. I. Iguchi, T. Yamaguchi and A. Sugimoto, Nature (London) **412**, 420 (2001)
5. H. H. Wen, Z.Y. Liu, Z. A. Xu, Z. Y. Weng, F. Zhou and Z. X. Zhao, cond-mat/0301367 (2003)
6. Z. Tesanovic, Phys. Rev. B **59**, 6449 (1999)
7. A. K. Nguyen and A. Sudbø, Phys. Rev. B **60**, 15307 (1999)

NON-LUTTINGER DYNAMICS IN A STRONGLY COUPLED ONE-DIMENSIONAL ELECTRON GAS

Vadim V. Cheianov (NORDITA, Copenhagen, Denmark) and Mikhail Zvonarev (Niels Bohr Institute, University of Copenhagen Niels Bohr Institute fAPG, University of Copenhagen, Denmark)

Zero-temperature asymptotics of two-point correlation functions of an integrable one-dimensional model describing spinful electrons with repulsive interactions are calculated in the limit of infinite repulsion. The correlation functions are consistent with a possibility of spin-charge separation in this limit. However, the critical behaviour turns out to be strikingly different from what could be expected based on the strong coupling limit of the corresponding Luttinger model.

FLUXON DYNAMICS SUPERCONDUCTING MULTILAYERS - MICROWAVE EMISSION

S. Madsen and N. F. Pedersen (Ørsted●DTU, Technical University of Denmark, Denmark)

The stacked Josephson junctions have been suggested for use as a microwave oscillator for very high frequencies. The junctions can be made artificially using low temperature superconducting materials or found naturally as single crystal $Bi_2Sr_2CaCu_2O_x$. For this, and other utilizations of the stacked Josephson junctions, the in-phase motion of fluxons in the different layers is highly desirable, but - as it turns out - difficult to obtain. In this presentation we will look at a possible solution to the problem.

HIGH-T_c SUPERCONDUCTIVITY VIA SUPERPROPAGATORS

G. P. Malik (Theory Group, School of Environmental Sciences, Jawaharlal Nehru University, New Delhi 110067, India) and Usha Malik (Physics Department, Miranda House, Delhi University, Delhi 110007, India)

We show that the high T_c of a multi-component superconductor comes about owing to multiple phonon exchanges between electrons in it. The demonstration makes use of the Bethe-Salpeter equation, which is temperature-generalized by invoking the Matsubara prescription; for multiple phonon exchanges, we use the elegant concept of a superpropagator.[1-4] The investigation is conducted at the level of the original Cooper problem.[5]

We are thus led to results[6] such as:

$$(T_c)_{Zn+Cd} = 12.6 \text{ K}; \; (T_c)_{Zn+Hg} = 17.2 \text{ K}; \; (T_c)_{Zn+Cd+Hg} = 32.4 \text{ K}.$$

REFERENCES

1. A. Salam in, *Nonpolynomial Lagrangians, Renormalization and Gravity* (Reviewer: A. Salam), Gordon and Breach, New York (1971)
2. S. N. Biswas, G. P. Malik and E. C. G. Sudarshan, Phys. Rev. D **7**, 2884 (1973)
3. S. Okubo, Progr. Theoret. Phys. (Kyoto) 1**1**, 80 (1954)
4. S. N. Biswas, R.N . Chaudhuri and G. P. Malik, Phys. Rev. D **8**, 1808 (1973)
5. L. N. Cooper, Phys. Rev. **104**, 1189 (1956)
6. G. P. Malik and Usha Malik, to appear in Physica B (2003)

FREE ENERGY ANALYSIS OF THE MAGNETIC AND SUPERCONDUCTING PHASES IN THULIUM BOROCARBIDE

Jens Jensen and Per Hedegård (Niels Bohr Institute fAPG, Ørsted Laboratory, University of Copenhagen, Denmark)

The rare-earth borocarbides $R\mathrm{Ni_2B_2C}$, with R = Dy, Er, Ho, and Tm, may be classified as unconventional superconductors in their own right, since superconductivity coexists and competes with antiferromagnetic ordering. It is usually assumed that they are isotropic singlet superconductors, but there are experimental observations questioning the assumption of isotropy. The localized magnetic rare-earth moments are coupled indirectly through the conduction electrons. The uniform component of the RKKY interaction is reduced in proportion to the superconducting order because of the Anderson-Suhl screening of the electronic bulk susceptibility. This screening implies that the upper critical field depends on the size of the uniform magnetization induced by an applied field, and H_{c2} thereby reflects the anisotropy of the magnetic system as discussed in reference 1.

Here we present a coarse-grained free-energy analysis of the competition between superconducting and magnetic order in these systems with focus on the Tm case. Due to low-lying excited vortex states the screening is assumed to be absent within the core of the vortices in the type II phase. This implies an excess magnetization of the flux lines in comparison with their surroundings and a radius of the cores, which increases with field. The theory accounts for the field dependence of the flux-line radius determined by neutron diffraction measurements.[2] It predicts a continuous transition at the upper critical field with a jump in the derivative of the magnetization of the size observed experimentally. The magnitude of the screening in $\mathrm{TmNi_2B_2C}$ is derived from the stability of the antiferromagnetic ordering in a c-axis field, see reference 1. In terms of this estimate it is found that the exchange splitting between the spin-up and spin-down states of the conduction electrons, just below the upper critical field, is four times larger than the superconducting energy gap. This finding suggests that the superconducting state in the Tm compound may involve triplet rather than singlet Cooper pairs close to the upper critical field.

REFERENCES

1. K. Nørgaard, M. R. Eskildsen, N. H. Andersen, J. Jensen, P. Hedegård, S. N. Klausen, and P. C. Canfield, Phys. Rev. Lett. **84**, 4982 (2000)
2. M. R. Eskildsen, *Small angle neutron scattering studies of the flux line lattices in the borocarbide superconductors*, Thesis (Risø National Laboratory, 1998)

ELECTRONIC SPECIFIC HEAT OF CHARGE-DENSITY-WAVE SUPERCONDUCTORS

A. M. Gabovich, A. I. Voitenko (Institute of Physics, pr. Nauki 46, 03028 Kiev, Ukraine), Mai Suan Li, H. Szymczak (Institute of Physics, Al. Lotnikow 32/46, PL-02-668 Warsaw, Poland)

Thermodynamical properties of superconductors with electron-hole correlations leading to charge-density-waves (CDWs) are considered on the basis of the model.[1] Strong mixing of states from dielectrised (*d*) and non-dielectrised (*nd*) Fermi surface (FS) sections is assumed leading to a single superconducting order parameter $\Delta(T)$ over the whole FS. A dielectric order parameter $\Sigma(T)$ driven by CDWs exists only on the *d*-sections. The temperature, T, dependences of $\Delta(T)$ and $\Sigma(T)$ are obtained self-consistently. It is shown that the structural critical temperature T_s always exceeds the superconducting critical temperature T_c and for close enough $T_s > T_c$, the CDW order parameter $\Sigma(T)$ may become smaller then $\Delta(T)$. Both energy gaps, i. e. $\Delta(T)$ at the *nd*-sections and $D(T)=(\Delta^2+\Sigma^2)^{1/2}$ at the *d*-sections, have the exact BCS form in the relevant T-regions.

The electronic specific heat $C(T)$ of the CDW superconductors was demonstrated to be a sum of contributions from gaps pertinent to the problem, with each contribution proportional to the specific heat dependence appropriate to the Bardeen-Cooper-Schrieffer (BCS) model. The normalized specific heat jump at T_c, $\alpha = \Delta C(T_c\}/C(T_c+0)$, is always reduced in comparison with the conventional $\alpha_{BCS} \leq 1.43$ value. In particular, it may be several times less for reasonable values of the model parameters. The ratio α is a non-monotonous function of the parameter μ, which characterizes the fraction of the FS covered by *d*-sections, and approaches α_{BCS} both for $\mu \to 0$ and $\mu \to 1$.

Experimental implications are made for CDW superconductors, such as A15 and C15 compounds or high-T_c cuprates.

REFERENCES

1. G. Bilbro and W. L. McMillan, Phys. Rev. B **14**, 1887 (1976)

SPECIFIC HEAT OF INHOMOGENEOUS S-WAVE SUPERCONDUCTORS: APPLICATION TO MgB_2

A. M. Gabovich, A. I. Voitenko (Institute of Physics, prospekt Nauki 46, 03028 Kiev, Ukraine), Mai Suan Li, H. Szymczak (Institute of Physics, Al. Lotnikow 32/46, PL-02-668 Warsaw, Poland), M. Pękała (Department of Chemistry, University of Warsaw, Al. Zwirki i Wigury 101, PL-02-089 Warsaw, Poland)

The recently discovered superconductor MgB_2 reveals multiple-gap behaviour. It is frequently explained as a manifestation of weakly connected σ- and π- band superconducting energy gaps, i. e. multiplicity has a k-space origin. The main objection to this interpretation is the robustness of these features with respect to alloying and disordering.

As an alternative, we consider MgB_2 as a configuration of mesoscopic domains, where (i) at temperature $T = 0$ each domain is described by a certain superconducting order parameter $\Delta_0 \le \Delta_0^{max}$; (ii) up to a relevant critical temperature T_{c0} its superconducting order parameter $\Delta(T)$ is the function $\Delta(T) = \Delta_{BCS}(\Delta_0, T)$. Thus, a given sample at any $T > 0$ eventually is a mixture of normal and superconducting regions. We calculate the electronic heat capacity of such a *spatial* ensemble with various gap\distributions. Calculations show that the superconducting contribution $<C_s(T)>$ at low T is quadratic in T and the validity range of this behaviour depends on the dispersion of the parameter Δ_0 over the ensemble. The low-T asymptotics for $<C_n(T)>$ is also proportional to T^2 due to the fact that the fraction of the normal phase varies with T. Thus, both normal and superconducting contributions to thermodynamic quantities are *functionally indistinguishable* from each other. Simultaneously, the *same* disorder of domain properties leads to the reduction and smearing of the BCS anomaly ΔC at T_c.

The theory explains well the experimental dependences $C(T)$ for MgB_2. For homogeneous samples it predicts the transitional T-intervals where $<C(T)>$ has an exponential behaviour with the apparent superconducting energy gaps being smaller than the BCS ones. The observed phase separation between Mg-vacancy rich and Mg-vacancy poor domains, superconductivity in MgB_2 exhibiting a percolative nature[1] directly supports our point of view.

The presented considerations can be applied, in principle, to any disordered superconductor with the specified relationship between different length scales. E.g., the power-law $C(T)$ in high-T_c oxides, exhibiting an intrinsic electronic phase-separation, may be explained in the same manner.

REFERENCES

1. P. A. Sharma et al., Phys. Rev. Lett. **89**, 167003 (2002)

STRUCTURE AND TRANSPORT PROPERTIES OF DOUBLE DOPED $Mg_{1-x}(Al_{0.5}Li_{0.5})_xB_2$

G.-J. Xu, J.-C. Grivel, A. B. Abrahamsen, N. H. Andersen (*Department of Materials Research, RisØ National Laboratory, 4000 Roskilde, Denmark*)

A series of polycrystalline samples of $Mg_{1-x}(Al_{0.5}Li_{0.5})_xB_2$ ($0 \le x \le 0.6$) and $Mg_{1-x}Al_xB_2$ ($0 \le x \le 0.4$) were synthesized by the conventional solid state reaction method and their structure and superconductivity were investigated by means of x-ray diffraction (XRD), ac susceptibility and resistivity. The XRD patterns of $Mg_{1-x}(Al_{0.5}Li_{0.5})_xB_2$ ($0 \le x \le 0.6$) samples show that the predominant phase was of MgB_2 type and there was a minor amount of impurity phases for the $x \le 0.4$ samples. A marked increase in intensity of impurity phases can be clearly observed for the $x = 0.6$ sample. Similar to Al doping, the double doping leads to a decrease in both the lattice parameters a and c as shown in the inset of Fig. 1.

To obtain the superconducting transition temperature, both resistivity and ac susceptibility measurement were made. The T_c obtained from magnetic measurement is approximately consistent with that from ρ-T curves. Fig. 1 illustrates the variation of zero resistivity, T_c^0, as a function of substitution level x for $Mg_{1-x}(Al_{0.5}Li_{0.5})_xB_2$ and $Mg_{1-x}Al_xB_2$. The T_cs for the double-doped samples are systematically higher than that of the single Al doped samples. The difference of T_c^0s between the two systems increases and it reaches about 10 K for the two $x = 0.4$ samples. High-pressure experimental results indicated that MgB_2 remains strictly hexagonal until the high pressure [1]. The large value of critical temperature variation with small modification in the unit-cell volume demonstrates that Mg-B and B-B bonding distances are crucial in the superconductivity, which can be used to understand our results, i.e., Al doping in $Mg_{1-x}Al_xB_2$ leads to a faster decrease in lattice parameters than the double doping with the same doping level, thus the decrease in T_c with Al doping is faster than that with double doping.

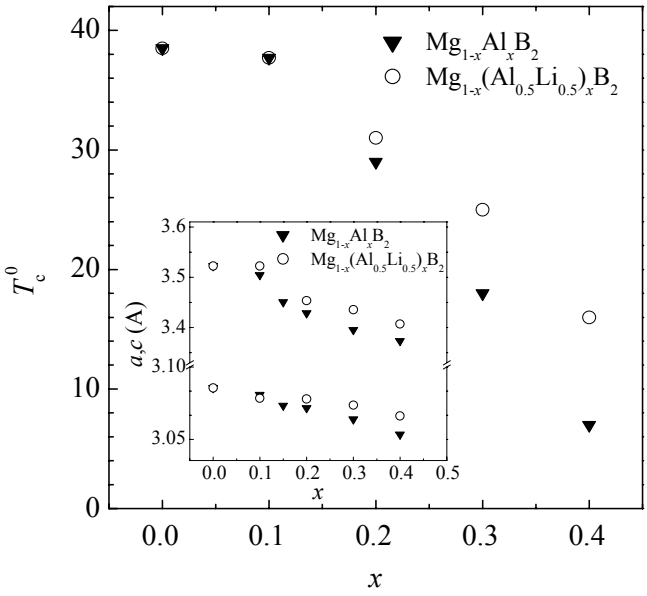

Fig. 1. T_c^0 dependence of doping level x for $Mg_{1-x}(Al_{0.5}Li_{0.5})_xB_2$ and $Mg_{1-x}Al_xB_2$. The inset illustrates the lattice parameter a and c as a function of x.

To clarify the factors that influence the superconducting transition temperature, we calculated the dependence of T_c on the unit-cell volume and plotted $T_c(V)$ in Figure 2. The result from high-pressure experiment was also given in the figure for comparison. At low doping level, the volume dependence of T_c values are close for the three cases and the T_cs show a approximately linear volume dependence. With further decreasing V, a remarkable deviation from linear $T_c(V)$ behavior for the chemical substituted cases can be clearly observed. The structural transition for the Al doped MgB_2 system taking place as $x \approx 0.1$ may be a possible factor causing the deviation. However, the structural transition, as well as the 'pressure effect', cannot be used to account for the fact that with same unit-cell volume the double-doped system has lower T_c than Al doped system. Obviously the change of carrier concentration is not the main cause resulting in different $T_c(V)$ between the two systems. In fact, the effect of carrier concentration on T_c is a little different between MgB_2 and high T_c cuprates. Hall effect experimental results [2] showed that the charge carriers in MgB_2 are holes with a density of $1.7 - 2.8\times10^{23}$ holes cm^{-3} at 300 K, which is about two orders of magnitude higher than the charge carrier density for high Tc cuprates. This value corresponds to 2.5 – 4 holes per unit-cell in MgB_2. Therefore a little change in carrier concentration may not show significant influence on T_c in MgB_2 system, which is in contrast to that in high-T_c cuprates. From the variation of lattice parameters with doping one may find that in order to get same unit-cell volume, the doping level for the double doped system is always higher than the Al doped system, which means that the disorder for the former is higher than that for the latter with same unit-cell volume. The strong disorder or localized structural distortion may be the origin causing the different T_c(V).

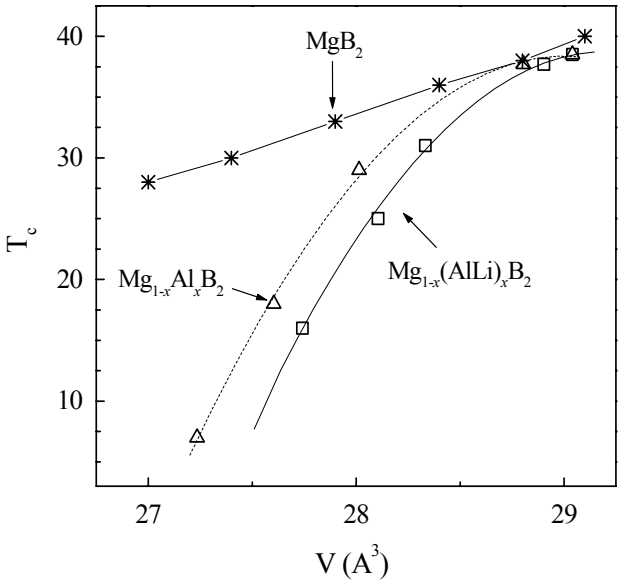

Fig.2 T_c as a function of unit-cell volume for $Mg_{1-x}(Al_{0.5}Li_{0.5})_xB_2$ and $Mg_{1-x}Al_xB_2$ and MgB_2.

References

1. A.F. Goncharov, V.V. Struzhkin, E. Gregoryanz, Phys. Rev. B **64** (2001) 100509.
2. C. Buzea and T. Yamashita, Supercond. Sci. Technol. **14** (2001) R115.

COMPARISON OF THE YIELD PROPERTIES OF MAGNESIUM DI-BORIDE AND BSCCO PRECURSOR POWDER

M. S. Nielsen, M. H. Hancock, M. Eriksen, J. I. Bech, N. Bay (Institute of Manufacturing Engineering and Management, Technical University of Denmark, DK-2800 Kgs. Lyngby, Denmark)

In order to analyse the plastic deformation process utilized in manufacture of a superconductor composite e.g. flat rolling of Ag/BSCCO or Fe/MgB_2 the Finite Element method is often utilized. With reference to basic literature on the subject the basis of such an analysis is a spatial discretisation of the principle of virtual work (PVW), which in rate formulation reads: $\Delta t \delta \dot{W}_{\text{int.}} = \Delta t \delta \dot{W}_{ext.}$ Here Δt is a pesudo time increment and $\delta W_{ext.}$ denotes the virtual work rate done by external forces to the body in question, i.e. a surface integral of the tractions given no body forces, and δW_{int} denotes the internal virtual work rate given by $\delta \dot{W}_{int.} = \int_V \partial(\boldsymbol{\sigma} : \boldsymbol{\delta\varepsilon})/\partial t \, dV$. The term $\boldsymbol{\sigma}$ is the Kirchoff stress tensor and $\boldsymbol{\varepsilon}$ is the Lagrangian strain which is a function of the material displacements $\boldsymbol{u}$. Solving for $\boldsymbol{u}$ thus defines the deformation. In order to solve the equation and find the deformation pattern one still needs to relate the stresses to the strains by a constitutive equation. Assuming that that the elastic contribution to the deformation may be neglected leaves the plastic properties to be measured. For metals the constitutive equation for plasticity is described adequately by isotropic hardening using a stress strain relation measured directly by an upsetting test. The challenge is to measure the plastic properties of the precursor powder adequately, which is the theme of the present work.

Looking at a stress situation given by the Cartesian components of the stress tensor σ_{ij} the plastic properties is usually formulated as a yield function, $f(\sigma_{ij})$ which has the properties $f<0$ when the material is in an elastic stress state and $f=0$ when the material is plastic. The plastic properties for the precursor powder may be assumed dependent of only of the first and second invariant of this stress tensor, J_1 and J_2. These are defined by $J_2 = (\sigma_{ij}\sigma_{ij} - \sigma_{ii}\sigma_{jj})/2$ and $J_1 = \sigma_{ii}$ adopting Einstein's summation convention. Using the hydrostatic pressure $p_m = -J_1/3$, and $q_{J2} = \sqrt{J_2}$, a quantity proportional to the von Mises or equivalent stress gives the yield function to be $f(\sigma_{ij}) = f(p_m, q_{J2})$. See Bech[1] for furter information.

Using three different mechanical tests with tools and procedures as described by Bech[1], the diametral fracture test, axial fracture test and die compression, three points may be determined on the yield surface for samples pre-compacted in a tool to a certain density. The tested powder was commercially available MgB_2 powder from Alfa Aesar. The density of fully compacted MgB_2 powder was measured by pycnometry in alcohol to be 2.50g/cm^3, which is lower than the value of 2.66g/cm^3.

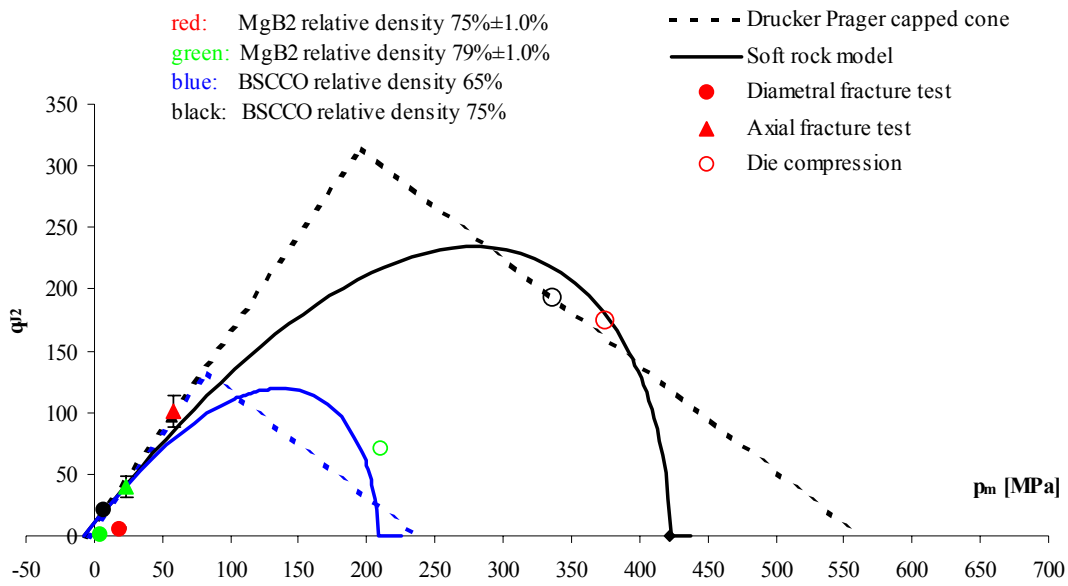

Fig. 1. Test data from mechanical testing of MgB2 with Drucker-Prager cone-cap and soft rock yield surfaces for BSCCO precursor powder.

Comparing the distribution of the test points for MgB_2 to the Drucker Prager capped cone model or the soft rock model as implemented in Elfen[3] fitted to BSCCO data from Bech[2] shows that the models are able to model the behaviour of MgB_2. However the hardening characteristics of the two powders is somewhat different. A change of 10%-point relative density for BSCCO results in the same increase in the yield surfaces as a relative density increase of 4%-point for MgB_2. This was a fact confirmed in the preparation of the samples: Where the maximal load in the preparation of samples for the diametral and axial fracture tests resulted in a relative density of 85% for BSCCO, it only resulted in approximately 80% relative density of MgB_2 samples. It is therefore to be expected that entirely mechanical methods will have difficulty in changing the final density of Fe/MgB_2 composites. An interesting result in Fig. 1 is that the diametral fracture tests points for MgB_2 is considerably lower than the yield surface (fracture line) for BSCCO. This indicates that the MgB_2 powder has only very little cohesion and internal friction, which facilitates the flow of the MgB_2-powder in manufacturing processes.

This work has been supported by the Danish Energy Research Program EFP, “DK Superconducting Tape Technology 2001-2003” and the Danish Technical Research Council in the project “New Superconductors: mechanisms, processes and products.

REFERENCES

J. I. Bech, "Manufacture of Superconductors", Ph. D. Thesis, IPL-DTU, DK-2800 Kgs. Lyngby, Denmark (2001)
Y. Takano, H. Takeya, H. Fuji, H. Kumakura,T. Hatano, K. Togano,Appl. Phys. Lett., **78**, 19 (2001)
Elfen FEM-program, Rockfield Software Ltd. Swansea, UK

CORRELATION BETWEEN ENHANCED CRITICAL TEMPERATURE, ORTHORHOMBICITY AND THE VOLUME OF THE UNIT CELL IN ARGON PREHEATED $(Y_{1-x}Sm_x)$ (Sr,Ba) $Cu_3 O_{6+z}$

Ab. Nafidi, M. Bellioua, A. El Kaaouachi, Ah. Nafidi, H. Sahsah, (Condensed Matter Physics Laboratory, Faculty of Sciences, B.P 8106 Hay Dakhla, University Ibn - Zohr, 80000 Agadir, Morocco) and R. Suryanarayanan (Physico-chemistry of Solid Laboratory, URA 446, Bât. 414, CNRS, University Paris Sud, 91405 Orsay, France)

We report here on the preparation, x-ray diffraction, resistivity and AC magnetic susceptibility measurements of the high T_c superconductor $(Y_{1-x}Sm_x)(SrBa)Cu_3O_{6+z}$. ($x$ = 0, 0.2, 0.4, 0.5, 0.6, 0.8 and 1). In addition we examine the effect of argon heat treatment followed by oxygen annealing that has considerable influence on the structural and superconducting properties. The samples were polycrystalline prepared by solid state sintering. We used two different heat treatments: (i) the sintered sample were annealed in oxygen at 450°C for three days, this sample was denoted as [O] and (ii) the same sample were heated in argon at 850°C for 1 days, cooled and later annealed in oxygen at 450°C for 3 days [AO]. The oxygen content (6 + z) of the samples was close to 6.94 ± 0.04 as determined by our iodometry measurements.

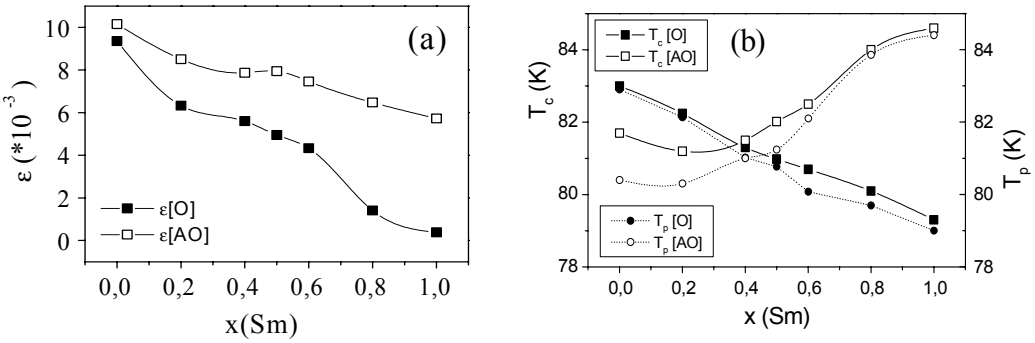

Fig. 1. (a) Variation of the orthorhombicity ε and (b) variation of T_c and T_p (b) of $(Y_{1-x}Sm_x)SrBaCu_3O_{6+z}$ as a function of x for Sm and heat treatment.

Figure 1 shown that when x increases from 0 to 1; in the samples [O] the orthorhombicity ε = $(b - a)/(b + a)$ decreases from 9.35 10^{-3} to 0.38 10^{-3} indicating a transition of structural phase from orthorhombic to tetragonal; and T_c decreases from 83 K to 79 K. While in the samples [AO], ε decreases by half from 10.14 10^{-3} to 5.72.10^{-3} with an orthorhombic symmetry. This were accompanied by an increase from T_c = 81.5 K to 85 K. This last evolution of T_c and ε in opposite sense is unusual and it's observed for the first time. For each x, the [AO] heat treatment increases the orthorhombicity (for $0 \le x \le 1$) and T_c (for $x \ge 0.4$). It is interesting to note, however, that the T_c of the sample $Sm(SrBa)Cu_3O_{6+z}$ [AO] increase remarkably by 6 K to 85 K.[1] The evolution of $T_p(x)$ (peak of the imaginary part of the AC susceptibility) follow essentially that of $T_c(x)$ as shown in Fig. 1b.

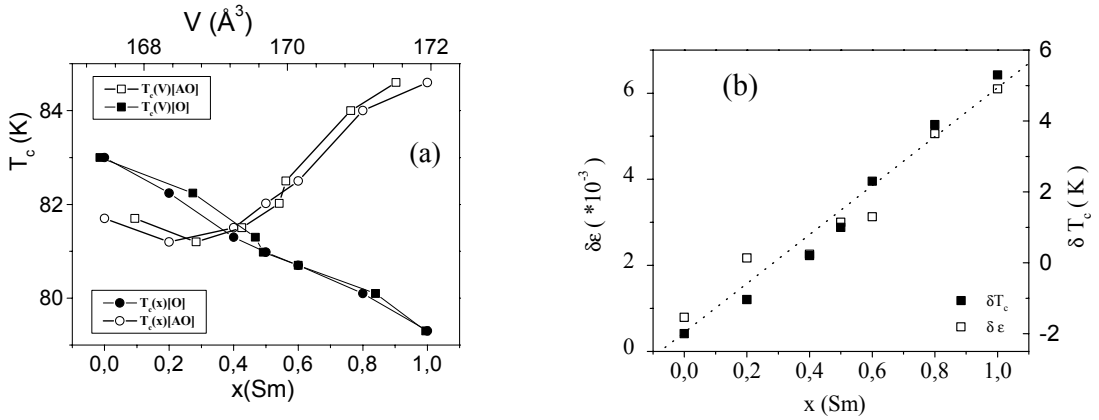

Fig. 2. (a) Correlation between T_c and the volume V of the unit cell and (b) $\delta T_c = T_c[AO] - T_c[O]$ and $\delta\varepsilon = \varepsilon[AO] - \varepsilon[O]$ as a function of x and heat treatment in $(Y_{1-x}Sm_x)SrBaCu_3O_{6+z}$.

We observed two remarkable correlations: between $T_c(x)$ and the volume $V(x)$ of the unit cell for the two heat treatments (Fig. 2a), and on the other hand, between the variation of critical temperature $\delta T_c(x) = T_c[AO] - T_c[O]$ and that of orthorhombicity $\delta\varepsilon(x) = \varepsilon[AO] - \varepsilon[O]$ (Fig. 2b). So the structural and superconducting properties are correlated with the effect of argon heat treatment. In addition we solved the controversy reported by [2,3] that indicated a tetragonal structure and a critical temperature T_c of 80 K and 37 K, respectively, in $Sm(SrBa)Cu_3O_{6+z}$.

These results are the outcome of interplay between cationic disorder and oxygen disorder in basal plane. A combination of several factors such as decrease in the Cu (1)-apical oxygen distance who enhance the mechanism of transfer of holes from the chains Cu(1)-O_p to the planes Cu(2)-O; cationic order of Sm_x on the (Sr, Ba) site, chain oxygen ordering on (O_4,O_5) site[4]; increase in p and in-phase purity for the (AO) samples (as observed respectively by thermoelectric power and neutrons diffraction measurements in $Nd(SrBa)Cu_3O_{6+z}$[5]) may qualitatively account for the observed data. We believe that the present data will be useful to test or improve certain theoretical models on electronic structure and the atomic disorder.

REFERENCES

1. M. Bellioua, A. Nafidi, A. El Kaaouachi, Ahmed Nafidi and R. Suryanarayanan, Physica C **383,** 183 (2002)
2. X. Z. Wang, B. Hellerbrand and D. Bruerle, Physica C **200**, 12 (1992)
3. V. Badri, U. V. Varadaraju and G. V. Subba Rao, in: *Physical and Material Properties of High Temperature Superconductors* (Eds. S.K. Malik and S.S. Shah, Nova Science, New York, 1994)
4. A. Nafidi and R. Suryanarayanan, Physica C **249**, 262 (1995)
5. A. Nafidi, A. El Kaaouachi, M. Bellioua, R. Suryanarayanan, I. Zelenay and C. Greaves, Moroccan Journal of condensed Matter **2**, 5 (1999)

TILTED-AXES YBCO THIN FILMS: FROM VICINAL RANGE TO STEP BUNCHING

P. B. Mozhaev, J. E. Mozhaeva (Institute of Radio Engineering and Electronics RAS, Moscow, Russia), I. K. Bdikin (Department of Ceramic and Glass Engineering, CICECO, University of Aveiro, Aveiro, Portugal), T. Donchev, E. Mateev, T. Nurgaliev (Institute of Electronics BAS, Sofia, Bulgaria), C. S. Jacobsen, J. B. Hansen (Physics Department, Technical University of Denmark, Denmark), S. A. Zhgoon, A. E. Barinov (Moscow Power Engineering Institute, Moscow, Russia)

Tilted-axes YBCO thin films were deposited on NdGaO3 (NGO) substrates with surface inclination from the standard (1 1 0) crystallographic plane. All deposited films were epitaxial with the (0 0 1) YBCO plane aligned with the {1 1 0} planes of the substrate. Structural and morphological studies revealed three angular ranges of film formation. In the small-angle "vicinal" range (L) the films do not differ much from films deposited on (1 1 0) NGO. The high-angle range (H) is characterized by "step bunching" during the thin film growth. The intermediate range (M) provides very smooth films with the best crystal structure. Measurements of (0 0 1) YBCO and (1 1 0) NGO planes alignment suggest an explanation of the smooth film formation. In the L-range the seeding of the film occurs randomly along the substrate surface. Collisions of the growing grains result in dislocations formation, and mis-orientation of individual grains from the substrate. For the H-range the step-terrace junctions on the substrate surface, acting as seeding centres, are very dense, again leading to grains collisions and inclination. Only in the M-range the density of seeding centres on the substrate surface corresponds to the diffusion length of the atoms along the surface, resulting in one grain per seeding centre and excellent crystallographic alignment.

This growth model is corroborated by differences in the M-range angles for different deposition techniques. The DC sputtering at high oxygen pressure provided smooth films for 1.5 to 3 degrees, while for laser ablation technique the M-range was 7 to 10 degrees. This difference can be explained by lower atomic mobility during laser ablation, resulting in smaller grains and good correlation with the seeding center density at higher inclination angles. The M-range thin films showed also the best electrical properties (T_c, J_c (77 K), Rs (77 K, 10 GHz)). Microwave resonators for the 1 and 10 GHz bands were patterned in the films and showed high Q-values.

EFFECT OF $AgNO_3$ ADDITIVE ON MICROSTRUCTURE AND SUPERCONDUCTIVITY OF THE Pb DOPED Hg:1223 THIN FILMS PREPARED THROUGH SPRAY PYROLYSIS

Suman Anand* and O.N. Srivastava (Department of Physics, Banaras Hindu University, Varanasi-221005, INDIA, *Present address: Optical Radiation Standards, National Physical Laboratory, *New Delhi-110012, INDIA)*

We report successful fabrication of Ag doped Hg:1223 films by reacting $Ba_2Ca_{2..3}Cu_{3..3}O_z(Ag_y)$ with y = 0, 0.02, 0.025, 0.05, 0.1, 0.2 precursors deposited by spray pyrolysis on $SrTiO_3(100)$ substrates, in controlled Hg+Pb ambient, in an evacuated sealed quartz tube at 820°C for four hours. The effects of $AgNO_3$ addition on the superconducting properties of Hg/(Pb):1223 films are studied. The addition of low concentration of silver e.g., $y \approx 0.025$ results in a slight increase of T_c (R = 0) from 125 K to 126 K and the *dc* critical current density (J_c) decreases with the increasing Ag in Hg(Pb):1223(Ag_y) films. The microstructural details exhibit the curious characteristics of spiral like features for lower concentrations of silver, i.e., up to y = 0.05. These improvements are believed to be due to the liberation of oxygen through the dissociation of $AgNO_3$ at higher temperature and passivation of weak link effects through the segregation of silver at these grain boundaries. The addition of silver content $y \geq 0.05$, resulted in the decrease of transition temperature. J_c is observed to decrease steadily with increasing Ag content. The microstructural feature, e.g. spiral, is also found to deteriorate with increasing silver content. The deterioration in superconducting properties at high Ag content is believed to be mainly due to the formation of AgHg amalgam.

YBCO/Ag PIT-TAPES PREPARED WITH NANOSIZED POWDER

P. Paturi, J. Raittila, R. Laiho (Wihuri Physical Laboratory, Physics Department, University of Turku, Finland), J.-C. Grivel, N. H. Andersen (Materials Research Department, Risø National Laboratory, Denmark)

YBCO single-filament powder-in-tube tapes were prepared using nanosized YBCO powder and annealing the tapes in N_2/O_2 atmosphere. This resulted in high critical current, I_c, tapes, with *ab*- and *c*-texturing at the interface between the silver sheath and the superconductor.

The YBCO nanopowder was prepared using the citrate-gel method[1, 2], where the nitrates of the metals are mixed together and citric acid is added. The gel is then dried and calcined at 500°C and the resulting powder is lightly ground. The powder is annealed in O_2 at 790°C resulting in X-phase YBCO. The conversion to fully oxygenized orthorhombic YBCO is done by annealing in Ar at 790°C and cooling in O_2. Annealing in Ar is repeated three times. This results in 1-3 nm thick and 50-100 nm wide particles with T_c = 92 K.

The tapes were prepared using the standard PIT-method.[3, 4] After drawing and rolling the tape was 2.2 mm wide and 200 μm thick with filling factor of 35 %. 4 cm long pieces of the tape were annealed in N_2 at 900 - 950°C for ten to twenty hours and cooled in O_2 with the cooling rate of 50 - 150°C/h to 650°C where the samples were kept for four hours. The cooling continued with the rate of 150°C/h to 440°C, where the temperature was dwelled for eight hours before cooling to room temperature with the rate of 50°C/h. The I_c was subsequently measured in liquid N_2 and self-field using the 1 μV/cm criterion. The highest I_c = 5.02 A, which corresponds to critical current density of 3300 A/cm^2, was obtained by annealing at 946°C for 10 h and cooling with 150°C/h. The magnetic measurements show that the tapes have critical temperature of 89 K and that the hysteresis loop is still open at 1 T, which suggests that the tapes perform better in magnetic field than the commercial BSCCO-tapes.

The texture of the tapes[5] was studied using XRD with a texture goniometer. First the silver sheath was removed either by dissolving it into mercury or with a knife. Dissolving does not affect the superconductor and exposes essentially the interface surface of the superconductor. Removing the silver with a knife on the other hand opens the tape nearer to the middle of the tape, which enables measurements at two different positions of the tape. The pole figures of (103) peaks were measured with $\Delta\phi = 5^o$ and $\Delta\psi = 5^o$. It was found that the texture clearly correlates with the observed I_c. The best tape had (Fig. 1a) two-fold symmetry distinctive of texturing in *ab*- and *c*-directions, whereas a tape with lower I_c = 1 A (Fig. 1b) had a ring type symmetry indicating *c*-axis texturing only. When the best tape was opened with a knife, it still showed 2-fold symmetry, but not so pronounced as in the Hg opened tape, indicating that the best texture is found at the interface between the silver and the superconductor, as has also been found for BSCCO tapes.[6]

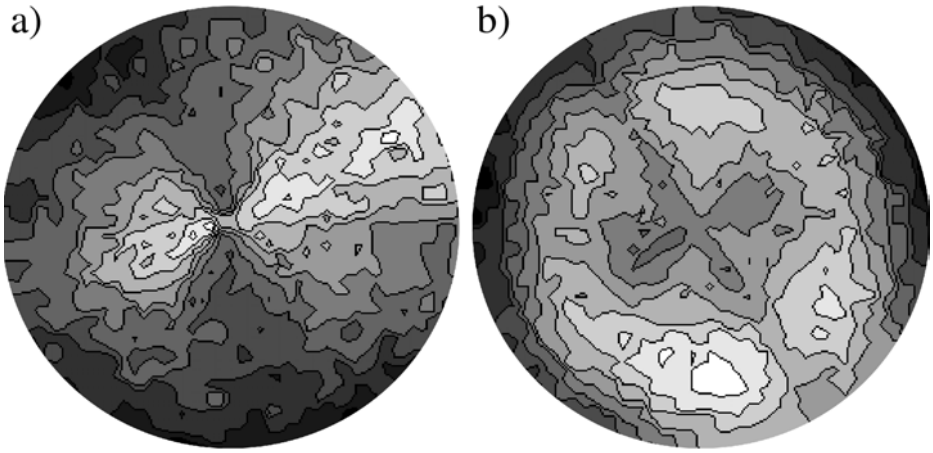

Fig. 1. Pole figures of (a) the best I_c = 5.02 A tape and (b) a I_c = 1.0 A tape. The best tape has a clear two-fold symmetry indicating *ab*-texturing, whereas the other tape exhibits ring-type symmetry and *c*-axis texturing only.

In conclusion we can say that using the nano-powder for manufacturing YBCO PIT-tapes has so far shown the largest I_c published and also to our knowledge the only evidence of *ab*-texturing in the superconductor. Since texturing is better at the silver-superconductor interface, the next logical step in the development of YBCO-tapes is multifilament tapes, where the interface area is maximized.

Academy of Finland, Graduate School of Materials Research and the Wihuri Foundation are acknowledged for financial support.

REFERENCES

1. E. Blinov, V. G. Fleisher, H. Huhtinen, R. Laiho, E. Lähderanta, P. Paturi, Y. P. Stepanov and L. Vlasenko, Supercon. Sci. Tech. **10**, 818 (1997)
2. J. Raittila, H. Huhtinen, P. Paturi and Y. P. Stepanov, Physica C **371**, 90 (2002)
3. P. Vase, R. Flükiger, M. Leghiss and B. Glowacki, Supercond. Sci. Technol. **13** , R71 (2000)
4. P. Paturi, J. Raittila, J.-C. Grivel, H. Huhtinen, B. Seifi, R. Laiho, N. H. Andersen, Physica C **372-376**, 779 (2002)
5. P. Paturi, T. Kulmala, J. Raittila, J.-C. Grivel, R. Laiho and N. H. Andersen, Physica C, submitted (2003)
6. B. Glowacki, Supercond. Sci. Technol. **11**, 989 (1998)

ANALYSIS OF Bi-2223 PHASE GROWTH IN Ag-SHEATHED $(Bi,Pb)_2Sr_2Ca_2Cu_3O_{10+\delta}$ TAPES

X. P. Chen (Applied Superconductivity Research Center, Tsinghua University, Beijing, 100084, China and Department of Materials Research, Risø National Laboratory, Denmark), Z. Han (Applied Superconductivity Research Center, Tsinghua University, Beijing, 100084, China), J.-C. Grivel and N. H. Andersen (Department of Materials Research, Risø National Laboratory, Denmark)

The evolution of the Liquid Phase (LP), the dissolution of the Bi-2212 phase and the growth of the Bi-2223 phase in sintered $(Bi, Pb)_2Sr_2Ca_2Cu_3O_{10+\delta}$/Ag tapes were investigated by SEM, EDS and XRD. The samples were sintered at 840 ^oC in 8.5% O_2 and quenched in air after sintering for 1, 2, 3, 5, 10, 20 and 50 hours.

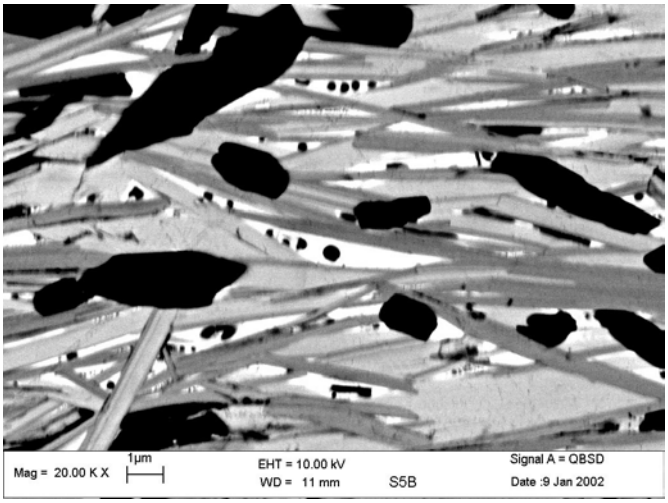

Fig. 1. The cross-section SEM images of sample sintering for 5 hours at 840 ^oC in 8.5% O_2. The white regions, the light grey regions and the dark grey regions represent LP, Bi-2212 phase and Bi-2223 phase, respectively. "jam-state" means the liquid region was covered by the Bi-2223 plates.

The cross-section SEM image of the sample sintered for 5 hours is shown in Fig. 1. It can be clearly observed that Bi-2223 phase always formed at the interfaces between the Bi-2212 phase and the liquid phase, indicating that Bi-2223 easily grows along the a-b plane of Bi-2212, and the Bi-2223 grains grow much faster along the ***ab*** plane than along the ***c***-axis. EDS analysis shows that the liquid region is rich in Bi, Pb, Ca and Cu, as originally reported by Morgan et al.[1], which implies that the Bi-2212 phase melt first to form the liquid phase and then the secondary phases dissolve into the liquid. It is also seen that some liquid regions were covered by the Bi-2223 plates, and we call this condition the "jam-state" (see Fig. 1). The average thickness along c-axis of Bi-2223 plates was obtained by measuring about 100 Bi-2223 plates. The thickness as a function of sintering time is shown in Fig. 2, which shows that the thickness increases with the sintering time, while the average growth rate of the Bi-2223 plate thickness decreases as the sintering time increases.

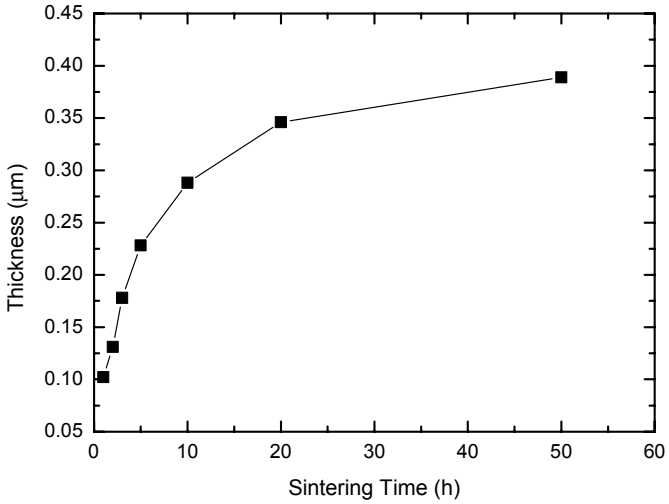

Fig. 2. The average thickness of Bi-2223 plates as a function of the sintering time.

The volume fraction of LP was measured by calculating the total area of all LP. It is found that the volume fraction of LP increases with sintering time and reaches maximum at a sintering time of 10 hours. Within the initial 10 hours, the increase of LP volume fraction is dominant; this is because that not all the liquid regions reach the "jam-state". Those that haven't reached the "jam-state" will dissolve the Bi-2212 phase plus secondary phase and grow larger continually. After sintering time of 10 hours, all liquid regions were covered by the Bi-2223 plates, the pure ***c***-axis growth of Bi-2223 phase begins. Since the growth of Bi-2223 plates consumes LP, and there is no supplementary to the LP, the total volume fraction of LP begins to fall down after 10 hours. The analysis of Bi-2223 growth using the Avrami equation reveals a two-stage kinetics process with a remarkable change of the n-exponent after about 10 hours' sintering, which can be well explained by the evolution of LP and the way of Bi-2223 phase growth.

REFERENCES

1. P. E. Morgan, R. M. Housley, J. R. Porter and J. J. Ratto, Physica C. **176,** 279 (1991)

EXACT DIAGONALIZATION ANALYSIS OF MAGNETIC BLOCH OSCILLATIONS

Heidi Kolmorgen Nielsen and Karen-Anne Holt Herdal (University of Roskilde, DK and Risø National Laboratory, Denmark), K. Lefmann (Risø National Laboratory, Denmark)

We consider an Ising-like ferromagnetic spin-1/2 chain with *x-y-z* anisotropy in the presence of an external magnetic field:

$$H = \Sigma_j \left(J_z S^z_j S^z_{j+1} + J_y S^y_j S^y_{j+1} + J_x S^x_j S^x_{j+1} - g \mu_B H S^z_j \right)$$

It has been predicted by Kyriakidis and Loss[1], that in this system magnetic domain walls will perform oscillating behaviour, the so-called magnetic Bloch-oscillations. Several candidate materials, where magnetic Bloch oscillations should be observable, have been suggested. Neutron scattering experiments has been carried out on one of the candidates, $CoCl_2 \cdot 2D_2O$, without success [2,3].

We study the dynamics of domain walls in a system similar to $CoCl_2 \cdot 2D_2O$ by simulating a ferromagnetic Ising-like chain of spin s=1/2 in an external magnetic field. Only nearest neighbour interactions are considered and we apply periodic boundary conditions. We formalize mathematically the description of the physical system of spins to block-diagonalize the Hamiltonian belonging to the system. Afterwards we calculate the eigenvalues and the eigenstates of the lowest excitations using the subspaces defined by the block-diagonalization of the Hamiltonian and the Lanczos-algorithm. Furthermore we calculate the dynamical structure factor of the relevant transitions corresponding to magnetic Bloch oscillations.

Our results for the dynamical structure factor show clear signs of magnetic Bloch oscillations for systems with the ideal case $J^{xy} = (J^x+J^y)/2 = 0$. However, the stability of the magnetic Bloch oscillations depends sensitively on the value of J^{xy}. When J^{xy} becomes comparable to $J^a = (J^x-J^y)/2$, the magnetic Bloch oscillations are suppressed. This suppression becomes more pronounced with increasing system size, whence we do not expect it to be a finite-size effect. We propose that the J^{xy} term present in the $CoCl_2 \cdot 2D_2O$ system is responsible for the non-observance of magnetic Bloch oscillations in this compound.

REFERENCES

1. J. Kyriakidis and D. Loss, Phys. Rev. B **5**8, 5568 (1996)
2. W. Montfrooij et al., Phys. Rev. B **64**, 4426 (2001)
3. N. B. Christensen et al., Physica B **276-278**, 784 (2000)

THE EUROPEAN SPALLATION SOURCE IN LUND – SCIENTIFIC OPPORTUNITIES IN AN EXCELLENT ENVIRONMENT

Patrik Carlsson and Karl-Fredrik Berggren (ESS-Scandinavia, Forskningsbyn Ideon, Scheelegatan 17, SE-223 70 Lund)

The European Spallation Source (ESS) will, when realised, be the premier facility for neutron scattering research in the world, provide orders of magnitude more powerful tools for studying the structure and dynamics of materials and most certainly provide new knowledge about superconductivity and magnetic properties of materials.

A proposal to host the ESS in Lund has been made by ESS-Scandinavia, a consortium of universities, research laboratories and authorities in Scandinaiva. The scientific opportunities of ESS and the merits of locating ESS to Lund is presented together with the latest news on the progress of the ESS-project in Europe and Scandinavia.

Previous Publications

Proceedings of the 1st Risø International Symposium on
"Recrystallization and Grain Growth of Multi-Phase and Particle Containing Materials"
Editors: N. Hansen, A.R. Jones, T. Leffers
Risø National Laboratory 1980

Proceedings of the 2nd Risø International Symposium on
"Deformation of Polycrystals: Mechanisms and Microstructures"
Editors: N. Hansen, A. Horsewell, T. Leffers, H. Lilholt
Risø National Laboratory 1981

Proceedings of the 3rd Risø International Symposium on
"Fatigue and Creep of Composites Materials"
Editors: H. Lilholt, R. Talreja
Risø National Laboratory 1982

Proceedings of the 4th Risø International Symposium on
"Deformation of Multi-Phase and Particle containing Materials"
Editors: J.B. Bilde-Sørensen, N. Hansen, A. Horsewell, T. Leffers, H. Lilholt
Risø National Laboratory 1983

Proceedings of the 5th Risø International Symposium on
"Microstructural Characterization of Materials by non-Microscopical Techniques"
Editors: N. Hessel Andersen, M. Eldrup, N. Hansen, D. Juul Jensen, T. Leffers, H. Lilholt, O.B. Pedersen, B.N. Singh
Risø National Laboratory 1984

Proceedings of the 6th Risø International Symposium on
"Transport-Structure Relations in Fast Ion and Mixed Conductors"
Editors: F.W. Poulsen, N. Hessel Andersen, K. Clausen, S. Skaarup, O. Toft Sørensen
Risø National Laboratory 1985

Proceedings of the 7th Risø International Symposium on
"Annealing Processes – Recovery, Recrystallization and Grain Growth"'
Editors: N. Hansen, D. Juul Jensen, T. Leffers, B. Ralph
Risø National Laboratory 1986

Proceedings of the 8th Risø International Symposium on
"Constitutive Relations and Their Physical Basis"
Editor: S.I. Andersen, J.B. Bilde-Sørensen, N. Hansen, T. Leffers, H. Lilholt, O.B. Pedersen, B. Ralph
Risø National Laboratory 1987

Proceedings of the 9th Risø International Symposium on

“Mechanical and Physical Behaviour of Metallic and Ceramic Composites”
Editors: S.I. Andersen, H. Lilholt, O.B. Pedersen
Risø National Laboratory 1988

Proceedings of the 10th Risø International Symposium on
“Materials Architecture”
Editors: J.B. Bilde-Sørensen, N. Hansen, D. Juul Jensen, T. Leffers, H. Lilholt, O.B. Pedersen
Risø National Laboratory 1989

Proceedings of the 11th Risø International Symposium on
“Structural Ceramics – Processing, Microstructure and Properties”
Editors: J.J. Bentzen, J.B. Bilde-Sørensen, N. Christansen, A. Horsewell, B. Ralph
Risø National Laboratory 1990

Proceedings of the 12th Risø International Symposium on
“Metal Matrix Composites – Processing, Microstructure and Properties”
Editors: N. Hansen, D. Juul Jensen, T. Leffers, H. Lilholt, T. Lorentzen, A.S. Pedersen, O.B. Pedersen
Risø National Laboratory 1991

Proceedings of the 13th Risø International Symposium on
“Modelling of Plastic Deformation and Its Engineering Applications”
Editors: S.I. Andersen, J.B. Bilde-Sørensen, N. Hansen, D. Juul Jensen, T. Leffers, H. Lilholt, T. Lorentzen, O.B. Pedersen, B. Ralph
Risø National Laboratory 1992

Proceedings of the 14th Risø International Symposium on
“High Temperature Electrochemical Behaviour of Fast Ion and Mixed Conductors”
Editors: F.W. Poulsen, J.J. Bentzen, T. Jacobsen, E. Skov, M.J.L. Østergård,
Risø National Laboratory 1993

Proceedings of the 15th Risø International Symposium on
“Numerical Predictions of Deformation Processes and the Behaviour of Real Materials”
Editors: S.I. Andersen, J.B. Bilde-Sørensen, T. Lorentzen, O.B. Pedersen, N.J. Sørensen
Risø National Laboratory 1994

Proceedings of the 16th Risø International Symposium on
“Microstructural and Crystallographic Aspects of Recrystallization”
Editors: N. Hansen, D. Juul Jensen, Y.-L. Liu, B. Ralph
Risø National Laboratory 1995

Proceedings of the 17th Risø International Symposium on
“High Temperature electrochemistry: Ceramics and Metals”
Editors: F.W. Poulsen, N. Bonanos, S. Linderoth, M. Mogensen, B. Zachau-Christensen

Risø National Laboratory 1996

Proceedings of the 18th Risø International Symposium on
"Polymeric Composites – Expanding the Limits"
Editors: S.I. Andersen, P. Brønsted, H. Lilholt, Aa. Lystrup, J.T. Rheinländer, B.F. Sørensen, H. Toftegaard
Risø National Laboratory 1997

Proceedings of the 19th Risø International Symposium on
"Modelling of Structure and Mechanics of Materials from Microscale to Product"
Editors: J.V. Carstensen, T. Leffers, T. Lorentzen, O.B. Pedersen, B.F. Sørensen, G. Winther
Risø National Laboratory 1998

Proceedings of the 20th Risø International Symposium on
"Deformation-Induced Microstructures: Analysis and Relation to Properties"
Editors: J.B. Bilde-Sørensen, J.V. Carstensen, N. Hansen, D. Juul Jensen, T. Leffers, W. Pantleon, O.B. Pedersen, G. Winther
Risø National Laboratory 1999

Proceedings of the 21st Risø International Symposium on
"Recrystallization – Fundamental Aspects and Relations to Deformation Microstructure"
Editors: N. Hansen, X. Huang, D. Juul Jensen, E.M. Lauridsen, T. Leffers,
W. Pantleon, T.J. Sabin, J.A. Wert
Risø National Laboratory 2000

Proceedings of the 22 nd Risø International Symposium on
"Science of Metastable and Nanocrystalline Alloys – Structure, Properties and Modelling"
Editors: A.R. Dinesen, M. Eldrup, D. Juul Jensen, S. Linderoth,
T.B. Pedersen, N.H. Pryds, A. Schrøder Pedersen, J.A. Wert
Risø National Laboratory 2001

Proceedings of the 23 nd Risø International Symposium on
"Sustainable Natural and Polymeric Composites – Science and Technology"
Editors: H. Lilholt, B. Madsen, H.L. Toftegaard, E. Cendre, M. Megnis,
L.P. Mikkelsen, B.S. Sørensen
Risø National Laboratory 2002

AUTHOR INDEX

RISØ

ISBN 87-550-3244-3

ISSN 0907-0079

Holmen Center- Tryk A/S, Holbæk